博士論文

Studies on effects of climate change on ocean environment and fisheries resources in the western coast of Kyushu

(気候変動が九州西岸域の海洋環境および水産資源に及ぼす影響に関する研究)

竹茂　愛吾

Contents

Chapter 1
General introduction

1.1 Climate change and its impact on coastal ocean

In recent years, much attention has been directed to the long-term changes in biotic and abiotic environment in ocean (Harley et al., 2006; Hollowed et al., 2009). Above all things, variations in seawater temperature associated with global climate change particularly play an important role in atmosphere–ocean interactions through heat exchange and can affect marine ecosystems (Heyward, 1997; Neumann, 2010; Iida et al., 2012; Brochier et al., 2013). As an example of the relationships between climatic conditions and seawater temperature, the Pacific decadal oscillation (PDO) and El-Nino/Southern Oscillation (ENSO) are both related to sea surface temperature (SST) around Japan (Nakamura et al., 1997; Gordon and Giulivi, 2004).

From a marine ecological viewpoint, variations in water temperature can also result in a change in species composition, distribution, productivity, and mortality of marine organisms. For example, the fish community structure has changed with variations in seawater temperature related to climatic regime shifts in the Sea of Japan (Tian et al., 2006). The latitudinal shift of fish distributions occurred corresponding to the warming trend in seawater temperature in the North Sea (Perry et al., 2005). The phytoplankton concentration in the North Pacific has declined since the 1900s (Boyce et al., 2010). The variations in water temperature is also known to have an influence in a smaller scale. A significant shift in the composition of coral species has occurred in Daya Bay, located in the northern part of the South China Sea between 1977 and 1993, corresponding to the increase in winter SST (Chen et al., 2009). The winter-spring phytoplankton bloom has declined over the last two decades due to the warming of water temperature in the Bay of Calvi, located in the northwestern Mediterranean Sea (Goffart et al., 2002). Cook et al. (1998) found that SST in Chesapeake Bay showed a significant warming trend in winter during the 1950s–1990s, which resulted in the outbreak of *Perkinsus marinus* epizootic in the northeastern United States. These studies suggest that the warming of seawater temperature commonly occur and is possibly caused by global climate change.

Several studies have been conducted on the long-term variations in seawater temperature in the coastal seas of Japan (Tomosada, 1994; Noguchi, 2001; Yamamoto, 2003). Productions of laver culture and shellfish fisheries in Tokyo Bay have declined since the 1960s. Regarding this phenomenon, Ishii et al. (2008) suggested that SST in Tokyo Bay during 1948

–2005 decreased in summer and increased in autumn–winter, and speculated that the decline of laver culture production was possibly caused by the increase in the water temperature in autumn–winter. In contrast, Ando et al. (2003) pointed out that these phenomena in Tokyo Bay could have been caused by an increase in the inflow from outer ocean characterized by colder water in summer and warmer water in winter than water inside of the bay. Similarly, SST in Fukuoka Bay tended to decrease in April–August and increase in September–March from 1975 to 2001 (Kondo et al., 2005). They showed that these trends could have been a result of the enhancement of estuarine circulation in summer and increased SST in the open ocean in winter. These previous studies imply that long-term trends of SST decrease in summer and increase in winter occurs in broad area. Quantitative explanation of the long-term temperature change has not been revealed in the coastal ocean because of the complexity of the environments. In addition, considering those spatially common phenomena, it is expected that those phenomena might be caused by large-scale atmospheric changes, and global climate change is a key factor controlling SST variations even in coastal waters.

1.2 Physical and biological characteristics of the East China Sea

The East China Sea (ECS) is known as one of the highest productivity zones in the Large Marine Ecosystems (LMEs, Sherman et al., 2009). This high productivity is supported by the freshwater discharges from Yangtze River (Gong et al, 2006). A number of commercially valuable fisheries resources therefore inhabits this sea, and the area has an important role as spawning and nursery grounds for many fishes such as yellowtail (*Seriola quinqueradiata*), jack mackerel (*Trachurus japonicus*) and Japanese common squid (*Todarodes pacificus*) (Murayama 1991; Yoda et al., 2004; Hatanaka et al., 1967). The western Kyushu is located in the continental margin of the ECS, and the hydrodynamics is strongly influenced by the Kuroshio and the Tsushima Warm Current (Katoh et al., 1996). This local region is important for the fish growth and survival because the Kuroshio and the Tsushima Warm Current transport larvae and juveniles from the southern spawning ground to the waters off western Kyushu (Sassa et al., 2006; Okazaki and Nakata, 2007).

It is also noted that the area is one of the fastest warming oceans in the LMEs (Belkin, 2009), and the SST in the ECS has increased by 0.6˚C since the 1960s (Fig. 1.1). In addition, this sea is also regarded as the area where the human impact on marine ecosystems is large (Halpern et al., 2008). Therefore, the signs of the changes in the marine ecosystems are likely

to appear earlier than the other seas, and hence it is urgent to recognize the mechanism of the responses of fisheries resources to the climate change in the ECS and its marginal seas. Omura Bay, located in northwestern Kyushu is characterized by enclosed sea. It has been pointed out that fisheries catch of pelagic and demersal fishes in the bay has decreased since the 1970s (Nagasaki Prefecture, 2006). In addition, recent outbreaks of red tides of the dinoflagellate *Heterocapsa circularisquama* that originates from tropical ocean, could damage the oyster cultures in this bay. These problems are possibly due to environmental degradation. However no studies have reported the long-term environmental condition changes in the bay, and therefore its effect on the fishery resources also remained to be delineated.

1.3 Climate change and fisheries resources

Since the fisheries resources are highly vulnerable to the environmental changes in the ocean (Brander, 2010), mechanisms of fluctuations in fisheries resources needs to be understood for the sustainable fisheries management (Perry et al., 2010). In the western coast of Kyushu, Japanese anchovy (*Engraulis japonicus*) is one of the most important commercial fisheries resources. In the coastal waters around Japan, the anchovy population consists of three major stocks, namely the Pacific stock, the Tsushima Warm Current stock and the Seto Inland Sea stock (Zenitani et al., 2007). Anchovy off the western coast of Kyushu are classified as the Tsushima Warm Current stock, and have been harvested using purse-seine mainly targeting juvenile and immature stages (Tanaka et al., 2010). The annual catch of juvenile and immature anchovies in Nagasaki Prefecture exceeds 50 thousand tons (Fig. 1.2).

It is well known that anchovy has exhibited multi-decadal fluctuations (Kawasaki, 1983; Lluch-Belda, 1989) synchronizing with ocean-climate regime shifts (Schwartzlose et al., 1999; Chavez et al., 2003). One possible explanation is “optimal growth temperature“ hypothesis proposed by Takasuka et al. (2007). The variation in ambient temperature induced by oceanic regime shifts could regulate the stock fluctuations through the growth and survival of larvae. In the western North Pacific, fluctuations in abundance of small pelagic fishes such as the Japanese anchovy, the Japanese sardine (*Sardinops meranostictus*) and the Japanese jack mackerel are known to correspond to PDO (Takasuka et al., 2008).

In the waters off northwestern Kyushu, the spawning of anchovy typically occurs from March to May with a peak in April in the Goto-Nada Sea (Yamashita, 1984), and eggs and larvae are gradually dispersed to the northern area. Furthermore, Tanaka et al. (2010) have

investigated the origin of larval anchovy caught in coastal fishing ground in Nagasaki Prefecture by analyzing carbon and nitrogen stable isotope ratios, and suggested that the spring-spawned anchovy larvae originate from the offshore region, and migrates, or are transported, to the nearshore fishing areas. It is assumed that spring-spawning anchovy has a reproductive strategy utilizing the offshore warm water as a spawning ground and the inshore food-rich water as a nursery ground (Kozasa, 1975). Thus, the disruption of the connectivity between spawning and nursery grounds could exert a serious influence on their successful recruitment (Gaines and Bertness, 1992; Cowen and Sponaugle, 2009). Of multiple factors affecting fish recruitment, the transport process during early life stages could be a crucial factor particularly in the regional scale. Therefore, the transport process would be one of the important factors controlling their recruitment variability. This species also has an important role in the marine ecosystems as a food source for predatory fishes (Yamanaka et al., 1963), and hence the fluctuation in anchovy stock would have a major influence on the other species population dynamics.

Intergovernmental Panel on Climate Change (IPCC) announced that the warming trend in global climate system is now an undisputed fact and the human activities probably would be main factor explaining the observed warming trend in the 21th century (IPCC, 2013). Global warming certainly affects marine ecosystems, and several studies have been projected to clarify various effects of global warming on fish recruitment (Stenevik and Sandby, 2007; Lehodey et al., 2010). However, future fluctuation in the fisheries resources in the regional seas is still unclear.

1.4 Objectives and structure of the following chapters

The aims of this study are to clarify the effects of climate change on the coastal ocean environment and to investigate its influence on the Japanese anchovy as a proxy of important fisheries resources, which is responsive to climate change. In Chapter 2, long-term change in ocean-atmospheric changes in Omura Bay is investigated with a special interest of relationship with large-scale climate change. In Chapter 3, an influence of environmental change such as the seawater temperature and wind on the anchovy catch is investigated. In Chapter 4, the transport process of anchovy eggs and larvae is examined using a coupled hydrodynamic and particle tracking model. After investigating the present climate and fisheries resources relationship, future projection of the regional ocean and climatic changes, and its impact on

fisheries resources are discussed focusing on transport conditions and biological factors in Chapter 5. Based on the results obtained throughout this study, the impacts of climate change on regional ocean environment and fisheries resources are discussed in Chapter 6. Contributions of this study to the natural environmental science and future works are also discussed.

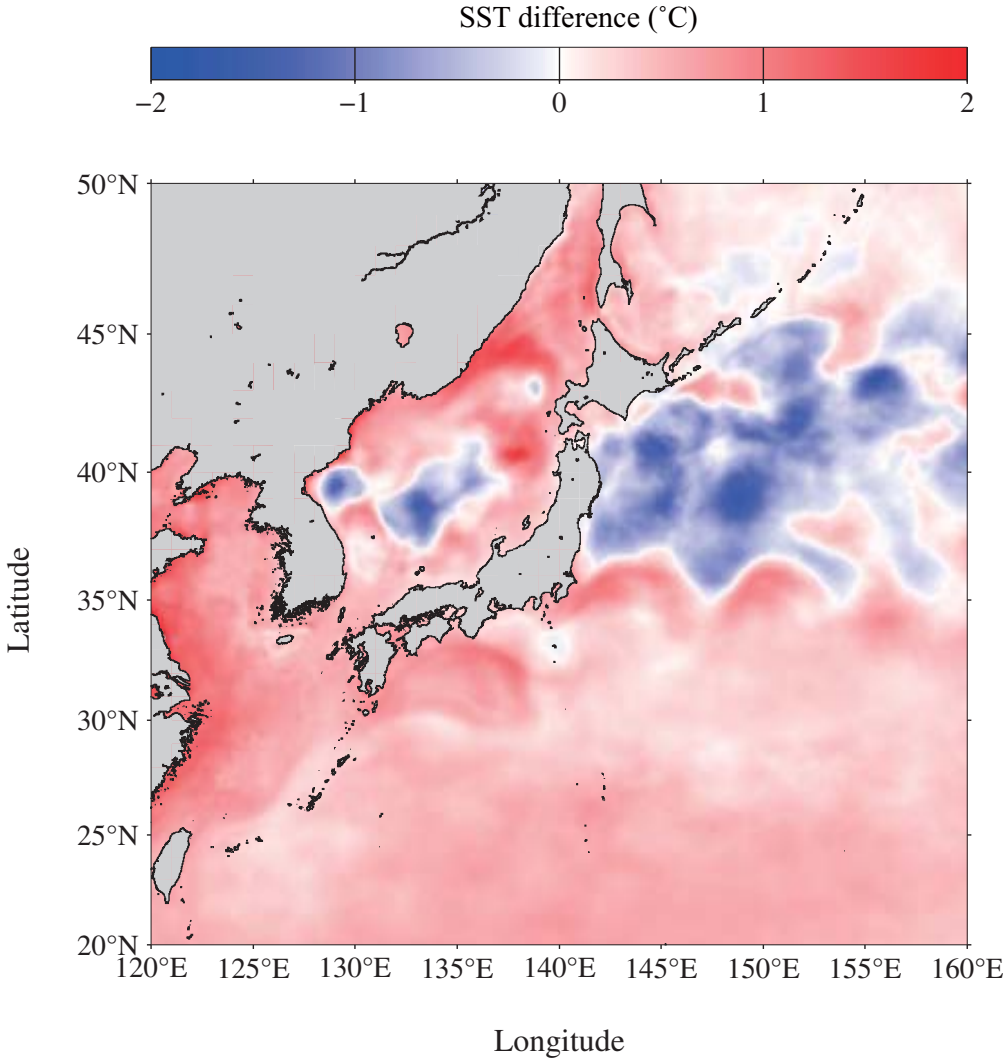

Fig. 1.1 Horizontal distribution of the SST difference between 1960s and 2000s around Japan based on the hindcast data of the Ocean General Circulation Model for the Earth Simulator.

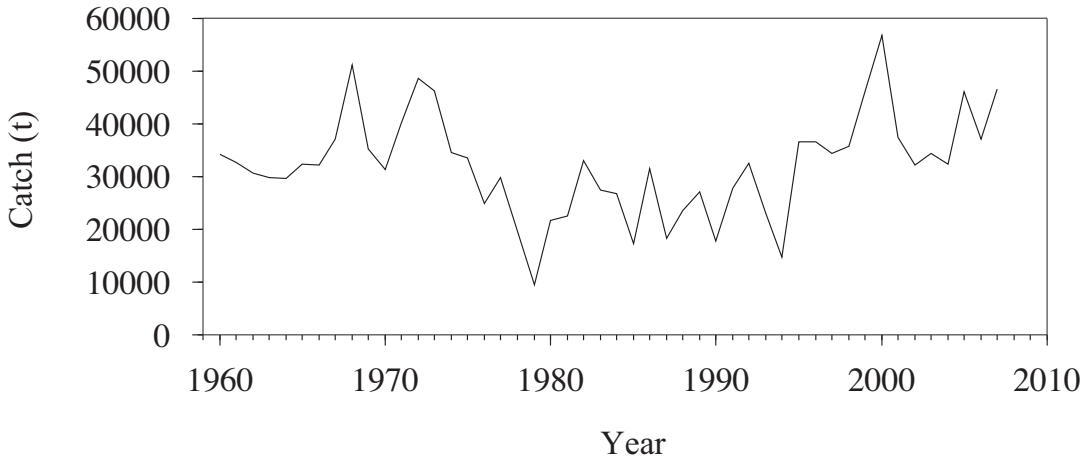

Fig. 1.2 Times series of the total catch of Japanese anchovy in Nagasaki Prefecture.

Chapter 2

Long-term trends in ocean-climate conditions in coastal sea

Seawater temperature is one of the determinant factors that influence on the distribution, growth and survival of marine organisms. For the understanding of fluctuation mechanism of fisheries resources, seawater temperature variation and its controlling factor should be revealed. In this chapter, to clarify the effect of climate change on the physical environment in the coastal sea, long-term SST variation in Omura Bay was investigated. In particular, the controlling factors of the long-term SST variations were clarified through the sea surface heat balance analysis. The relationship between regional ocean-climatic conditions and global climate change is discussed.

2.1 Data and methods

2.1.1 Study site

Omura Bay is an enclosed bay located in the central Nagasaki Prefecture, Japan (Fig. 2.1). The width and length of the bay are approximately 10 and 26 km, respectively. The area and average depth of the bay are approximately 320 km^2 and 14.5 m, respectively (Iizuka and Min, 1989). The bay is connected to neighboring Sasebo Bay and further to the ECS mainly through Hario Strait, a narrow passage with 200 m width and 30 m mean depth. This geographic feature causes quite small tidal transport and exchange of the seawater with the outer seas.

2.1.2 Seawater temperature and specific gravity

Seawater temperature and specific gravity were measured daily at 10 a.m. from January 1955 to January 1995 by the National Pearl Research Laboratory at a coastal station having a depth of 5.0 m (Fig. 2.1). Measurement depths were 0, 0.5, 1.0, 2.0 and 3.0 m. Missing data were inserted into the data set using linear interpolation. This study focused on SST for the following analysis. The SST data in the north part of the ECS (refer to http://www.data.kishou.go.jp/kaiyou/shindan/a_1/japan_warm/japan_warm.html) in summer and winter during the period of 1900-2009 were obtained from the Japan Meteorological Agency (JMA).

2.1.3 Climatic and meteorological data

Meteorological data, such as air temperature, solar radiation, wind speed, amount of cloud, atmospheric pressure, vapor pressure, and sea level pressure (SLP), were obtained from the Nagasaki Marine Observatory, JMA (Fig. 2.1). The daily averaged data for 34 years from January 1961 to December 1994 were used for estimating the sea surface heat balance. To investigate the influence of global climate change on the SST variations in Omura Bay, the monsoon circulation over East Asia was also examined. The East Asian summer monsoon index (EASMI) was used for the analysis in summer (June–August). EASMI is defined as the normalized zonal wind shear between 850 and 200 hPa averaged over 20˚–40˚N and 110˚–140˚E in summer (Han and Wang, 2007). The 2.5˚ × 2.5˚ square grids supplied by the National Centers for Environmental Prediction/National Center for Atmospheric Research (NCEP/NCAR) was used for calculation of the EASMI. EASMI was then compared with the mean summer wind speed, the air temperature and SST in Omura Bay. As for the effect of the winter (December–February) monsoon circulation, the East Asian winter monsoon index (EAWMI) proposed by Watanabe (1990) was used for the analysis. This index is characterized by a strong northwesterly wind, and it is defined as the difference in SLP between Irkutsk, Russia, and Nemuro, Japan. The monthly average SLP data at Irkutsk and Nemuro were also obtained from NCEP/NCAR. Similar to the analysis of EASMI, EAWMI was compared with the mean winter wind speed, the air temperature, and SST.

2.1.4 Methods for calculating sea surface heat balance

In order to detect factors affecting the SST variations, the heat balance analyses for August and January were conducted. Heat exchange through the atmosphere–ocean interface is given as follows. The net heat flux (Q_{NET}) consists of the incoming shortwave radiation flux (Q_{SW}) and the outgoing flux from the sea surface to the atmosphere such as the longwave radiation flux (Q_{LW}), latent heat flux (Q_E), and sensible heat flux (Q_H). It should be noted that positive values of Q_{SW} represent the downward flux to the sea surface, while negative values of Q_{LW}, Q_E and Q_H are upward fluxes representing heat loss from the sea surface to the atmosphere.

The sea surface absorption of shortwave radiation flux Q_{SW} (W m^{-2}) is estimated as follows,

$$Q_{SW} = S(1-\alpha) \tag{2.1}$$

where S (W m^{-2}) is the observed solar radiation at Nagasaki, α is the albedo at the sea surface. The α values of 0.06 and 0.09 were used in August and January, respectively (Budyko, 1956). Net flux of the longwave radiation Q_{LW} (W m^{-2}) is represented by the difference between the incoming and outgoing longwave radiations from the atmosphere and the sea surface. This flux is estimated by a following equation (Clark et al., 1974),

$$Q_{LW} = -\varepsilon\sigma T_S^4(0.39 - 0.00495e^{1/2})(1 - kC^2) - 4\varepsilon\sigma T_S^3(T_S - T_A) \tag{2.2}$$

where T_A and T_S are absolute air temperature and SST (K), respectively, and e is the atmospheric vapor pressure (hPa). C is the amount of cloud. Constants ε (= 0.98), σ (= 5.670×10^{-8} W m^{-2} K^{-4}) are the ratio of sea surface radiation to a black body, the Stefan–Boltzmann constant, respectively. k is the cloud coefficient which is a function of latitude, and 0.65 was applied with reference to Nakamura et al. (1989).

Q_E (W m^{-2}) is latent heat caused by evaporation, and Q_H (W m^{-2}) is sensible heat generated by the difference between water and air temperatures. Q_E and Q_H are calculated by bulk formulas as follows,

$$Q_E = -\rho_A L C_E(q_S - q_A)W \tag{2.3}$$

$$Q_H = -\rho_A C_P C_H(T_S - T_A)W \tag{2.4}$$

C_E and C_H are transfer coefficients of latent and sensible heat. These values are calculated considering its dependence on the wind speed and atmospheric stability proposed by Kondo (1975). The variable q_A denotes specific humidity, q_S denotes saturated specific humidity at seawater temperature and W denotes wind speed (m s^{-1}). It should be noted that the wind speed observed at Nagasaki Airport (Fig. 2.1) is generally 1.5–2.0 times stronger than that of observed at Nagasaki Marine Observatory due to the geographic feature of Omura Bay which is surrounded by mountains on west and east sides. Therefore, wind speed data observed at Nagasaki in each month was corrected by the regression analysis using wind speed at Nagasaki

Airport (available since January 1997). The coefficients of determination of the regression between wind data at Nagasaki Marine Observatory and Nagasaki Airport were 0.54–0.78 from January to December. ρ_A is density of the air expressed as a function of temperature and sea level pressure. Constant C_P (=1.006 × 10^3 J K^{-1} m^{-3}) is the specific heat at constant pressure. L is latent heat of evaporation which is dependent on the temperature.

$$L = (2.501\text{-}0.00237T_S)\times 10^{10} \tag{2.5}$$

From these equations, net heat flux Q_{NET} (W m^{-2}) is determined as follows,

$$Q_{NET} = Q_{SW} + Q_{LW} + Q_E + Q_H \tag{2.6}$$

Because of the limitation of available data, this calculation was conducted during 1961–1994 with a time step of one day.

Net heat budget at the seas surface consists of surface and horizontal fluxes, however, Hyodo and Gotoh (2000) estimated tidal exchange ratio of Omura Bay to be 0.2–0.4% per a tidal day using a numerical simulation. In addition, Hamada and Kyozuka (2001) also evaluated the value of tidal exchange ratio to be 5% per 10 days using a numerical model. Since horizontal heat transport could be quite small due to very small tidal exchange between the bay and outer seas, the horizontal heat exchange was neglected in the present analysis. In addition, because of the limitation of available data, long-term change in the effect of vertical mixing was not discussed in this study.

2.2 Results

2.2.1 Long-term variations in seawater temperature

The long-term variations in SST in Omura Bay were in the range of 4.7–32.3˚C with an averaged SST of 18.4˚C during 1955–1995 (Fig. 2.2). Monthly averaged SST reached a maximum in August (28.6˚C) and a minimum in February (8.3˚C), as shown in Figure 2.3. Hereafter, heating and cooling periods are defined as periods from March to August and from September to February, respectively according to the annual cycle of heat flux. Definitions of the heating and cooling periods are described in some detail in a later section.

The SST trends determined by linear regressions revealed a decrease in the heating period and an increase in the cooling period except for September (Table 2.1). The rate of SST decrease in the heating period was highest in August (−0.020˚C year^{-1}, Table 2.1). SST in August decreased by approximately 0.8˚C over 40 years based on the regression line (y = −0.020x + 28.97, $R^2 = 0.05$, $p = 0.13$, Fig. 2.4a). In contrast, the highest rate of increase in SST in the cooling period occurred in January (0.028˚C year^{-1}, Table 2.1). The increase in SST of approximately 1.2˚C in January over 40 years was estimated from the regression line (y = 0.028x + 8.21, $R^2 = 0.10$, $p < 0.05$, Fig. 2.4b).

2.2.2 Sea surface heat balance

Annual cycle of heat fluxes and meteorological parameters averaged for 1961–1994 are described in Figure 2.5 and 2.6, respectively. Monthly averaged Q_{NET} reached a maximum in July and a minimum in November. Q_{SW} reached a maximum in July and a minimum in November, corresponding to the annual cycle of solar radiation (Fig. 2.6). The amount of outgoing heat such as Q_{LW}, Q_E and Q_H was higher in the cooling period than in the heating period, in response to annual cycle of air temperature, wind speed and vapor pressure (Fig. 2.6). Note that air temperature in August (27.6˚C) is lower than SST in August (28.6˚C) in this bay (Figs. 2.3 and 2.6). In this study, the heating period was defined as March to August and cooling period as September to February, based on the sign of the annul cycle of Q_{NET}. Long-term trend in Q_{SW} showed a significant decreasing trend in both August ($r_S = -0.492$, $p < 0.01$, Fig. 2.7a) and January ($r_S = -0.605$, $p < 0.01$, Fig. 2.7b). Decreasing trends in Q_E and Q_H were also found in both August and January (Figs. 2.7a and b), but only Q_E was significant.

To elucidate the factors controlling SST, correlations between Q_{NET} and each component of the heat flux were analyzed for both August and January. These results are summarized in Table 2.2. In August, Q_{NET} showed a significant positive correlation with Q_{SW} and negative correlations with Q_{LW}, Q_E, and Q_H. In January, no significant correlation was obtained between Q_{NET} and Q_{SW}, Q_{LW}, however, Q_{NET} was significantly negatively correlated with Q_E and Q_H, as shown in Table 2.2. As the results of comparison between SST and each heat flux, Q_{SW}, Q_E and Q_H showed significant correlations with the SST in August (Table 2.3). On the other hand, only Q_H showed a significant correlation with the SST in January.

2.2.3 Long-term trends in climatic and meteorological parameters

On the basis of the results of the heat flux estimation, the long-term variations in meteorological parameters, which could be particularly important in determining the variations in heat fluxes were further investigated. Figure 2.8 shows long-term variations in the meteorological parameters. Note that to detect the critical factors controlling SST, this study particularly focused on the meteorological parameters determining the heat flux variation. As mentioned in the previous section, Q_{SW}, Q_{LW}, Q_E and Q_H components of the heat flux showed significant correlations with Q_{NET} in August. In addition, solar radiation and the wind speed in August decreased by approximately 38.4 W m^{-2} ($y = -1.441x + 239.5$, $R^2 = 0.23$, $p < 0.05$) and 1.1 m s^{-1} ($y = -0.0325x + 4.8$, $R^2 = 0.37$, $p < 0.05$), respectively, during 1961–1994, as shown in Figure 2.8a.

In contrast, in January, Q_{NET} showed significant correlations with Q_E and Q_H (Table 2.2). As shown in Fig. 2.8b, the air temperature in January increased by approximately 1.65˚C ($y = 0.050x–5.638$, $R^2 = 0.11$, $p = 0.06$), while the wind speed in January decreased by approximately 2.0 m s^{-1} ($y = -0.062x + 6.1$, $R^2 = 0.51$, $p < 0.01$) during 1961–1994.

2.2.4 Relationship between East Asian monsoon circulation and wind

As mentioned in the previous section, the significant decreasing trend in the wind speed was detected in both August and January. The wind speed decrease observed at Nagasaki could be affected by changes in the large-scale atmospheric circulation. Thus, EASMI was compared with the mean summer wind speed observed at Nagasaki, the air temperature and SST. Long-term variations in EASMI and the mean summer wind speed are shown in Figures 2.9a and b, respectively. It is clear that EASMI has decreased during 1955–1995, and the mean summer wind speed also tended to decrease, corresponding to the decrease in EASMI. Moreover, EASMI showed significant correlations with the mean summer wind speed, the air temperature and SST, as shown in Figures 2.10a–c, respectively. As for winter, EAWMI was compared with the mean winter wind speed, the air temperature, and SST averaged from December to February. As the results, EAWMI also showed a decreasing trend during the study period (Fig. 2.9c), and the mean winter wind speed tended to decrease, corresponding to the decrease in EAWMI (Fig. 2.9d). It is evident from Figures 2.10d–f that EAWMI also significantly correlated with the mean winter wind speed, the air temperature and SST.

2.3 Discussion

In this study, it was revealed that SST in Omura Bay has decreased and increased in the heating period and cooling period during 40 years, respectively. In addition, sea surface heat balance analysis detected that solar radiation was a primary factor contributing to the SST variation in the heating period. Furthermore, the SST trend in the cooling period was primarily related to the trends in air temperature and the wind speed. These results indicate that the dominant process influencing the SST variation differs in the heating and cooling periods. In a previous study, Tanaka and Nakajima (1975) investigated the seasonal heat balance in the Hiuchi-nada Sea, located in the Seto Inland Sea, and pointed out that the shortwave radiation flux was the dominant factor in the variation of water temperature in summer, whereas latent and sensible heat fluxes controlled the SST variation in winter. Ishii and Kondo (1987) also studied seasonal variations in sea surface heat balance in the ECS and found that solar radiation and horizontal heat transport played a primary role in the heating process in summer, and latent and sensible heat fluxes became dominant in the cooling process in winter.

Based on the above mechanism of SST variation, it is suggested that in Omura Bay, the SST in August was closely associated with the reduction of solar radiation, further indicating that sunlight reduction caused the SST decrease in the heating period because of reduction of incoming heat. In fact, extremely low shortwave radiation was detected in 1980 and 1993 (Figs. 2.7a and 2.8a), and the lowest and the second-lowest SST were observed in Omura Bay during these two years (Fig. 2.4). Another factor contributing to the SST variation in August was wind speed. A significant decreasing trend in the wind speed was detected in August. This trend can be explained by the effect of EASM. The EASM circulation is mainly driven by pressure gradients between the high pressure over the South China Sea and the western North Pacific and the low pressure over East Asia (Ding, 1994). Xu et al. (2006) reported that the decreasing trend in the wind speed was consistent with the weakening of EASM over China during 1969–2000. Li et al. (2010) showed that an interdecadal warming trend in SST in the tropics of the central and eastern Pacific is the primary cause of the weakening of EASM. An obvious decreasing trend in the mean summer wind speed was detected in summer in this study, and the mean wind speed, the air temperature and SST in summer were positively correlated with EASMI. These results imply that the weakened EASM circulation potentially causes the SST increase through heat accumulation at the sea surface due to the decrease in the wind speed during summer. In order to quantitatively verify the potential effect of those changes in

meteorological conditions on SST variation, the SST change between 1961 and 1994 was calculated. The calculated SST ($T_{cal.}$) can be estimated by the following equation.

$$T_{cal.} = T_{ini.} + \frac{Q}{\rho C_{PW} h} \tag{2.7}$$

The initial temperature ($T_{ini.}$) for August and January are defined as the SST in preceding month such as July and December, respectively. σ_S (kg m^{-3}) is the seawater density averaged for 34 years, the value of 1019 and 1025 are used for August and January, respectively. Specific heat of seawater C_{PW} is 4.2 × 10^3 J kg^{-1} K^{-1}. The depth of the turbulent mixing layer (h) in Omura Bay in summer is assumed to be 7.5 m in August according to Nakamura and Furushima (2000), and 14.5 m in January assuming the vertical mixing to the bottom. Q (W m^{-2} day^{-1}) is the amount of the heat at the sea surface. Since this study focuses on the effect of the meteorological factor primarily contributing variation in heat flux, the sum of Q_{SW}, Q_{LW}, Q_E and Q_H was substituted Q in August, whereas the sum of Q_E and Q_H was applied to Q in January, based on the results of the correlation analysis (Table 2.2). Using Eq. (2.6), $T_{cal.}$ in August 1961 was estimated to be 31.52˚C, whereas 30.37˚C in August 1994 (Table 2.3). Thus, the decrease in the SST in August was estimated to be 1.15˚C for obtaining the decrease of 17.62 W m^{-2} due to the greater decrease of Q_{SW} than Q_E and Q_H. This simple estimation indicates that change in the amount of the surface heat alone potentially have the effect of lowering SST approximately 1.0˚C during 34 years. Although this analysis could not estimate the contribution of horizontal heat exchange on SST change in Omura Bay, Ishii and Kondo (1993) suggested the dominant contribution of the horizontal heat transport in summer in the ECS, thus discrepancy between estimated SST change (-1.15˚C) and observed value (-0.70˚C) might be occurred by neglect of horizontal heat exchanges.

In contrast, the increasing trend in SST in January was largely associated with the increase in the air temperature. The decrease in the wind speed also contributed to the increase in SST through the decrease in the amount of heat loss from the sea surface to the atmosphere as latent heat and sensible heat. The possible reason for the increase in the air temperature and the decrease in the wind speed is the weakened EAWM circulation, which covers the mid-latitudes of the western North Pacific, including Japan (Yasuda and Hanawa, 1999).

Watanabe (1990) showed that EAWMI has a significant negative correlation with winter SST in the western part of the mid-latitudes of the North Pacific, and strong EAWM is associated with low SST in the northern part of the subtropical gyre in winter (Suga and Hanawa, 1995). Yeh and Kim (2010) showed a warming trend in winter SST in the Yellow/East China Seas (YES) during 1950–2008. They reported that a decrease in the northerly wind associated with the weakening of EAWM could result in a decrease in the latent heat and an increase in SST in the YES. Furthermore, Hori and Ueda (2006) estimated the impact of global warming on the EAWM circulation with an atmosphere–ocean general circulation model. Under the global warming scenario, their model showed weakening of the EAWM circulation. Further, Xu et al. (2006) indicated that the decreasing trend in the wind speed and the increasing trend in the air temperature over China corresponded to the weakening of EAWM during 1969–2000. An obvious decreasing trend in EAWMI could potentially influence an increase in the air temperature and SST in Omura Bay through a decrease in the wind speed. A weakened EAWM circulation leads to weak winds and reduces the advection of cold air masses from Eurasia in winter, therefore, consequently the winter air temperature and SST become relatively high compared to the year in which EAWM is strong. In fact, extremely strong EAWM was observed in 1963, resulting in strong wind, a low air temperature, and low SST (Figs. 2.4b and 2.8b). Note that the SST continued to increase since 1987 causing warming trend in the SST, and this sudden change was triggered by the negative phase of EAWMI since 1987. These results indicate that the winter SST warming trend is largely associated with the large-scale atmospheric circulation. In the same manner as August, calculated SST was estimated to be 8.78˚C in January 1961, whereas 10.37˚C for January 1994 obtaining 28.19 W m^{-2} decrease in heat loss caused by the weakened wind speed (−2.0 m s^{-1}) and the increased air temperature (1.65˚C) between 1961 and 1994. Thus, SST increase in January was estimated to be 1.59˚C (Table 2.3), and this is almost consistent with observed SST increase 1.25˚C.

The increase in the SST has potential to impact on the biological and ecological perspective in the bay. The red tide caused by *Heterocapsa circularisquama* in Omura Bay was first recorded in 1995. Since this species cannot survive at 10˚C or lower (Matsuyama, 2004), SST rise in cooling period could benefit this species surviving during winter and make its red tide occurrence possible from summer to autumn. If the warm winter trend continues, red tide by *Heterocapsa circularisquama* would become a more serious concern for aquaculture industry such as pearl and oyster cultures in the bay.

The effects of large-scale climate change on SST variations are not limited only to Omura Bay. In fact, similar trends of SST in this bay have been reported in many coastal seas (e.g., Chen et al. 2009; Ishii et al. 2008; Kondo et al. 2005; Paraso and Valle-Levinson, 2009; Rouault et al., 2010). Moreover, the reduction of solar radiation was reported in a number of worldwide sites, for example, Germany, Russia, Turkey, Canada, Hong Kong, New Zealand, China and Japan as "global dimming" (Abakumova et al., 1996; Aksoy, 1997; Cutforth and Judiesch, 2007; Liepert et al., 1997; Liley, 2009; Sato and Takahashi, 2001; Stanhill and Kalma, 1995; Yang et al., 2009). In addition, using the Global Energy Balance Archive data, Liepert (2002) reported that solar radiation in the United States showed a decrease of 19 W m^{-2} during 1961–1990. Furthermore, they pointed out that this decrease in solar radiation was attributed to an increase in aerosol emission and evaporation caused by global warming. The increase in evaporation and aerosol emission could have a synergistic effect, leading to an increase in cloud cover and a decrease in sunlight. Wild (2009) described potential impact of increased regional aerosol emission on large-scale dimming through the intercontinental aerosol transport, therefore, observed decline of the solar radiation at Nagasaki during the1960s to the 1990s could be related to the global dimming (Fig. 2.11).

Although this study focused on the coastal bay, atmospheric conditions are able to impact on the entire ECS. Long-term variations in SST in the ECS in summer and winter during the period of 1900-2009 are shown in Figure 2.12. The SST in the ECS tended to increase both in summer (0.008˚C $year^{-1}$) and winter (0.016˚C $year^{-1}$), however, for the period of 1955–1995, which was analyzed in the present study, showed a decreasing trend in summer (-0.007˚C $year^{-1}$) and an increasing trend in winter (0.011˚C $year^{-1}$). These variations were significantly correlated with the SST in Omura Bay (Fig. 2.13). As expected, the SST in the ECS significantly correlated with the monsoon index both in winter and summer (Fig. 2.14). Therefore, SST variations in the ECS may also be regulated by the same mechanism indicated in Omura Bay.

In this chapter, long-term trends of the SST in Omura Bay and their possible causes were investigated by primarily using surface heat flux analysis. Although only a small tidal exchange occurs because of the narrow entrance of the bay, horizontal heat exchange between the bay and the outer seas is necessary for any future study to explore the interaction between the ECS and Omura Bay in more detail.

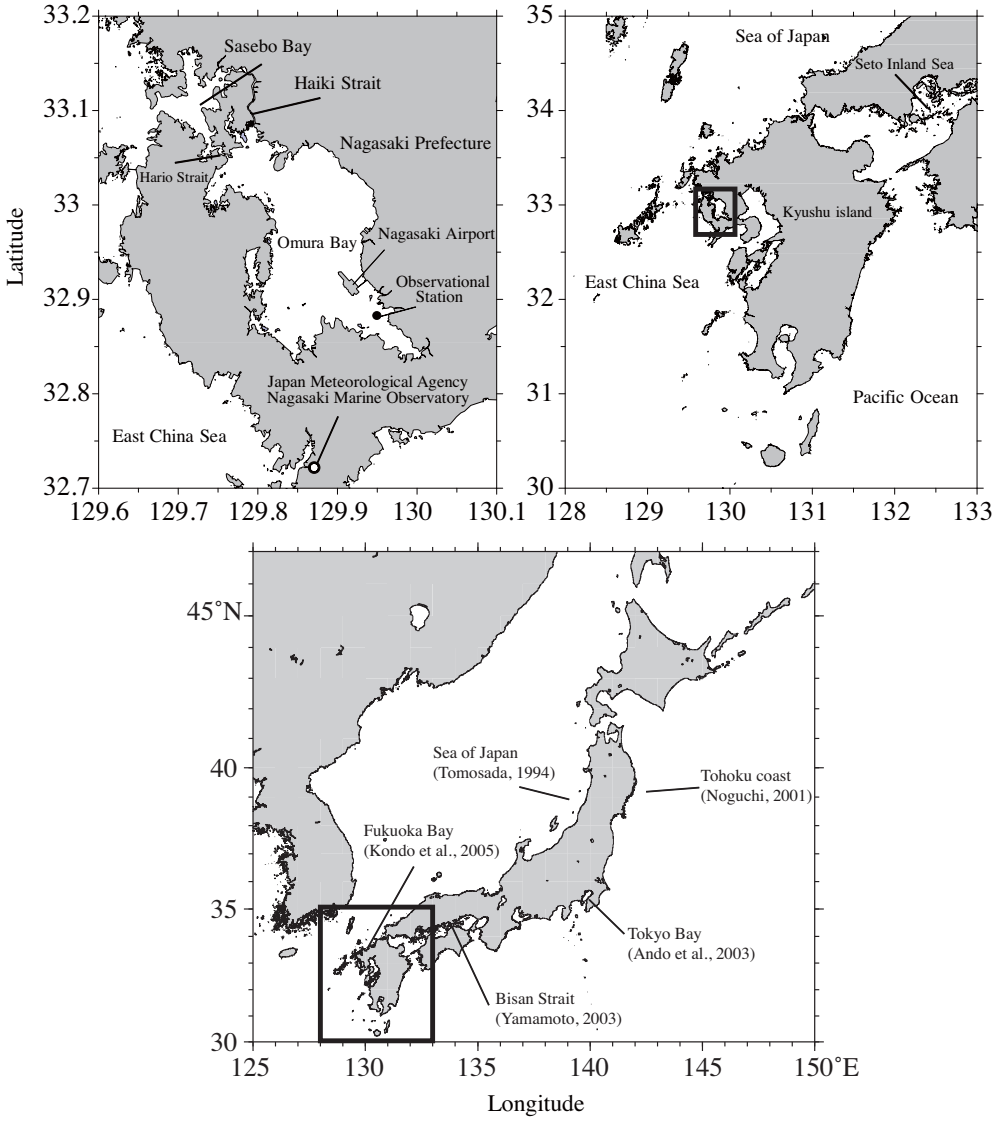

Fig. 2.1 Location of the study area including Omura Bay. The closed circle shows the observational station at which water temperature and specific gravity were measured during 1955–1995. The open circle shows the location of the Nagasaki Marine Observatory, Japan Meteorological Agency. References in the lower panel indicate previous studies reporting the SST trends.

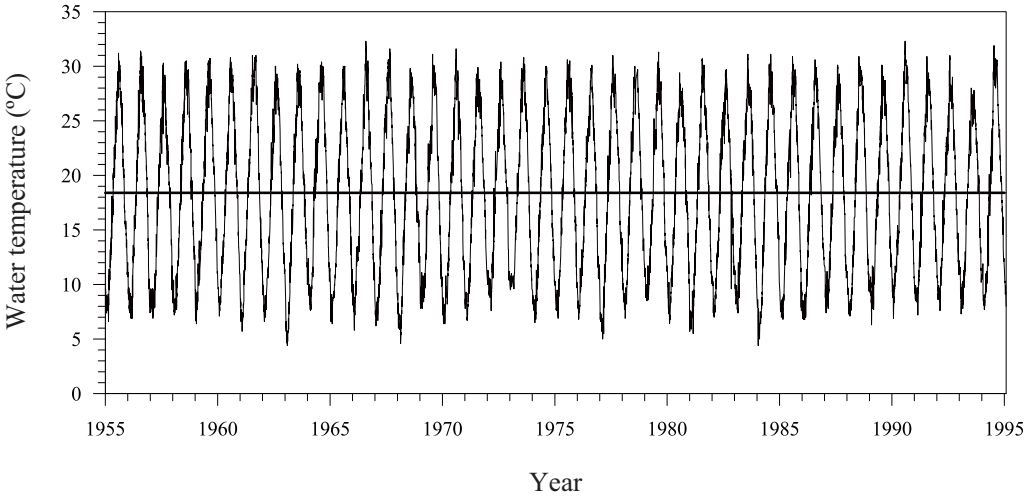

Fig. 2.2 Time series of daily SST during 1955–1995. A horizontal line shows the averaged SST (18.4˚C) for 40 years.

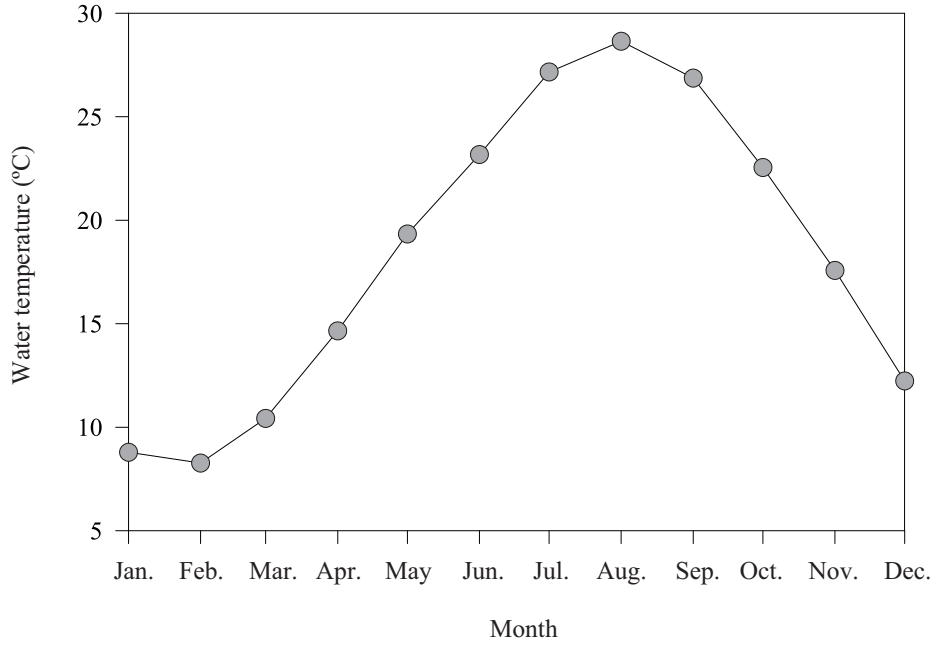

Fig. 2.3 Annual cycle of SST averaged for 1961–1994.

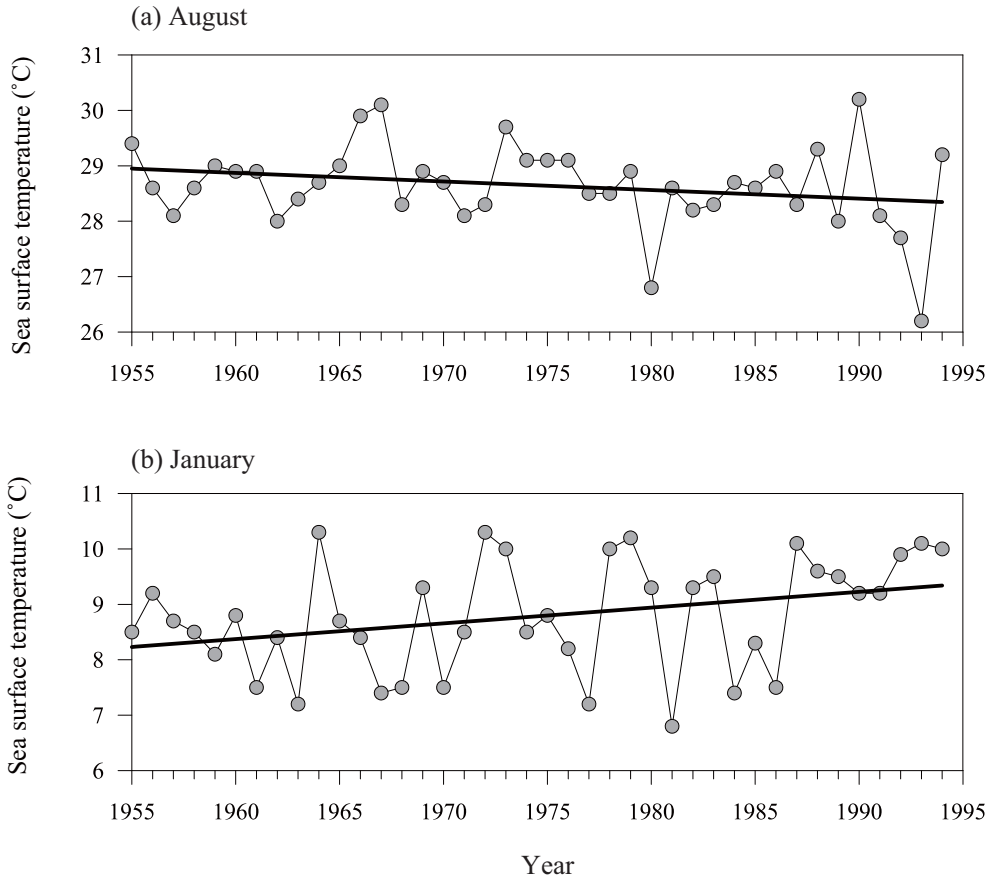

Fig. 2.4 Time series of monthly mean SST in August (a) and January (b) during 1955–1994. Bold lines show liner trends calculated by the method of least squares.

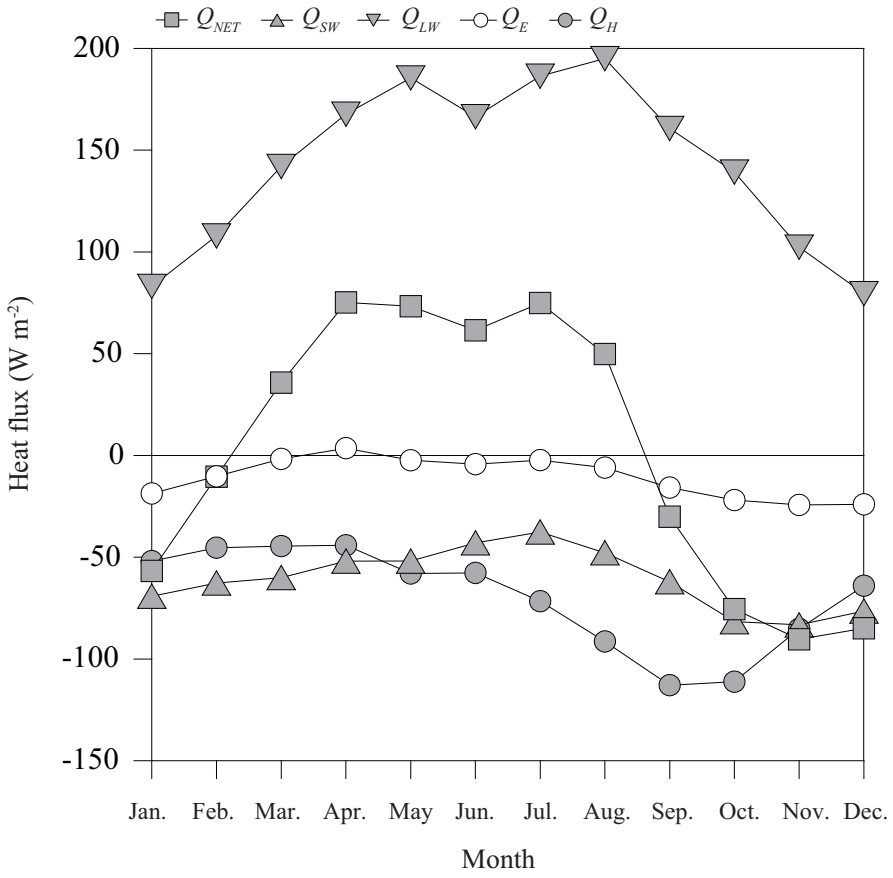

Fig. 2.5 Annual cycle of heat fluxes averaged for 1961–1994.

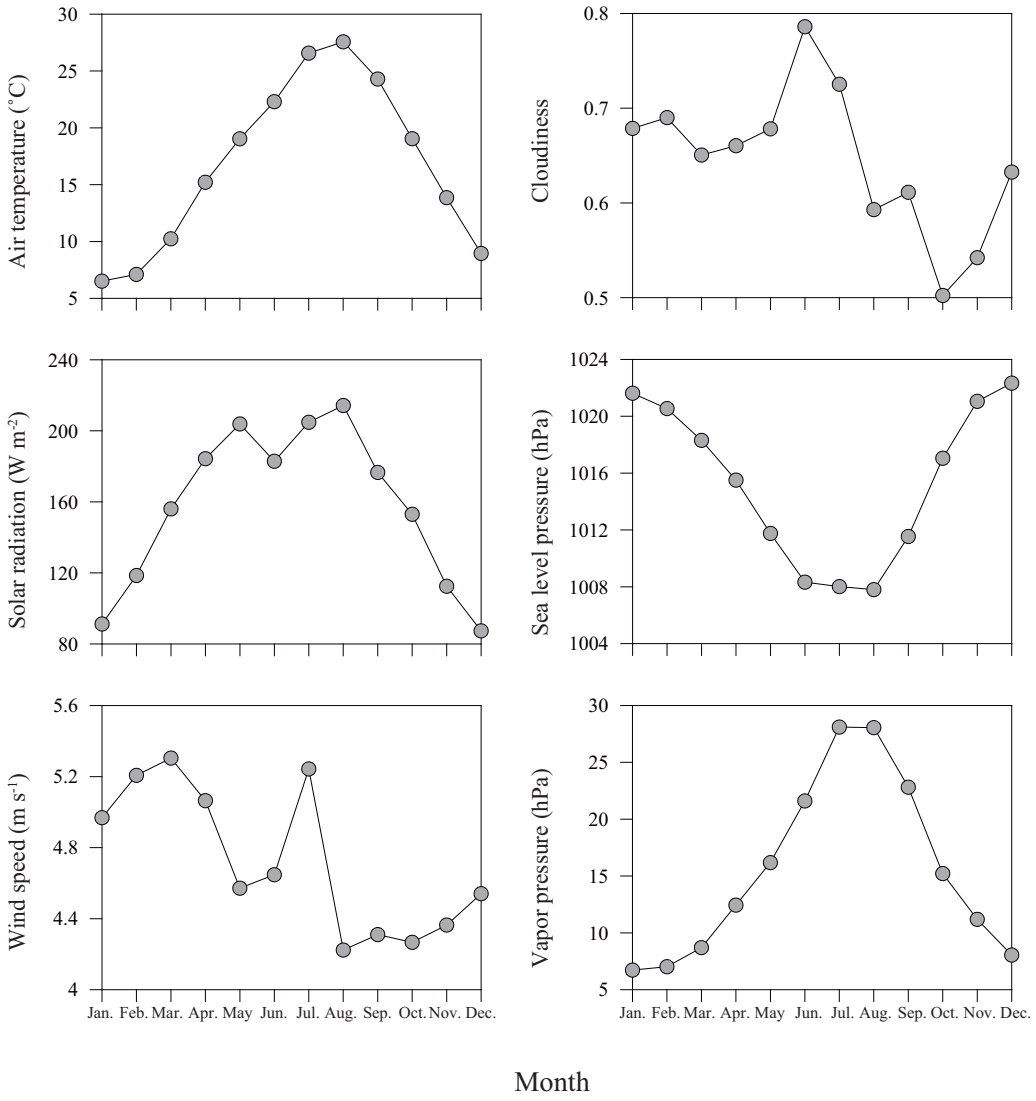

Fig. 2.6 Annual cycle of meteorological parameter averaged for 1961–1994.

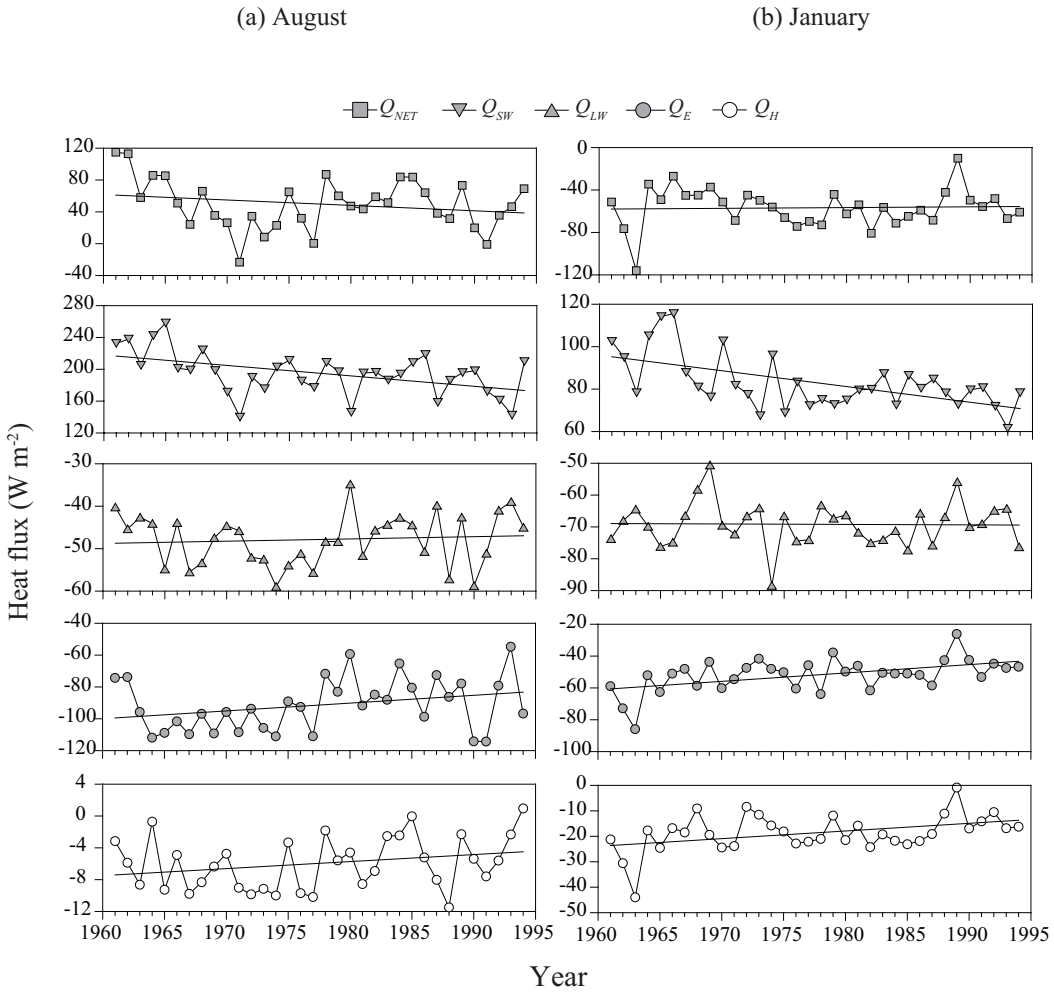

Fig. 2.7 Time series of monthly averages of heat fluxes in August (a) and January (b). Straight lines show liner trends calculated by the method of least squares.

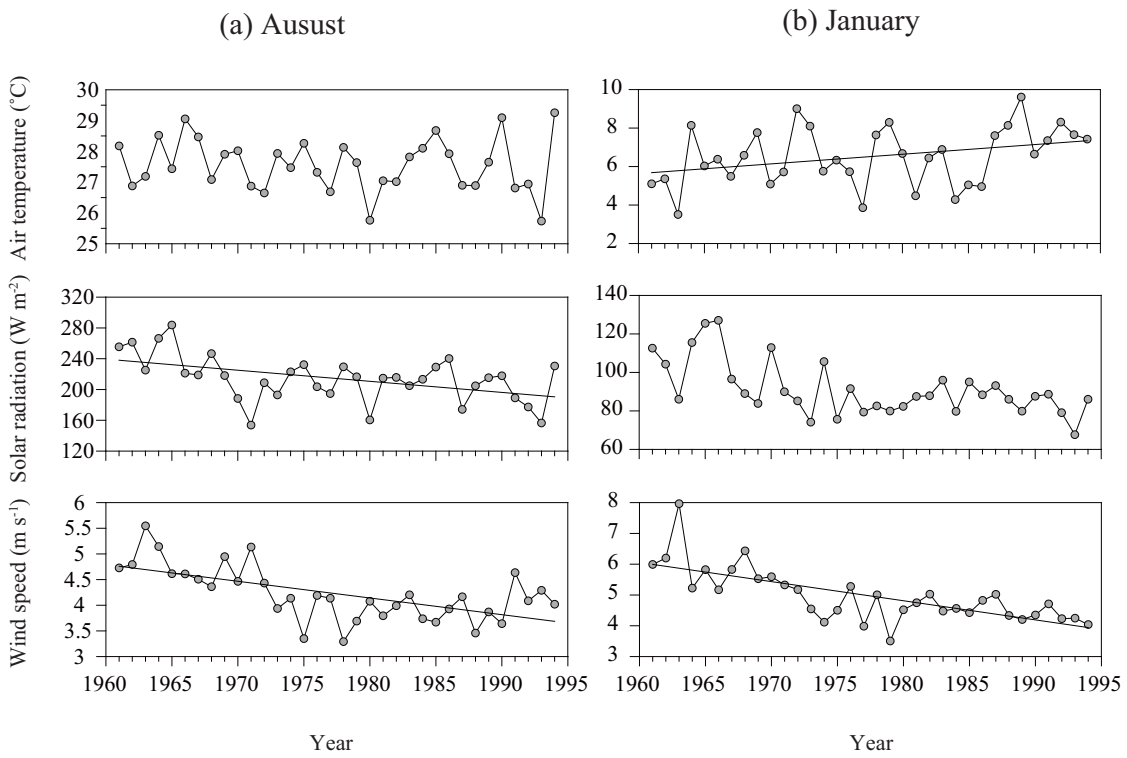

Fig. 2.8 Time series of monthly mean meteorological parameters (air temperature, solar radiation and wind speed) at Nagasaki Marine Observatory in August (a) and January (b) between 1955 and 1994. Regressions are fitted in parameters which could be important in determination of heat fluxes variation.

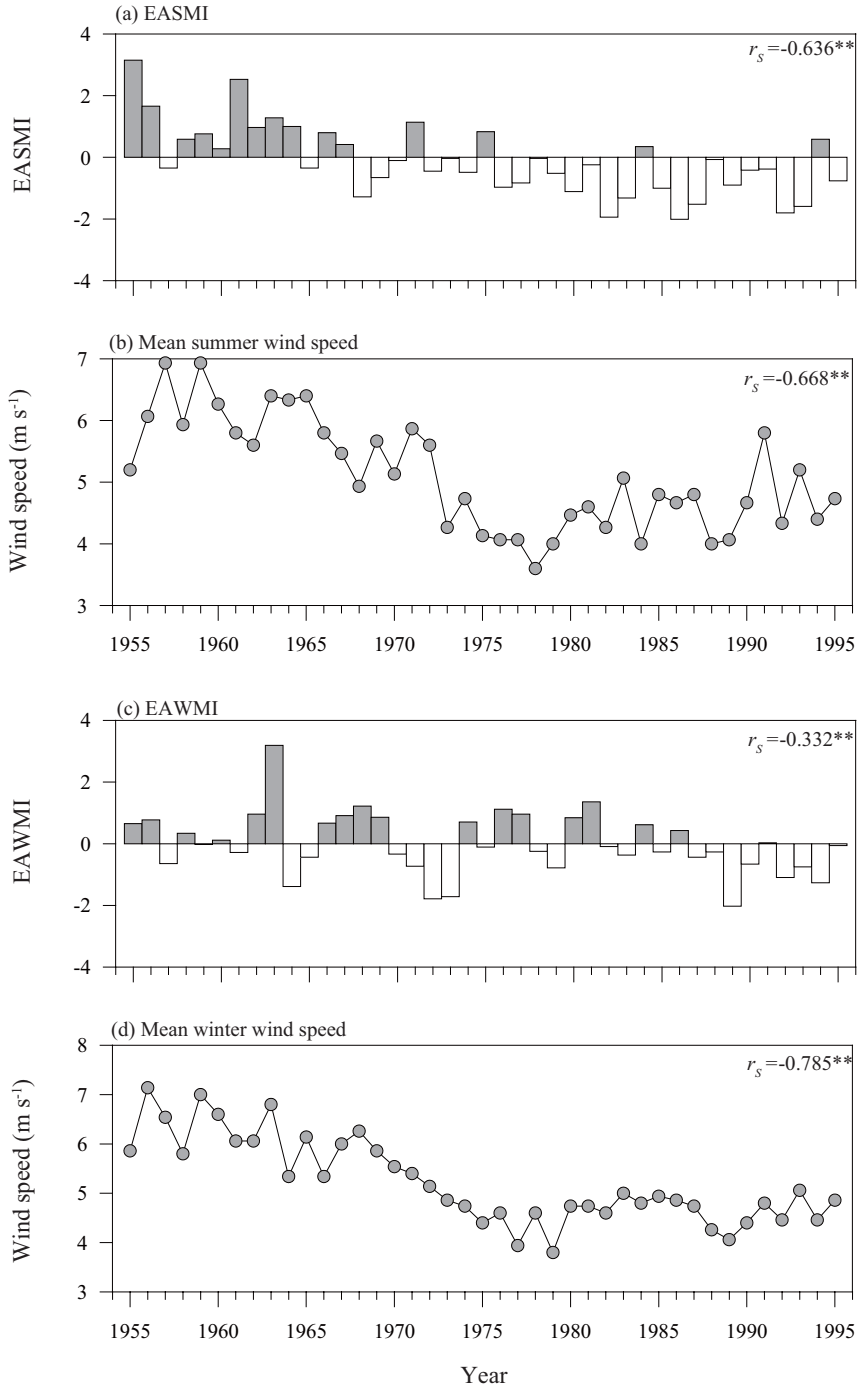

Fig. 2.9 Time series of the standardized East Asian monsoon index and seasonal mean wind speed during 1955–1995. East Asian summer monsoon index (EASMI) (a), mean summer wind speed (b), East Asian winter monsoon index (EAWMI) (c), and mean winter wind speed (d). ** represents $p < 0.01$.

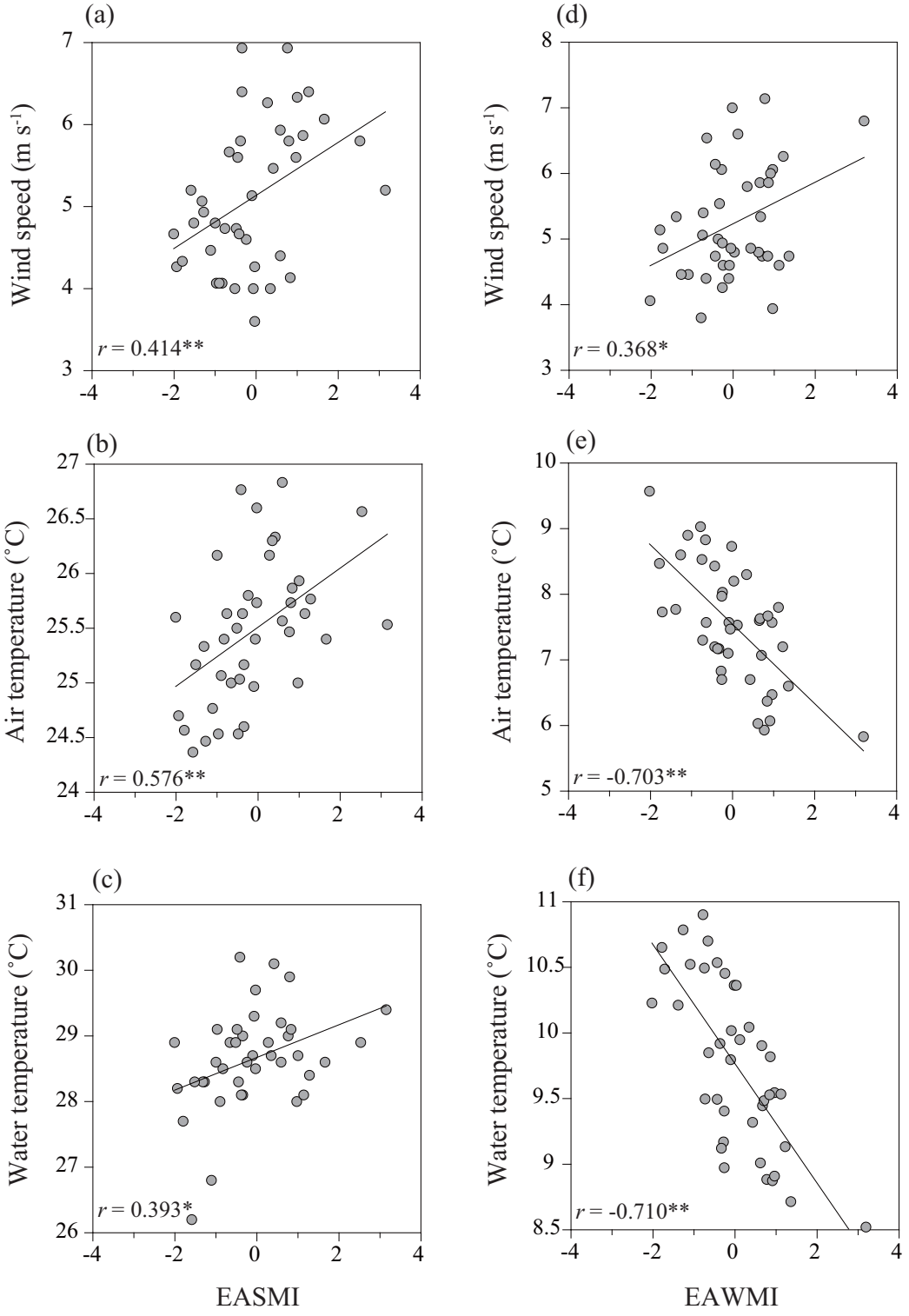

Fig. 2.10 Correlations between the East Asian summer monsoon index and mean summer wind speed (a), air temperature (b), and SST (c), and correlations between the East Asian winter monsoon index and mean winter wind speed (d), air temperature (e), and SST (f). ** and * represent $p < 0.01$ and $p < 0.05$, respectively. Straight lines show liner trends calculated by the method of least squares.

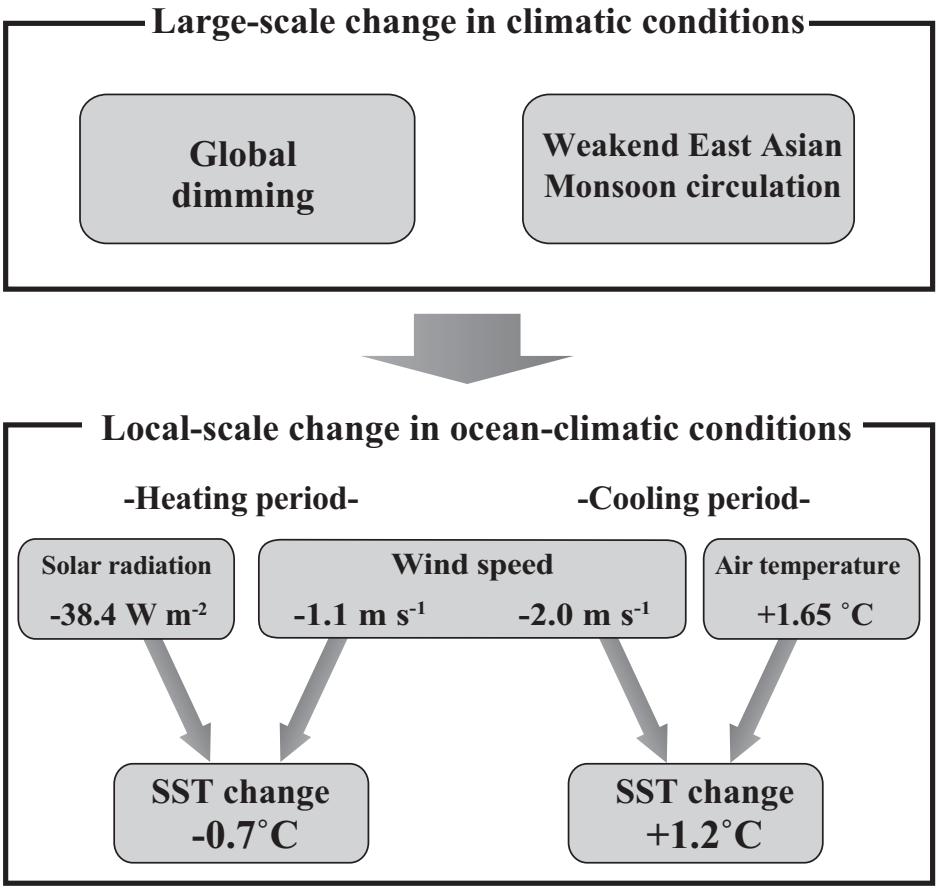

Fig. 2.11 Schematic diagram of the impact of large-scale climate change on local-scale oceanic-climatic conditions.

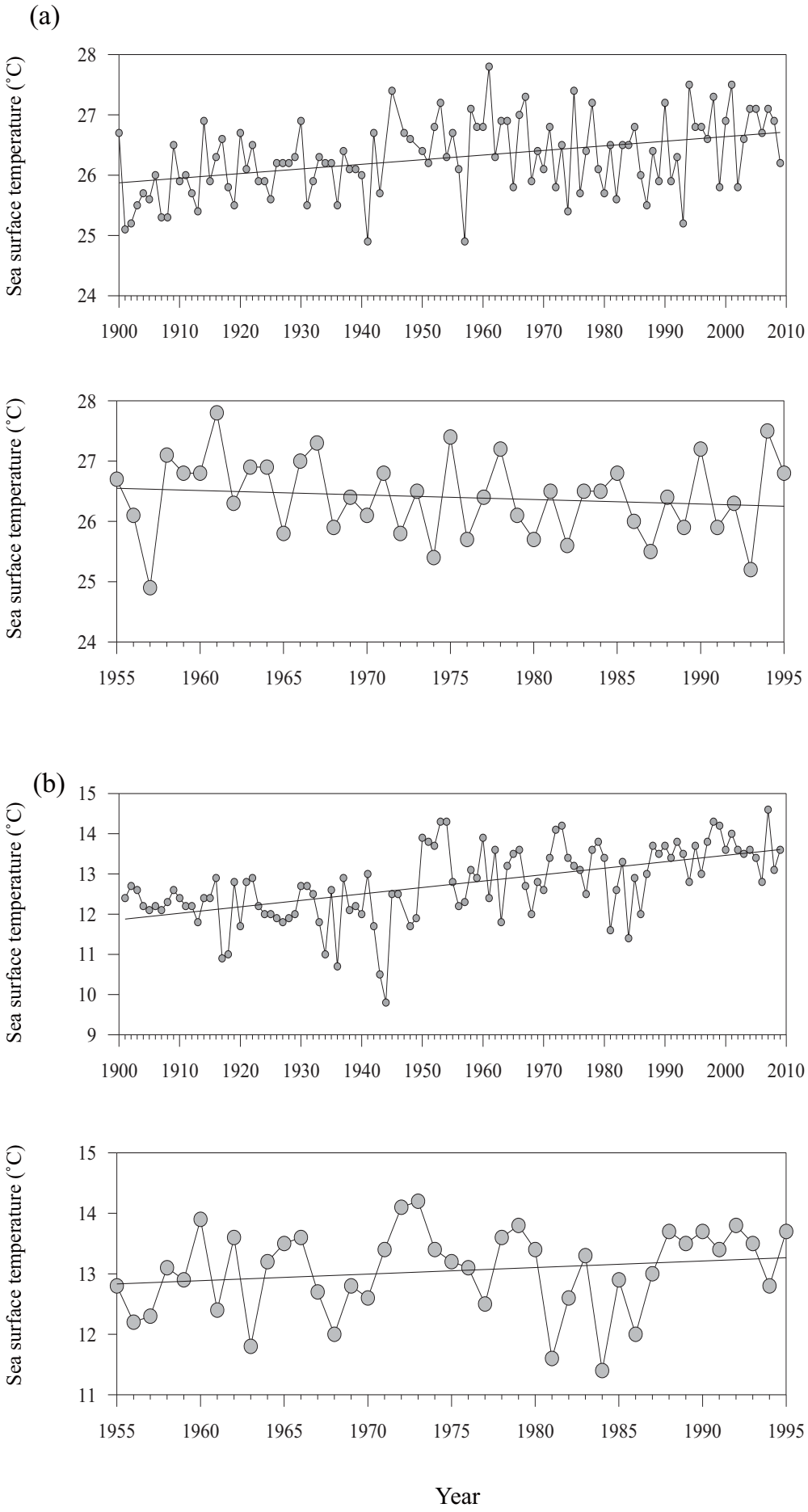

Fig. 2.12 Long-term variations in SST in the East China Sea during 1900-2009. summer (a) and winter (b). Straight lines show the regression.

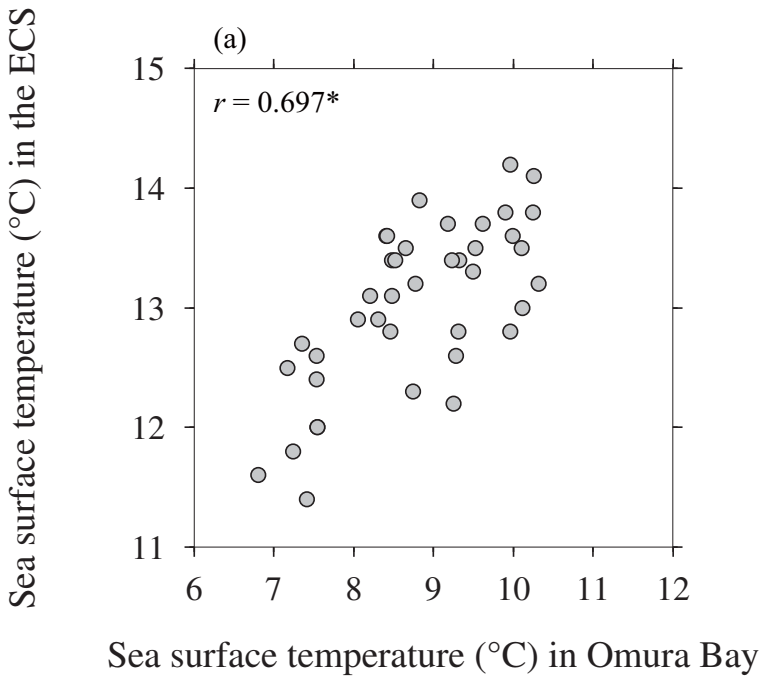

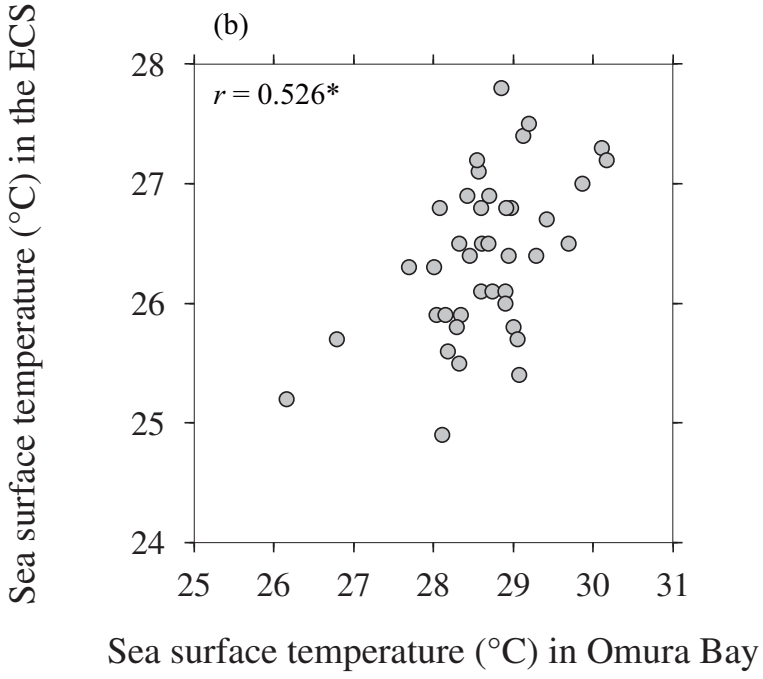

Fig. 2.13 Relationships between the SST in summer (a) and in winter (b) in the ECS and Omura Bay. * represents $p < 0.01$.

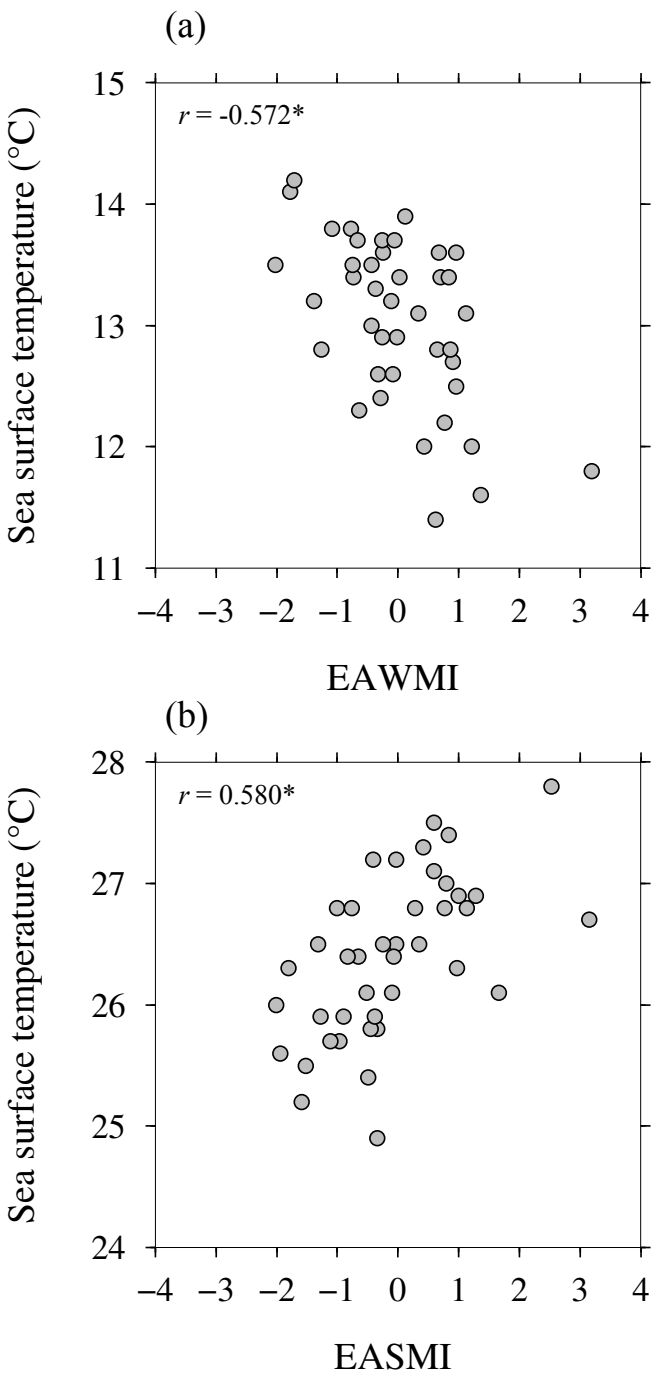

Fig. 2.14 Correlations between the East Asian summer monsoon index (EASMI) and the SST in the ECS in winter (a), and correlations between the East Asian winter monsoon index (EAWMI) and the SST in the ECS in summer (b). * represents $p < 0.01$.

Table 2.1 Rate of SST variation in each month during 1955–1994 and Spearman rank correlation coefficient r_S.

Month	Rate (˚C year^{-1})	Spearman rank correlation coefficient r_S
January	0.028	0.346*
February	0.010	0.129
March	-0.006	-0.058
April	-0.004	-0.022
May	-0.004	-0.068
June	-0.007	-0.195
July	-0.006	-0.069
August	-0.020	-0.185
September	-0.005	-0.078
October	0.008	0.187
November	0.005	0.076
December	0.010	0.105

*represents $p < 0.05$.

Table 2.2 Coefficient of correlation (r) between each heat flux and net heat flux (Q_{NET}).

	Heating period (Aug.)	Cooling period (Jan.)
Q_{SW}	0.706**	0.226
Q_{LW}	-0.352**	-0.252
Q_{E}	-0.490**	-0.736**
Q_{H}	-0.580**	-0.798**

**represents $p < 0.01$.

Table 2.3 Coefficient of correlation (r) between each heat flux and the SST.

	August	January
Q_{NET}	-0.020	0.120
Q_{SW}	0.441*	-0.242
Q_{LW}	-0.571*	0.018
Q_{E}	-0.546*	0.316
Q_{H}	-0.178	0.419*

* represents $p < 0.05$.

Table 2.4 List of the initial temperature ($T_{ini.}$), amount of heat (Q) and calculated temperature ($T_{cal.}$) in 1961 and 1994.

	August			January		
	$T_{ini.}$	Q	$T_{cal.}$	$T_{ini.}$	Q	$T_{cal.}$
1961	26.81	57.83	31.52	12.04	-78.78	8.78
1994	27.04	40.21	30.37	12.47	-50.59	10.37
1994-1961	0.23	-17.62	-1.15	0.43	28.19	1.59

Chapter 3

Effect of wind-stress on the fluctuation of the recruitment of Japanese anchovy

Japanese anchovy is an important fisheries resource in the western coast of Kyushu. Anchovy has a relative short life span (matures at age 1), and is known to spawn offshore waters and migrate inshore waters. The main food of anchovy is zooplankton, and both ambient temperature and food availability during their early life stages would be critical factors determining their recruitment. In the previous chapter, significant changes in the regional ocean-climate conditions related to the global climate change were identified. Of multiple climatic conditions, the importance of wind condition on the coastal ocean environment was suggested. The purpose of this chapter is to investigate the decadal fluctuations in regional anchovy catch and to reveal the fluctuation mechanism off northwestern Kyushu with a special interest in egg and larval transport process focusing on wind-induced currents.

3.1 Data and methods

3.1.1 Catch data

Annual anchovy catch data from 1960 to 2009 were derived from the Fisheries Statistical Yearbooks of the Ministry of Agriculture, Forestry and Fisheries. Abundance of the Tsushima Warm Current stock (from Niigata Prefecture to Kagoshima Prefecture) in 1977–2009 was derived from Kuroda et al. (2012). The stock abundance was estimated using cohort analysis and was compared with the total catch in Nagasaki Prefecture for evaluating the usefulness of the annual catch data as the stock abundance. The main fishing area in Nagasaki Prefecture is divided into five regional sub zones, namely such as Hokusho, Omura Bay, Goto, Seihi and Tachibana Bay (Fig. 3.1). In the study region, purse-seine fishery is typically conducted within a zone extending almost up to 20 km offshore (Kuwaoka, 1976) from May to August, mainly targeting juvenile and immature anchovies (Ogawa, 1976). It is reported that the catch from August to December correlated with the catch of juvenile anchovy from May to July (Nagasaki Prefecture, 2008). Acoustic survey showed that the anchovy biomass and the annual catch in the Tsushima Warm Current region (from Niigata Prefecture to Kagoshima Prefecture) had significant correlation (Ohshimo, 2004), indicating that usefulness of the catch data as an indicator of the recruitment. The fluctuation in the annual total catch in Nagasaki Prefecture was significantly correlated with the fluctuation in the abundance of the Tsushima

Warm Current stock (Fig. 3.2, $r = 0.740$, $p < 0.01$). The stock recruitment index for similar pelagic fishes such as Japanese sardine and chub mackerel (*Scomber japonicus*) in the Tsushima Warm Current has been studied (Hiyama et al., 2002; Ohshimo et al., 2009). These studies suggested that the relationships between stock recruitment and environmental factors such as the SST, monsoon index and Arctic oscillation. Although it is better to analyze the stock abundance using recruitment relationship, the recruitment relationship of the anchovy of the Tsushima Warm Current stock has not been reported. For this reason, catch data were analyzed instead of the stock abundance.

To detect the regime shift in catch, wind-stress and SST, sequential *t*-test analysis of regime shifts (STARS) method developed by Rodionov and Overland (2005) was applied. Cut-off length for a regime was set to 10, and Regime Shift Index (RSI) was tested based on 95% confidence interval. In order to clarify regional fluctuation patterns, the regional catch data were clustered using Ward's method (Ward, 1963) based on the similarity of the time-series of the catch.

3.1.2 Environmental data

Daily seawater temperature and horizontal current velocity data from 1993 to 2009 were derived from the Japan Coastal Ocean Predictability Experiment 2 (FRA-JCOPE2) (Miyazawa et al., 2009). The FRA-JCOPE2 reanalysis data has a horizontal resolution of 1/12 degree around Japan. According to the method of Warner (2005), the model applicability was evaluated using coastal mooring data obtained from the Japan Oceanographic Data Center (JODC, Fig. 3.1). The model skill score was relatively high (0.6), and thus it was considered the FRA-JCOPE2 reanalysis data can be regarded as reliable hydrodynamic data for the study area. The reanalysis data were used for the analysis of hydrodynamic features and SST distribution. In the present study, the Goto-Nada Sea was defined as the area within 32.5–33.25˚N and 129.0–129.75˚E (Fig. 3.1). Since anchovy larvae are distributed in the surface water of 0–20m (Iseki and Kiyomoto, 1997; Nakata and Imai, 1981), surface data of the FRA-JCOPE2 were used for the analysis. In order to recognize the temporal variations in SST and horizontal velocity in spring, all grid data at the surface layer within the Goto-Nada Sea were spatially and temporally averaged from 1993 to 2009. To explore the effect of wind on the surface current, wind-stress (N m^{-2}) was calculated from daily maximum wind speed, averaged air temperature and sea level pressure observed at Fukue meteorological station of

the JMA for the period between 1963 and 2009 (Fig. 3.1) based on the following equations,

$$\tau_x = C_D \rho W u \quad (3.1)$$

$$\tau_y = C_D \rho W v \quad (3.2)$$

$$C_D = 1.085 W 10^{-1.5} \quad (0.3 \leq W < 2.2) \quad (3.3)$$

$$C_D = 0.771 + 0.0858 W 10^{-3} \quad (2.2 \leq W < 5.0) \quad (3.4)$$

$$C_D = 0.867 + 0.0667 W 10^{-3} \quad (5.0 \leq W < 8.0) \quad (3.5)$$

$$C_D = 1.2 + 0.025 W 10^{-3} \quad (8.0 \leq W < 25.0) \quad (3.6)$$

$$C_D = 0.073 W 10^{-3} \quad (25.0 \leq W < 50.0) \quad (3.7)$$

where, τ_x and τ_y are zonal and meridional wind-stress components, respectively. C_D is drag coefficient which depends on intensity of wind speed (Kondo, 1975). ρ is density of air (kg m^{-3}) calculated using air temperature (˚C) and sea level pressure (hPa). W, u and v are scalar, zonal and meridional wind speeds (m s^{-1}), respectively. Positive signs of zonal and meridional wind-stress represent eastward and northward directions, respectively. Daily average of surface current velocity and wind-stress from March to May (averages of 1993–2009) were compared to clarify the relationship between surface current and wind-stress. To test the hypothesis of the potential effect of the long-term variation in wind-stress on the fluctuation in catch of anchovy, annual wind-stress was calculated by cumulating daily wind-stress from April 1 to May 31 for each year. Mean spring SST in the northern part of the ECS from 1960 to 2009 was also obtained from JMA. The linear trend was removed from the time-series of the SST, and then oceanic regime shift was examined based on the cumulated SST anomaly.

3.2 Results

3.2.1 Long-term fluctuations in anchovy catch off northwestern Kyushu

It was found that anchovies caught in the five sub zones have commonly experienced high stock phases from the 1960s to 1970s and low stock phase from the 1980s to the 1990s (Fig. 3.3). As a result of STARS analysis, although there were slight difference in the timing of the shift among the sub zones, most of the negative shift and positive shift were detected in the mid–1970s and mid–1990s. The negative and positive shifts were detected in the total catch in 1977/78 and 1994/95, respectively. As a result of cluster analysis, fishery sub zones were grouped into two major clusters. The first cluster was composed of Omura Bay, Seihi and

Tachibana Bay (Fig. 3.4). These three sub zones are located along the coast of northwestern Kyushu. The second group was composed of the Goto and Hokusho, and these two sub zones are located offshore. As the results of regime shift patterns and cluster analysis, sub zones were simply divided into offshore zone (the total of Hokusho and Goto zones) and coastal zone (the total of Omura Bay, Seihi and Tachibana Bay). In general, negative shifts were detected in 1975/76 and 1984/85 in the coastal zone (Fig. 3.3). In the offshore zones, a negative shift occurred in 1974/75, and two positive shifts were detected in 1985/86 and 1994/95. In these two regions, the timing of shifts to low-level in the coastal zone and to high-level in the offshore zone has occurred in the mid-1980s and mid-1990s, respectively.

3.2.2 Changes in oceanographic conditions

Mean surface current condition off northwestern Kyushu is illustrated in Figure 3.5, which shows the surface current in the northern Goto Islands flowing towards the northeast (Tsushima Warm Current) and Kuroshio intrusion in the southern area. Spatially-averaged daily surface current velocity and SST in the Goto-Nada Sea in spring (March to May, 1993–2009) are shown in Figure 3.6. There were considerable variations in surface current. Zonal and meridional components became relatively strong and almost directed northward and eastward from early April to May, respectively. Meanwhile the SST reached the lower-limit of spawning temperature of the Japanese anchovy (15.6˚C, Fig. 3.6) suggested by Takasuka et al. (2007). The spring SST in the northern ECS showed an increasing trend between 1960 and 2009 with the averaged SST 17.6˚C. The SST has increased by 0.9˚C during 1963–2009 (Fig. 3.7). The STARS analysis for the SST detected a statistically significant negative regime shift in 1975/76 and a positive shift in 1994/95 (Fig. 3.7). Based on the regime shift in the SST, the time-series data were divided into three fixed regimes such as 1963–1975 (warm-regime I), 1976–1994 (cold-regime) and 1995–2009 (warm-regime II). The averaged SST in the warm-regime II (18.0˚C) was 0.7˚C higher than that in the warm-regime I (17.3˚C) (Table 3.1). In order to examine the effect of the increased SST on the distribution of the spawning ground, the SST in 1996 (spatially averaged SST 16.4˚C) and 1997 (17.3˚C) were compared using the FRA-JCOPE2 reanalysis data. Those two years were selected considering the above SST change between the warm-regime I and warm-regime II. As a result, the 15.6˚C contour line in 1997 was located further north, compared with that in 1996 (Fig. 3.8).

3.2.3 Wind condition change

In order to examine the effect of wind on the surface current in the Goto-Nada Sea, wind-stress observed at Fukue meteorological station was analyzed. In this region, north-northeast to south-southwest axis winds are the most prevailing directions (both exceeds 10%), followed by southeastward wind (12%) in April–May (Fig. 3.9). To clarify the causal factor of the eastward current, daily zonal surface current velocity and meridional wind-stress were compared. The result showed a significant correlation (r = 0.450, $p < 0.01$, Fig. 3.10), indicating that northward wind-stress drives eastward Ekman currents over the Goto-Nada Sea from April to May. According to this result in 1993–2009, the meridional wind-stress can be an indicative parameter for the surface current variability. Thus, the long-term (1963–2009) meridional wind-stress data was used to discuss the change in surface current in the following analyses. Long-term variation in north-northeastward wind-stress exhibited a decreasing trend from the 1960s to the 2000s (Fig. 3.11). The STARS analysis indicated that wind-stress shifted to a negative regime in 1974/75, and has been lowered until a positive shift occurred in 2003/04.

3.2.4 Relationship between wind-stress and anchovy catch

Long-term variations in cumulative north-northeastward wind-stress from April to May were compared with the catches in each fishery sub zone (Fig. 3.12). Annual catches in Omura Bay, Seihi, Tachibana Bay and the coastal zone were significantly correlated with the north-northeastward wind-stress (r = 0.652, 0.479, 0.386 and 0.518, all $p < 0.01$). Conversely, no positive correlations were found in the offshore zone including Hokusho and Goto (Fig. 3.12). It should be noted that significant correlations were found only with the sub zone located along the coast of northwestern Kyushu. To distinguish the effect of the different strength of wind-stress, the surface current in the Goto-Nada Sea under the weak and strong north-northeastward wind conditions were compared (Fig. 3.13). In 2003, surface current directed north-northwestward, and spatially averaged current velocity over the Goto-Nada Sea was 0.08 m s^{-1} under the average north-northeastward wind-stress 2.6 N m^{-2}. On the other hand, surface current directed to east with the spatially averaged current velocity 0.12 m s^{-1} when the strong north-northeastward wind-stress 4.6 N m^{-2} was observed in 2004.

Based on the regime shift in the SST, catch and wind-stress were averaged for each regime (Table 3.1). Averaged catch in the coastal zone in warm-regime II was almost half of

that in warm-regime I, whereas the offshore catch in warm-regime II was twice as high as that in warm regime I. It is clear that averaged north-northeastward wind-stress in warm-regime II has weakened by more than 1.6 N m^{-2}, compared to that in warm-regime I.

3.3 Discussion

According to the previous study, high and low regimes in the total catch may be resulted from warm and cold regime changes in the SST through the temperature-dependent biological processes, respectively (Takasuka et al., 2007). Similar climatic and fish regime shifts were reported by Tian et al. (2006) in the Tsushima Warm Current region and the Sea of Japan. They have detected a negative shift in pelagic species including anchovy in 1977/78, and a positive shift between 1989 and 1992. This positive shift in the Sea of Japan has occurred earlier than the beginning of warm-regime II in the northern ECS, possibly due to faster increasing rate of SST in the ECS.

However, the fluctuations in the regional catches were not explained by the above SST step changes. In the coastal zone, a negative shift was detected in the mid-1980s, and the catch continued to decrease. The discrepancy between the SST regime shift and the catch fluctuation indicates that the other mechanism would have a great influence on the anchovy population in this region. Recent Acoustic Doppler Current Profiler (ADCP) observations conducted by Takagi et al. (2009) detected north to north-northeastward current on the continental margin of the southern part of the Goto-Nada Sea between winter and spring, and they also mentioned its importance in recruitment of anchovy into the coastal fishing zone. The significant correlations between the catches in the coastal zones and wind-stress indicate that anchovy recruitment off northwestern Kyushu partly depends on the eastward Ekman transport during their early life stages. Similar studies have revealed the importance of wind-driven current in successful fish recruitment (Borja et al., 1996; Nielsen et al., 1998; Hinrichsen et al., 2001; Linnane et al., 2010). In Shijiki Bay, located in the northern part of the Goto-Nada Sea, Nakata and Hirano (1988) reported that prevailing southerly winds during the spawning season of red sea bream (*Pagrus major*) possibly contributes to the increase in the amount of transported larvae into the bay. In the western Gulf of Maine, modeling approach suggested that high retention rate of larval Atlantic cod (*Gadus morhua*) in nearshore habitat is attributed to the downwelling favorable winds which prevents cod larvae from drifting by the offshore western Maine Coastal Current (Churchill et al., 2011). In the present study, it was found that a strong

northward wind causes eastward current, and therefore, the weakened Ekman current, due to the decreased north-northeastward wind-stress, was found to be a potential environmental factor responsible for the recent decrease in the catch of anchovy in Omura Bay, Seihi and Tachibana Bay through reduced onshore transport of eggs and larvae. Despite a shift to warm-regime II in the mid-1990s, anchovy catch in the coastal zone did not recover to that level of warm-regime I because the wind-stress did not shift to a positive regime. It indicates that a certain level of strong north-northeastward wind is also required for successful recruitment in order to take advantage of eastward transport, which would result in a higher growth rate due to higher food availability in the coastal waters than that in the offshore (discuss in the next chapter). In regard to the long-term change in local wind, this study pointed out that the weakened East Asian monsoon circulation led to the decrease in wind speed observed in Nagasaki Prefecture between the 1950s and the mid-1990s (Chapter 2). Thus, the large-scale atmospheric circulation, such as the East Asian monsoon, is possibly related to the long-term decrease in wind-stress and even to the fluctuations in anchovy catches.

On the other hand, a positive shift in the offshore catch was detected in the mid-1980s, and a second positive shift, coinciding with the warm-phase shift of SST, occurred in 1994/95. However, these increasing trends in the catches in Hokusho and Goto zones could not be explained by the variation in wind-stress alone. One of the possible factors influencing the offshore recruitment may exist in expanding of spawning ground due to SST warming trend. This study showed that the warming trend in the SST has potential to extend the spawning ground to the northern area (Fig. 3.8). Therefore, not only the regime shift, but the warming trend in the SST may also be responsible for the recent rapid increase in the offshore catch due to the expansion of the spawning ground, which is thought to be favorable for the retention of eggs and larvae in the offshore zone. This hypothesis is tested using a particle tracking simulation in the Chapter 4.

In conclusion, recovery of the catch in the coastal zone is unlikely unless the north-northeastward wind becomes strong, even if the ambient temperature is close to the optimal growth temperature. The change in the wind condition due to the future climate change could break connectivity between spawning and nursery areas (Aiken et al., 2011). The results suggested that the physical process could regulate fish recruitment, and future prediction of recruitment is difficult without the unveiling transport mechanism, especially in the coastal

waters (Fig. 3.14).

In waters off the western coast of Kyushu, the Tsushima Warm Current and the Kuroshio would affect coastal current (Lie et al., 1998). Thus, further understanding of the mechanism of larval transport related to the Tsushima Warm Current and the Kuroshio intrusion will be necessary, and it may require a new method of a numerical simulation. In addition, several studies have reported the distribution of anchovy in the ECS and Yellow Sea. Iversen et al. (1993) and Ohshimo (1996) have estimated the stock abundance in the ECS at 3,000,000 tons. This stock may affect the recruitment variability off northwestern Kyushu. Therefore, contribution of the stock from the other areas should be included in future analysis.

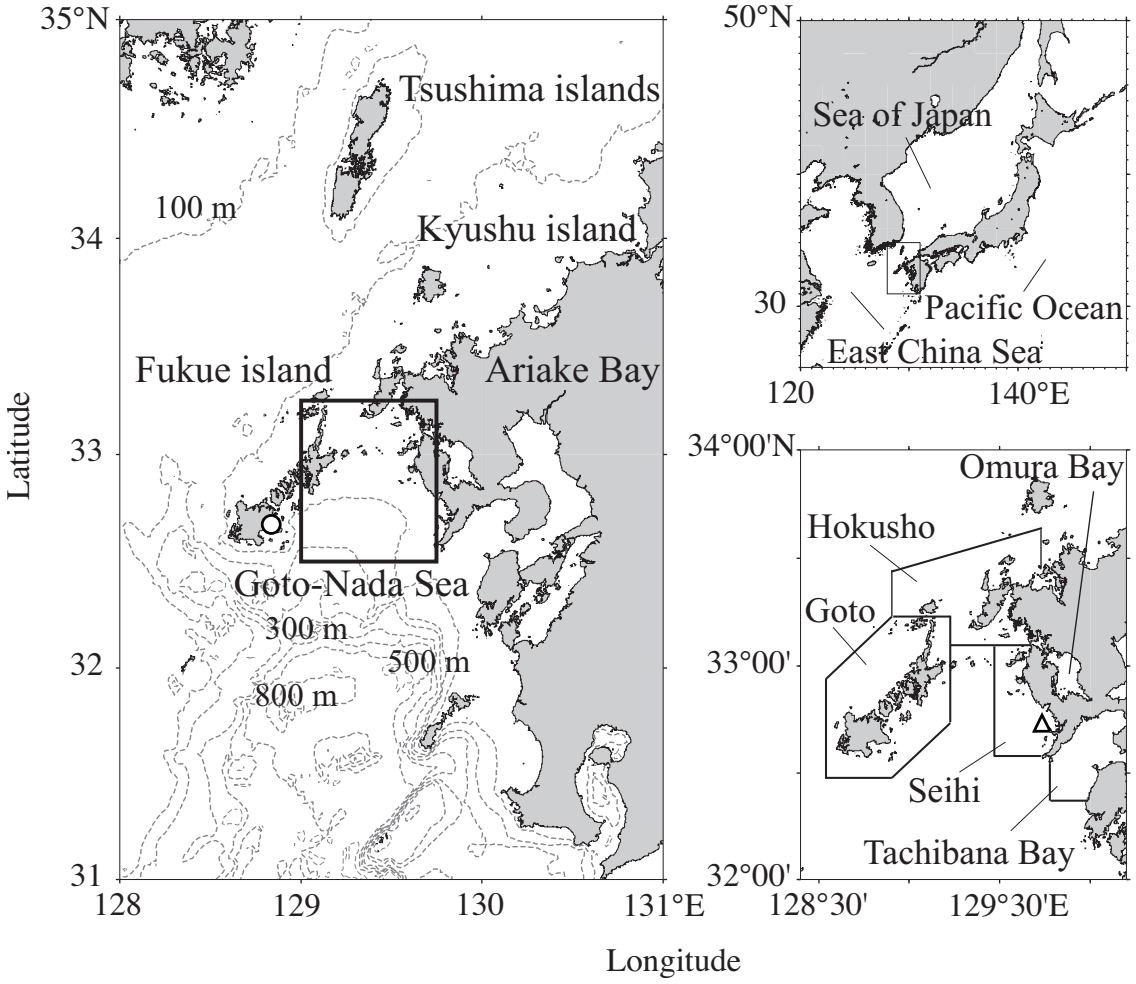

Fig. 3.1 Geophysical location of northwestern Kyushu. Fukue meteorological station of the Japan Meteorological Agency is represented by an open circle. Black solid lines in the lower right panel indicate borders of fishery sub zones in Nagasaki Prefecture. The Goto-Nada Sea is defined by the enclosed black-bold lines in the left panel. The coastal mooring station is indicated by a triangle.

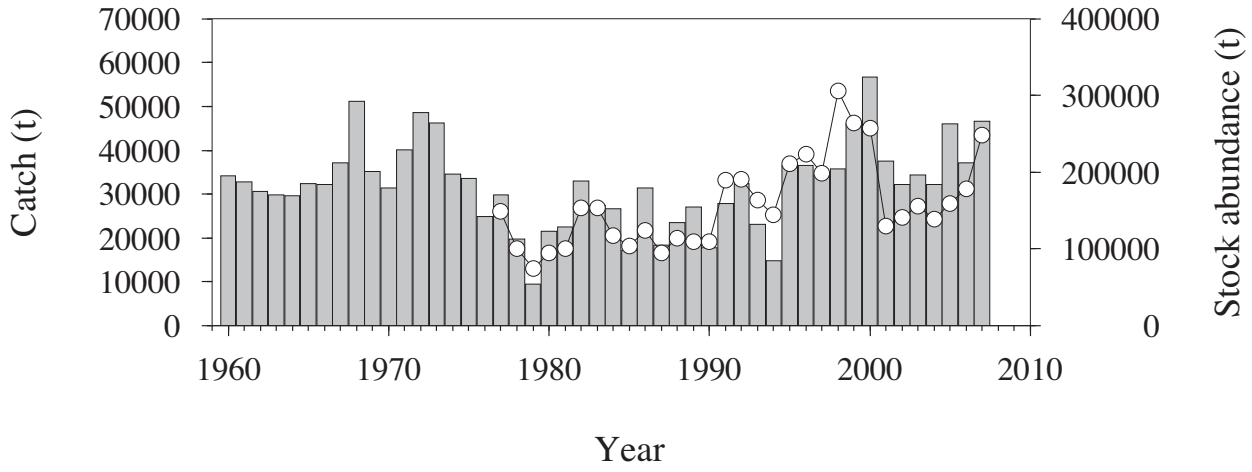

Fig. 3.2 Time series of the total catch in Nagasaki Prefecture (bar) and abundance of the Tsushima Warm Current stock (circle).

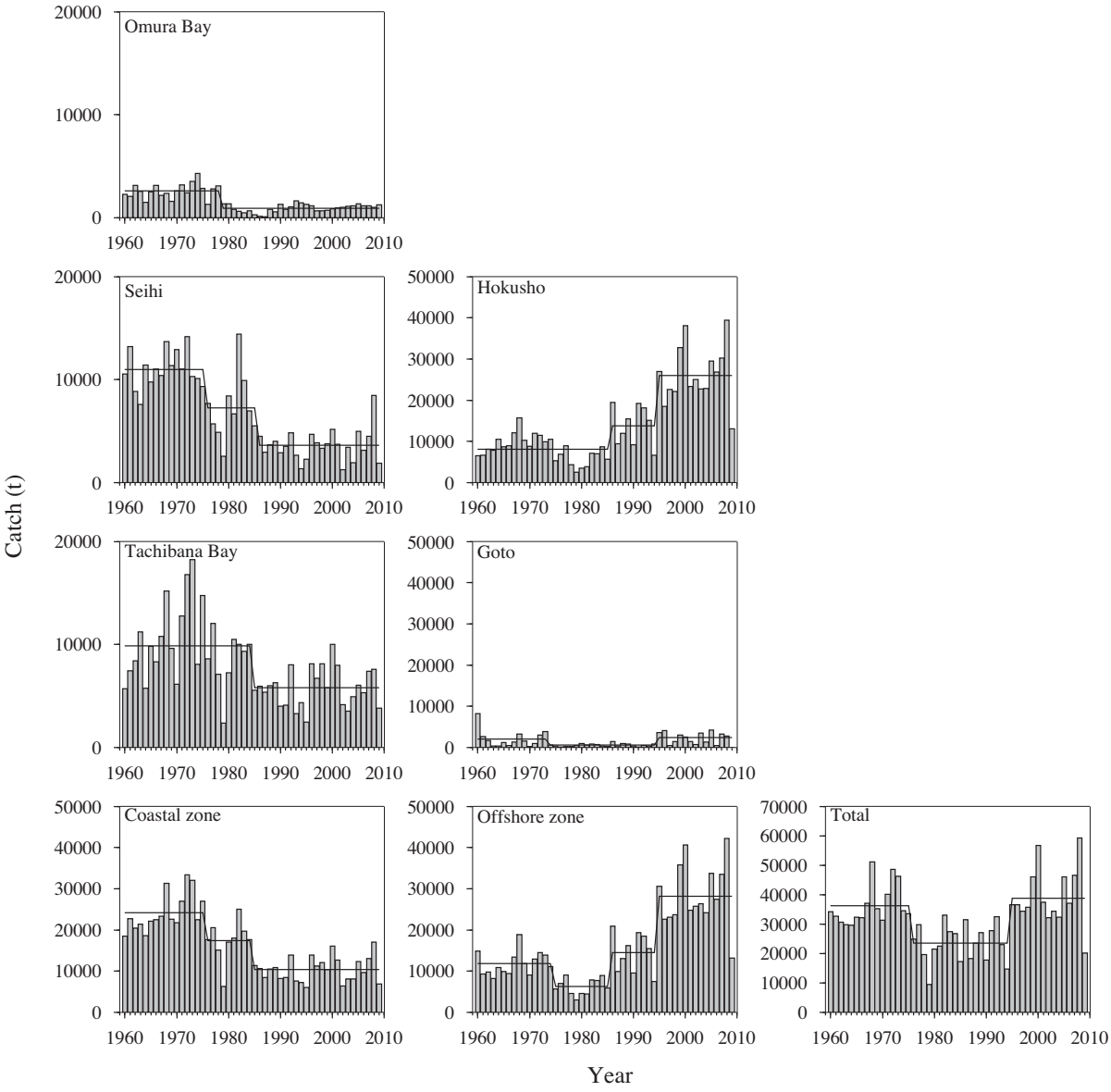

Fig. 3.3 Time series of annual catches of the Japanese anchovy in five sub-fishery zones, coastal zones (Omura Bay, Seihi and Tachibana Bay), offshore zones (Hokusho and Goto) and total. Solid lines indicate averages of each regime detected by STARS.

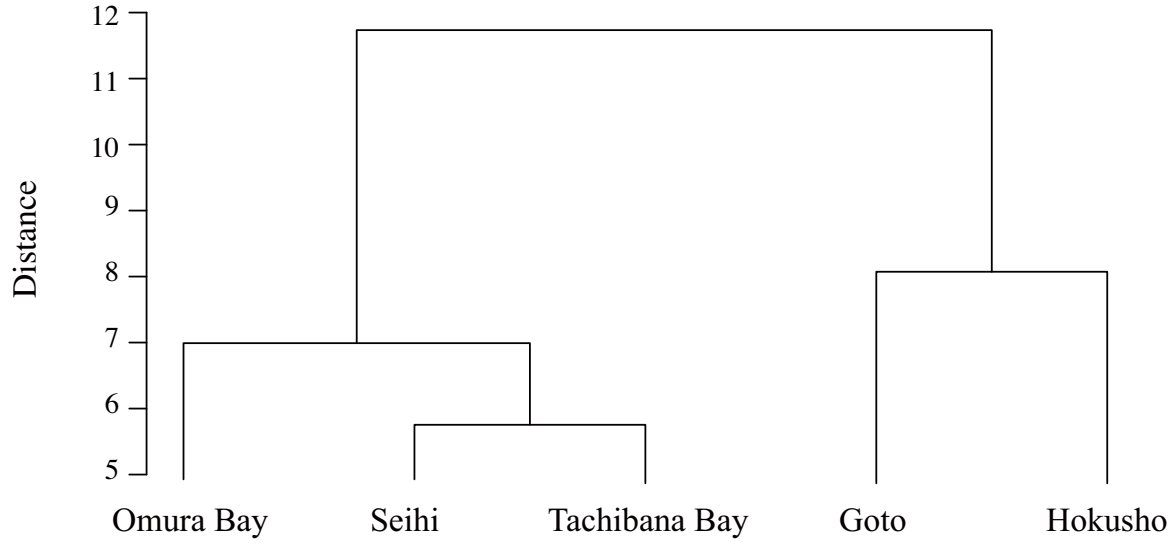

Fig. 3.4 Dendrogram for clustering the fluctuation in catch of anchovy in five sub zones.

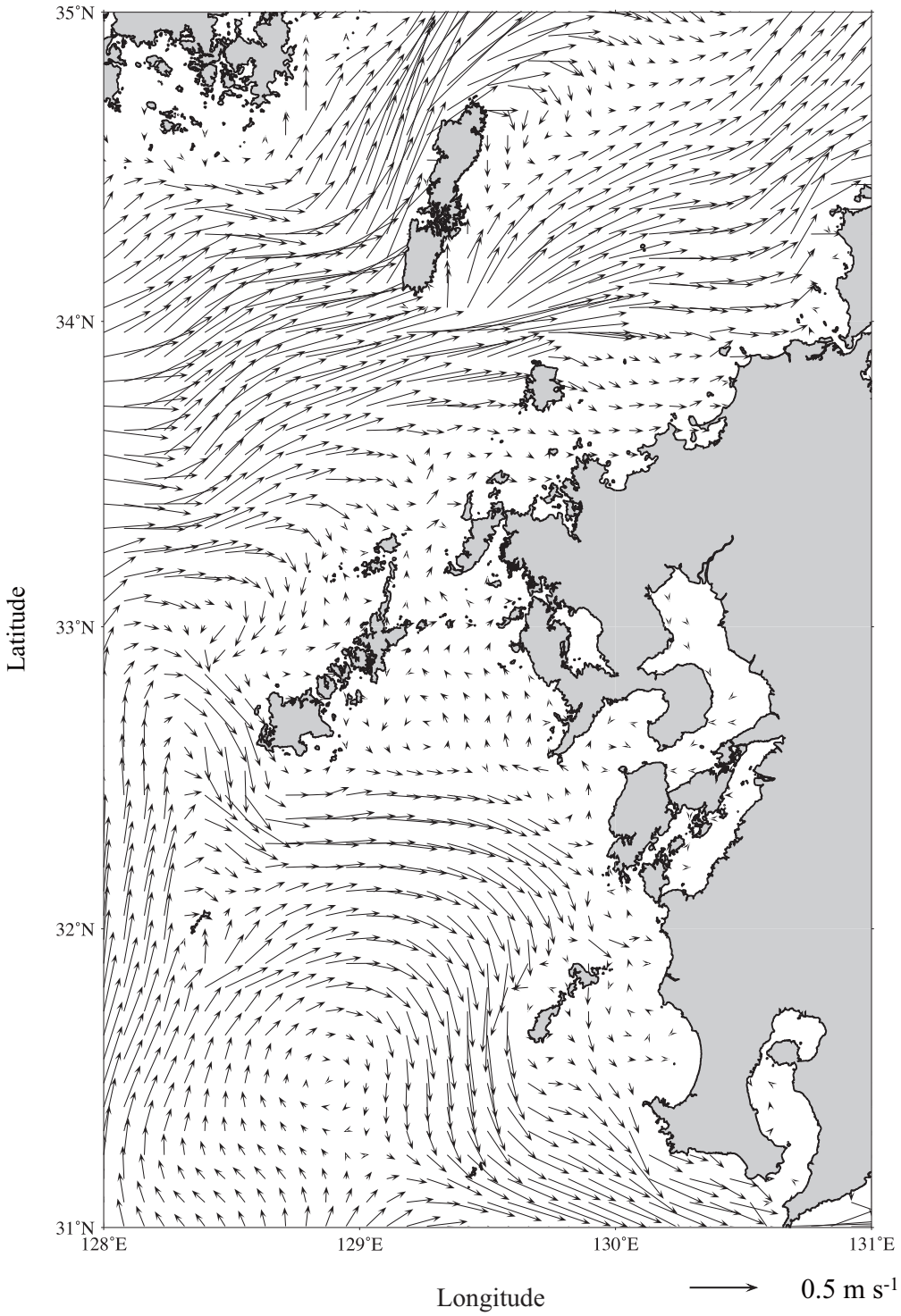

Fig. 3.5 Temporally-averaged surface circulation in the northeastern East China Sea during spring between 1993 and 2009. Arrows indicate the magnitude and directions of flow.

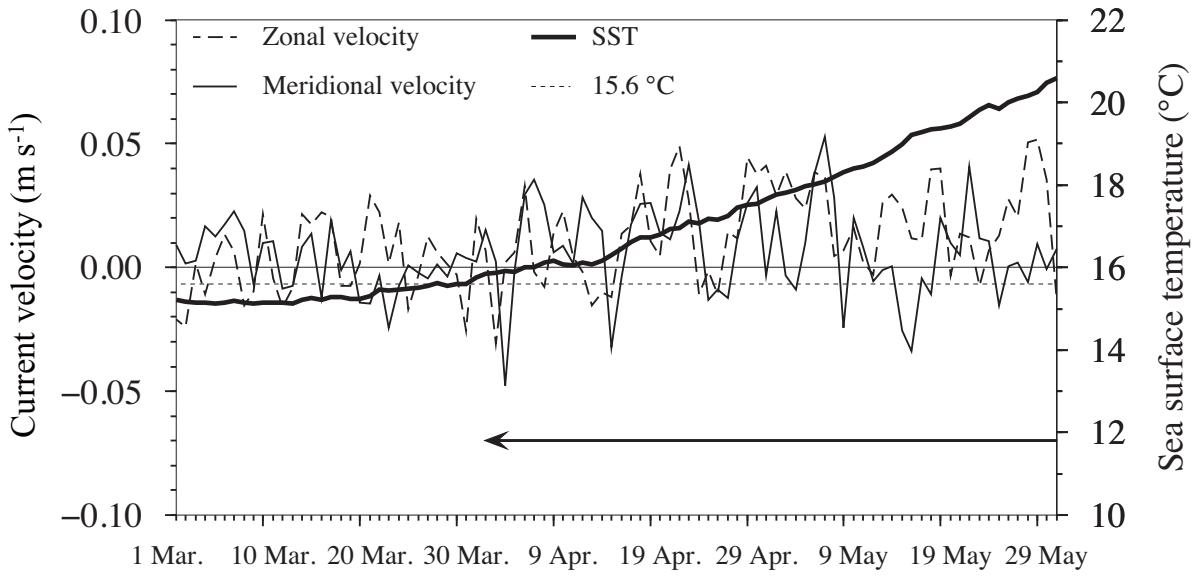

Fig. 3.6 Time series of spatially averaged daily surface current and sea surface temperature (SST) from March to May (average of 1993–2009 period). Arrow indicate the period in which SST exceeds 15.6 ˚C which is the lower limit of the spawning temperature according to Takasuka et al. (2007).

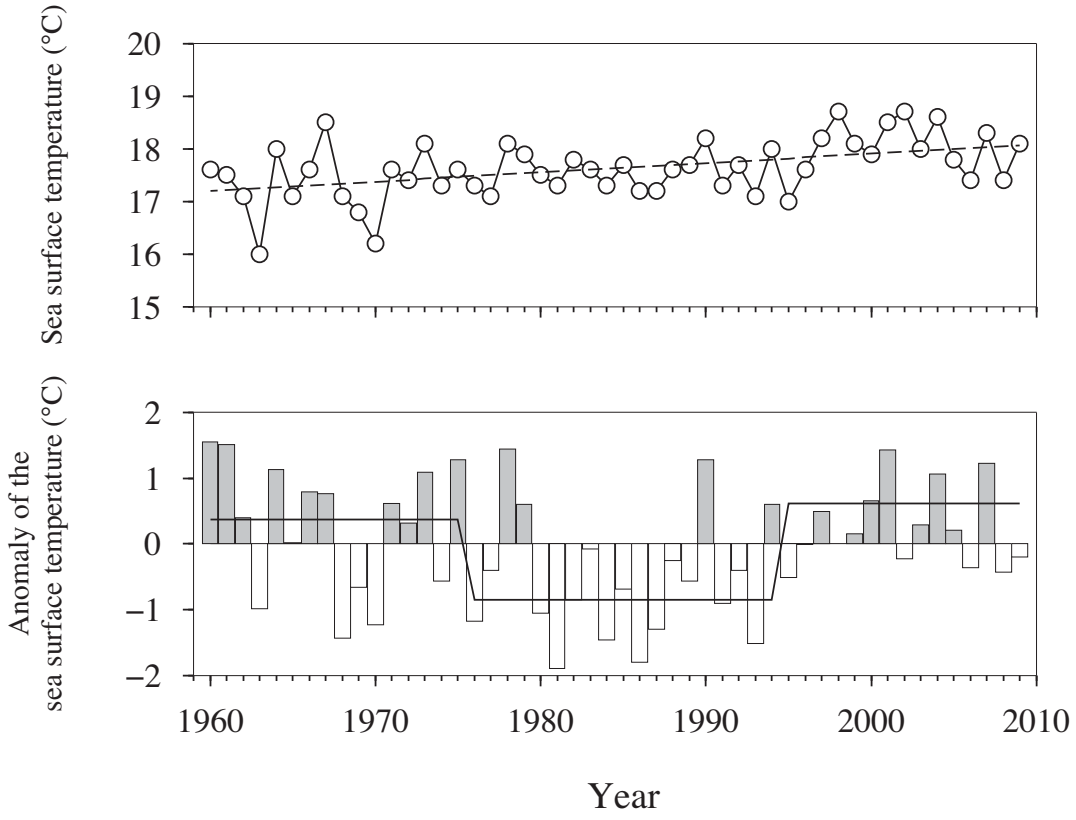

Fig. 3.7 Time-series of the SST in the northern East China Sea in spring (upper) and the cumulated SST anomaly (lower) during 1963–2009. Dashed line in the upper panel indicates a linear trend. Solid line in the lower panel indicates averages of SST regimes detected by STARS.

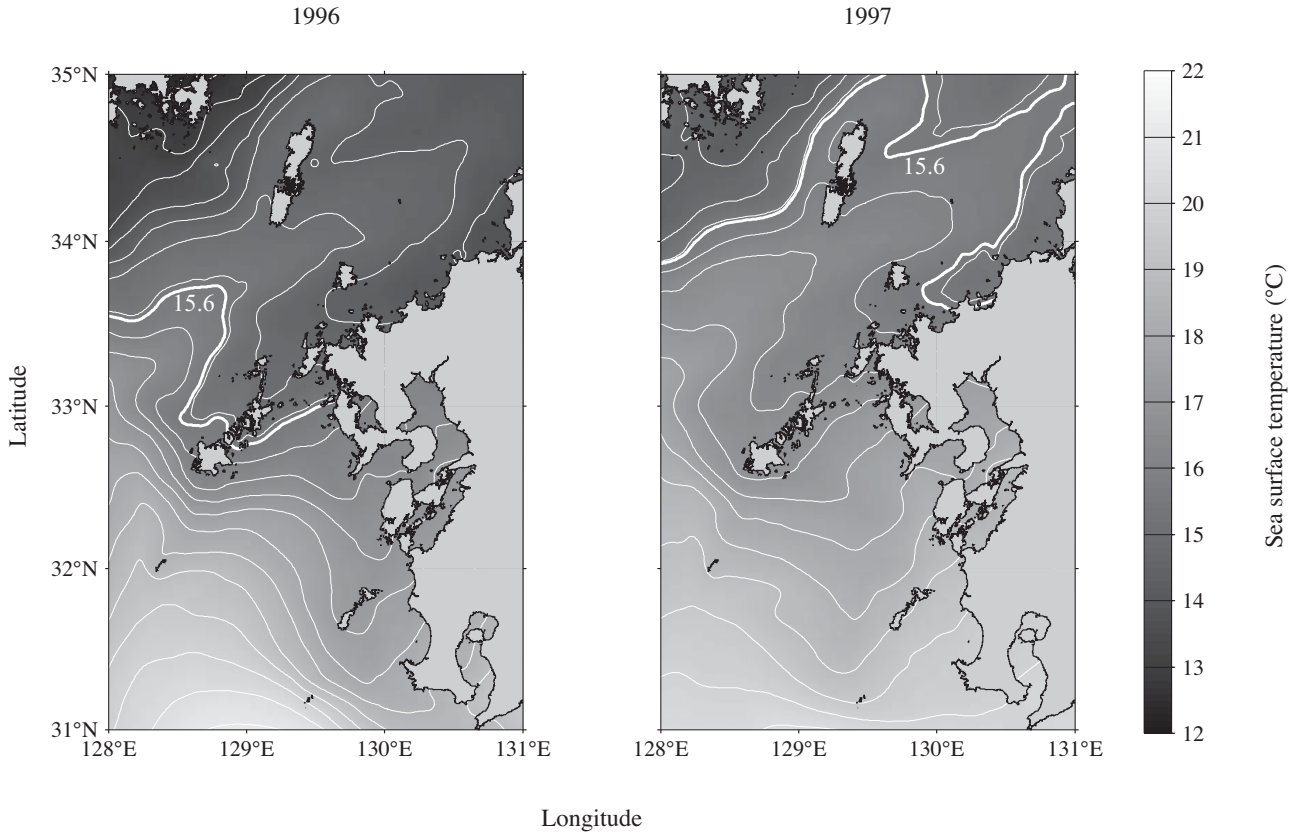

Fig. 3.8 Temporally-averaged SST in the study area from March to May in 1996 (left) and 1997 (right). The contour interval is 0.5 ˚C, and white bold lines indicate 15.6 ˚C.

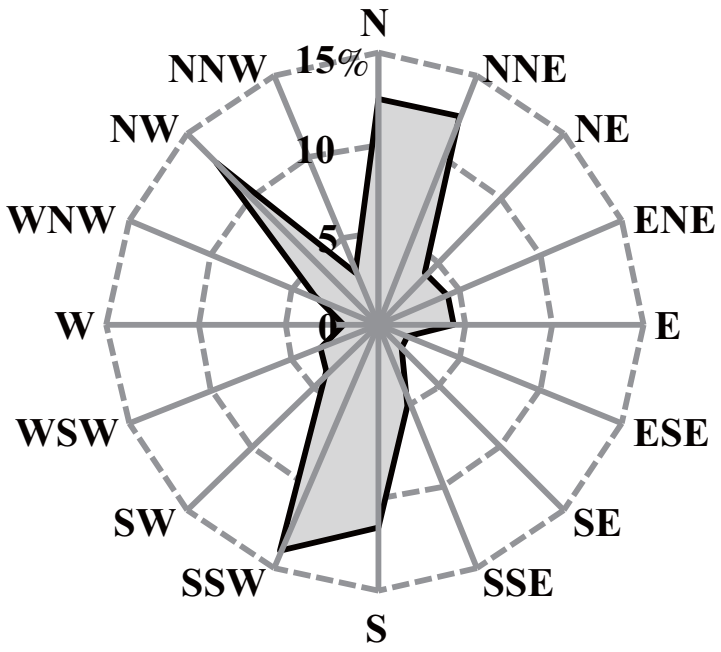

Fig. 3.9 Rose diagram for frequency of daily wind directions from April to May (averaged for 1993–2009).

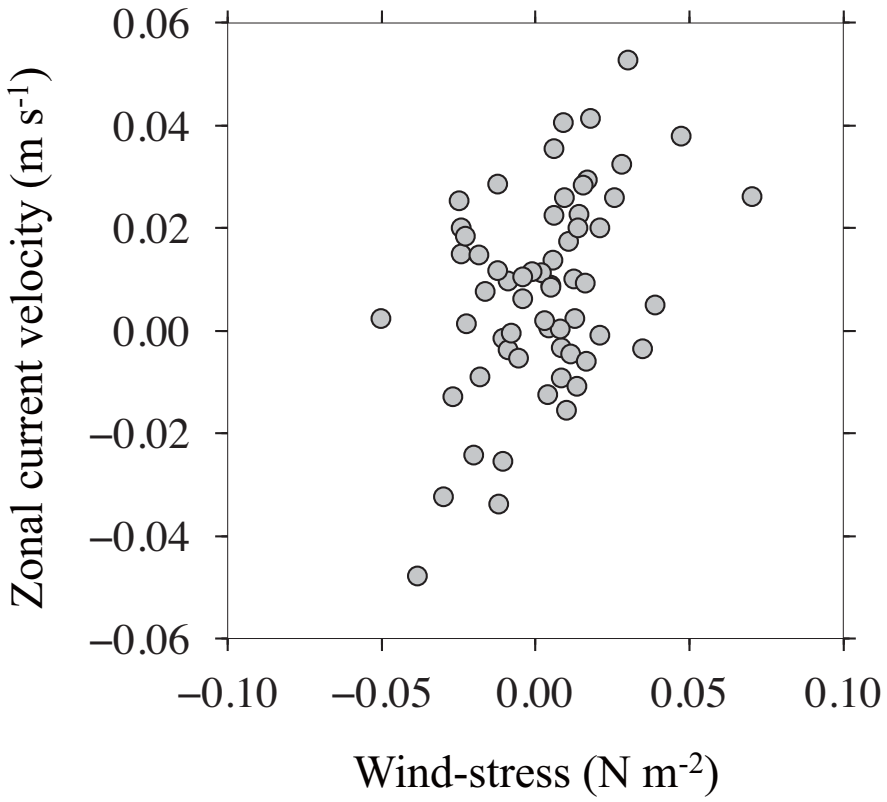

Fig. 3.10 Comparison of daily meridional wind-stress and zonal current velocity.

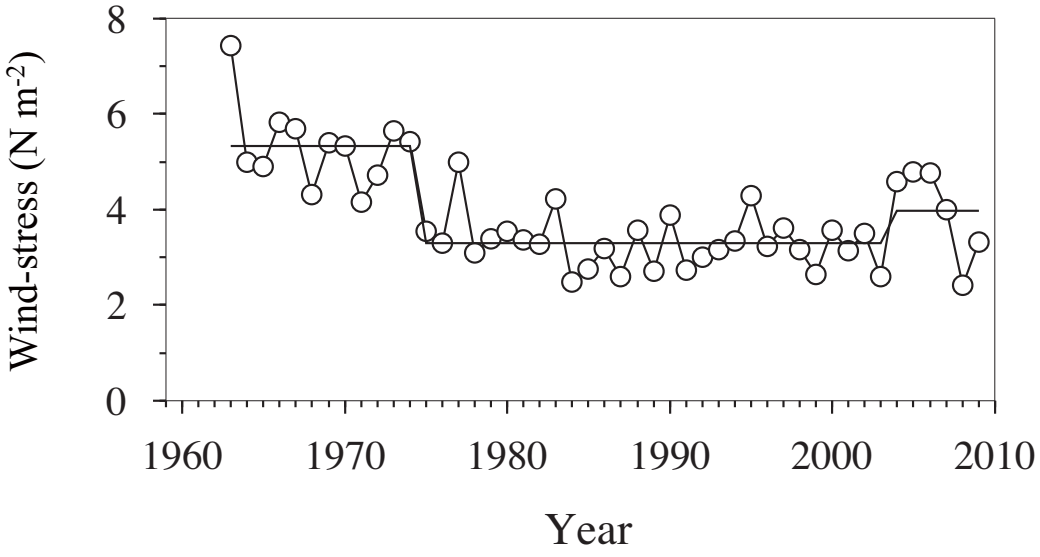

Fig. 3.11 Long–term variations in cumulated north-northeastward wind-stress from April to May during the period of 1963–2009. Solid line indicates averages of each regimes detected by STARS.

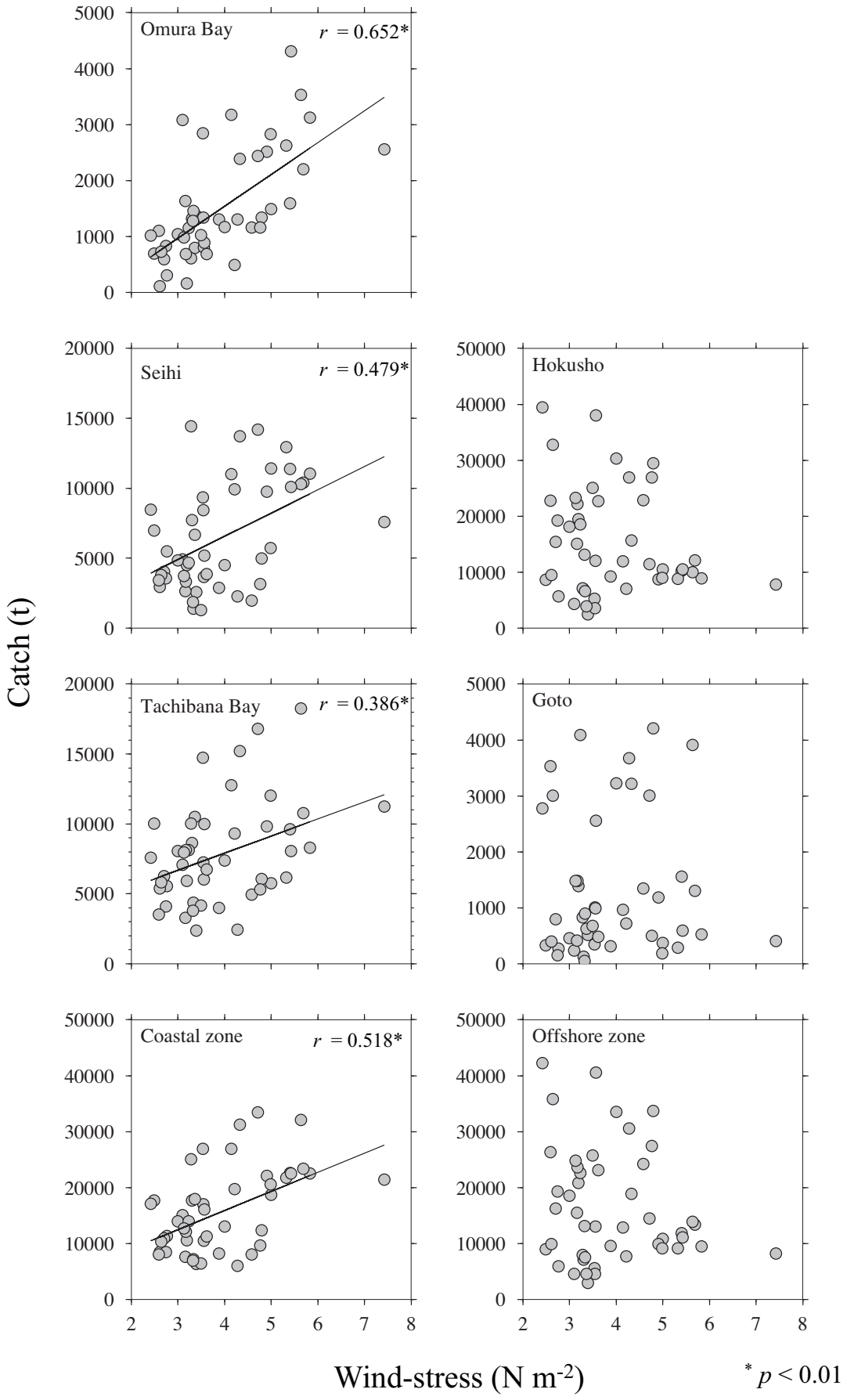

Fig. 3.12 Comparison of annual catch of anchovy in each sub zone with cumulated north-northeastward wind-stress from April to May.

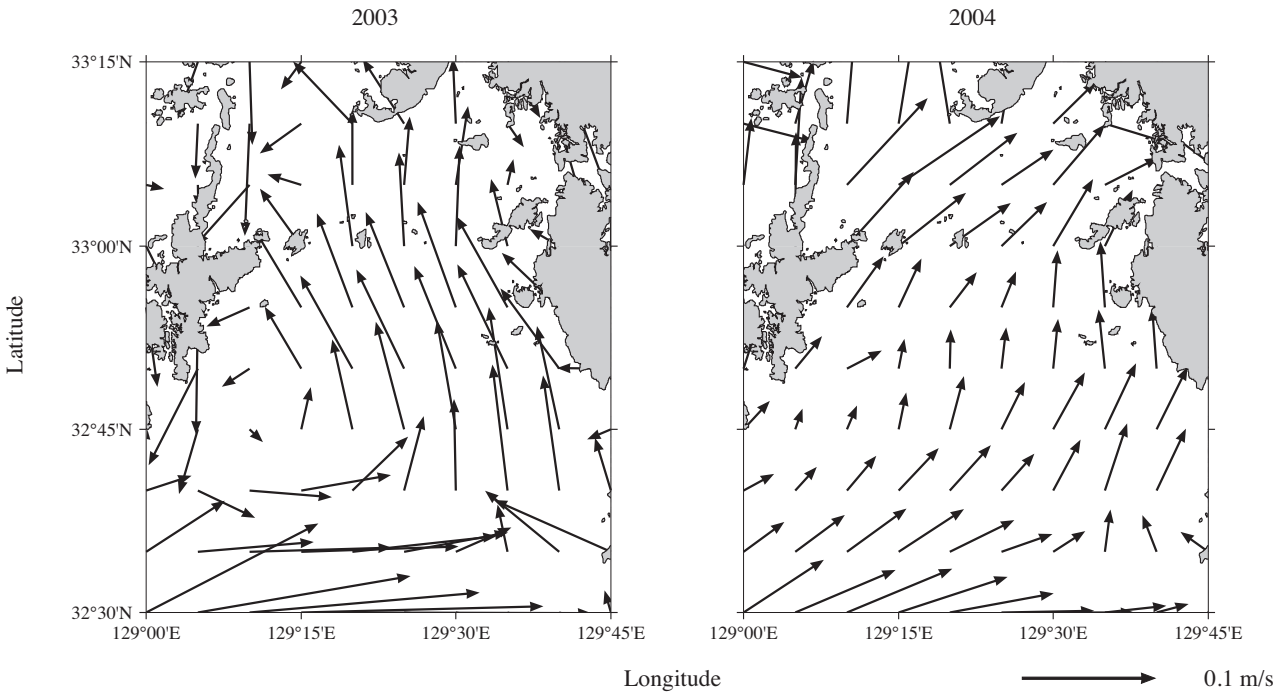

Fig. 3.13 Temporally-averaged surface circulation in the Goto-Nada Sea in April in 2003 (left) and 2004 (right). Arrows indicate the magnitude and directions of flow.

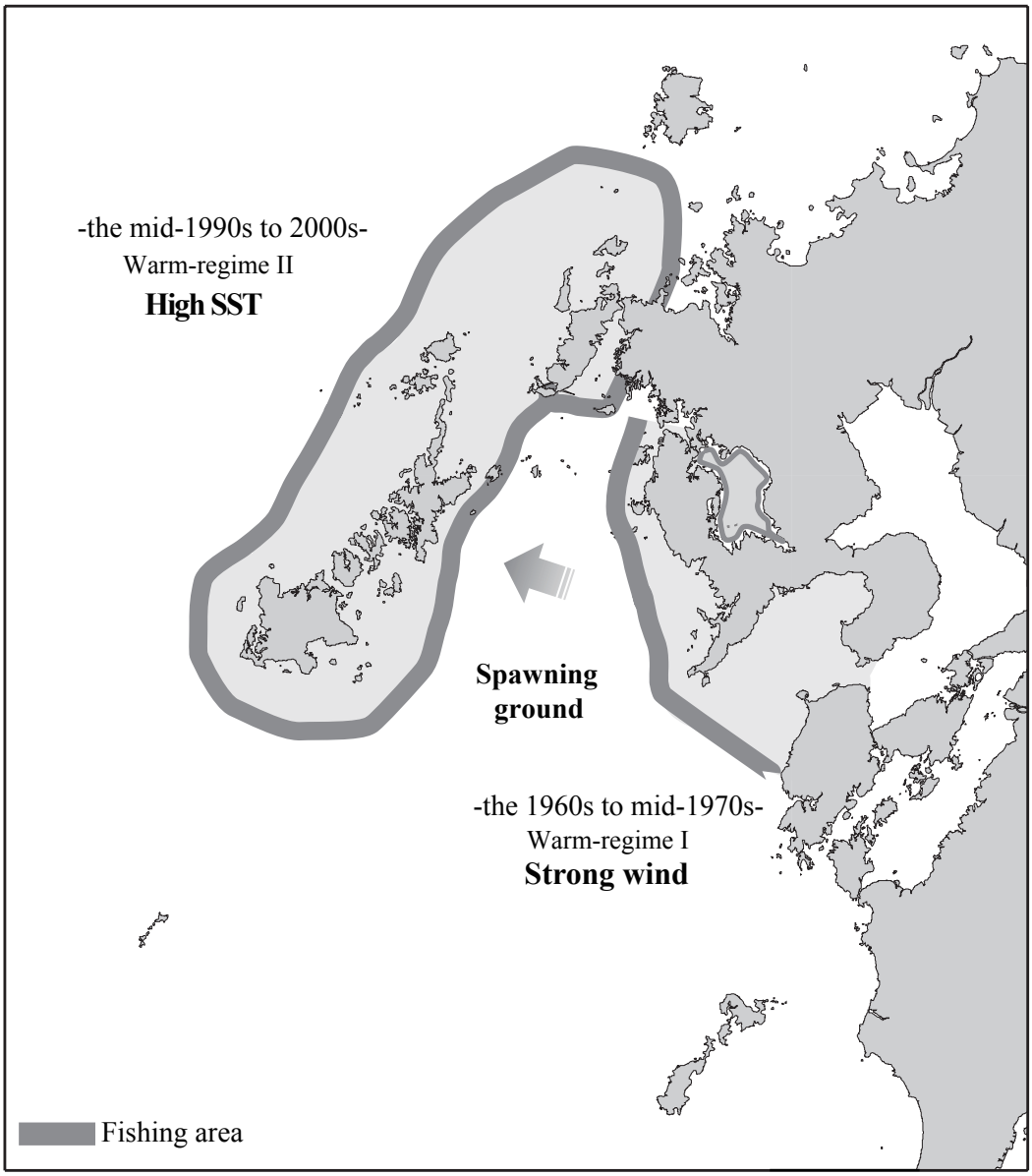

Fig. 3.14 Schematic diagram of shift of the fishing area between the 1960s–1970s and the 1990s–2000s.

Table 3.1 Averaged anchovy catch in each sub zone (t), wind-stress (N m^{-2}) and sea surface temperature (˚C) during 1963–1975, 1976–1994 and 1995–2009.

	Regime		
	Warm-regime I (1963–1975)	Cold-regime (1976–1994)	Warm-regime II (1995–2009)
Omura Bay	2,590	1,094	1,044
Seihi	10,737	5,432	3,765
Tachibana Bay	10,119	6,856	6,133
Coastal zone	24,196	13,383	10,943
Hokusho	9,424	9,641	26,295
Goto	2,099	561	2,205
Offshore zone	11,482	10,202	28,500
Total	36,215	23,609	39,452
Wind stress	5.2	3.3	3.6
Sea surface temperature	17.3	17.6	18.0

Chapter 4

Modeling eggs and larval transport and its relation to climate change

In the Chapter 3, the results showed that transport process has potential to affect the recruitment of anchovy off the western Kyushu. However, quantitative evaluation of eggs and larval transport and possible environmental factors influencing the transport success are still unrevealed. A particle tracking method is an effective approach to elucidate eggs and larval transport process. In this chapter, long-term transport success and its controlling factors were investigated by the modeling approach.

4.1 Data and methods

4.1.1 Egg and larval data

The time-series data of the abundance of anchovy eggs and larvae in the ECS from 1979–2007 was derived from Kuroda et al. (2013). The distributions of eggs and larvae were analyzed to investigate eggs and larval distribution characteristics and to determine the particle release location. Seikai National Fisheries Research Institute conducted monthly egg and larval census from 1959 to present, but only abundance of averages of 1959–1973 was available. The eggs and larvae were collected by plankton net (diameter of 45 cm and a mesh size of 0.33 mm) at the surface layer. The abundance of the eggs and larvae are represented by five levels (0, 1–9, 10–49, 50–99 and 100–499 ind. per tow). In order to specify the spawning ground, modeled SST and observed egg distribution were compared.

4.1.2 Hydrodynamic model

To reproduce fine scale coastal current field, a hydrodynamic model in the study area was developed using Delft3D-FLOW (Delft Hydraulics, 2008), applied over the domain extending from 31 to 35˚N and 128 to 131˚E (Fig. 4.1). The computational grid has 2 × 2 km resolutions in a horizontal direction with 5 σ-grid layers. From surface to bottom, the thickness of each layer was 20% at the given depth. The bathymetry data of 500 m resolutions were derived from JODC. The model boundary conditions were forced by daily horizontal current velocity at west and south boundaries, and hourly tidal height at north and east boundaries. The horizontal current velocity data were obtained from the Ocean General Circulation Model for Earth Simulator (OFES, Masumoto et al., 2004). The 0.1˚ grid zonal and meridional current

velocity data was linearly interpolated to 0.02˚ grid. The OFES data were also used for the initial condition such as the seawater temperature, salinity and water level. The tidal height at the north and east boundaries were calculated using NAO.99Jb model (Matsumoto et al., 2000). The model sea surface was forced by wind-stress obtained from OFES. The heat exchanges at the model surface was simulated with Ocean Heat Flux Model (Delft Hydraulics, 2007) using air temperature, relative humidity and cloudiness observed at Nagasaki Marine Observatory, JMA (Fig. 4.1). Secchi depth was used for the calculation of the heat flux and was set to 12 m with reference to Nagata et al. (1996). All lateral boundaries were forced by water temperature and salinity from the OFES. The horizontal eddy viscosity and diffusivity were set to 1.0 m^2 s^{-1} and 10 m^2 s^{-1}, respectively. Larger scale horizontal eddy turbulence was computed with Horizontal Larger Eddy Simulation (Delft Hydraulics, 2007). The background vertical eddy viscosity and diffusivity were set to 1.0×10^{-3} m^2 s^{-1}. The vertical viscosity and diffusivity were calculated by *k*-*ε* turbulence model. The model calculations were conducted from January 1 to May 31 in each year of 1960–2007 with a time step of 60s.

The model reproducibility was validated using coastal mooring data at M1 near the Sasebo Bay mouth observed from April 18 to May 3, 1997 and M2 near the Seihi Peninsula observed from February 14 to March 1 1999 obtained from JODC (Fig. 4.1). Modeled hydrodynamic was evaluated from the skill score (Warner et al., 2005) and root mean square error (RMSE).

4.1.3 Particle tracking experiment

The eggs and larval transport simulations were performed using Delft3D-PART (Delft Hydraulics, 2007) based on the result of hydrodynamic model. To focus on the variation of the transport condition, this study did not consider a spatial weighting of the egg abundance, and therefore a constant number of the particles (a thousand) were released from each release point over the area (Fig. 4.1). The release locations of the particles were determined by the SST. In order to estimate the spawning temperature, the relationship between the distributions of egg and the SST were analyzed. Using the SST data at the sampling station of egg, averaged egg density was calculated at every 0.1˚C interval from 13˚C to 23˚C. The range between minimum and maximum temperatures at which averaged egg density exceeds 1.0 ind. per tow then defined as the spawning temperature. From 1960 to 2007, the release site was determined applying the spawning temperature and the modeled SST distribution in each year. The

particles were released in April 1 and May 1 at 00:00 because these two months are thought to be main spawning season (Yamashita, 1984) and spawning takes place around midnight (22:00–2:00) (Matsuoka et al., 2002). Horizontal dispersion was set to 1.0 m s^{-2}. Since anchovy eggs are distributed in the surface water (Iseki and Kiyomoto, 1997), all particles were released from the surface layer, and the positions of the particles were calculated every 1 hour until 30 days after release. Particles were assumed to be passive drifter, and this study did not consider active vertical and horizontal movement of the particle. When the particles were located inside of the offshore or coastal zones after 30 days, it was considered successful transport (Fig. 4.1). Transport success was represented in percentage of transported particle to the total number of released particles. In this study, the transport success in April and May was averaged. To specify the range of distribution of particle, two dimensional kernel density method, which can smooth the density distribution, was performed at the end points of all released particle. The estimated kernel density of the particles was compared with the observed distribution of larval anchovy.

4.1.4 Analysis of the environmental conditions

To clarify the factors influencing the eggs and larval transport, the environmental conditions were analyzed. The volume transport of the Tsushima Warm Current was calculated from the current velocity passing through the eastern channel of the Tsushima Strait (Fig. 4.2). The effect of the Kuroshio was also considered. The volume transport of the Kuroshio passing through the section at 32˚N, 128.5–129.5˚E was calculated. The horizontal current velocity (zonal and meridional components) in the Goto-Nada Sea was defined as the same zone in the Chapter 3. In order to elucidate the effect of spawning ground condition on the transport success, the size and the center latitude of the spawning ground were considered. The size of the spawning ground was defined as the number of the release points. The center latitude of spawning ground was calculated by averaging the highest and lowest latitude of selected release points. The following analysis refers the size and center latitude of the spawning ground to “spawning area” and “spawning latitude”, respectively.

Satellite images of the SST and chlorophyll-*a* (chl-*a*) were derived from the Moderate Resolution Imaging Spectroradiometer (MODIS), on board the satellites Terra and Aqua. The daily MODIS data of 1 km horizontal resolutions were processed to Level 1b by the Earth Observation Center of the Japan Aerospace Exploration Agency. The satellite images were

analyzed with the vertical structure of modeled hydrodynamics.

4.1.5 Statistical analysis

To examine the difference in the transport success among three regimes, regime-averaged transport success was arc sine transformed before the *t*-test in order to postulate equal variance. The definition of the regimes are warm-regime I (1960–1975), cold-regime (1976–1994) and warm-regime II (1995–2007), following the definition of the Chapter 3.

In order to explore the possible non-linear relationship between the transport success and environmental variables, the generalized additive model (GAM) was used. The GAM represents non-linear relationships between a response and explanatory variables. The general equation of the GAM is given by,

$$\ln\left(transport\ success\right) = \alpha + \sum_{i=1}^{6} s(X_i) + \varepsilon \quad (4.1)$$

where α is the intercept of the model, *s* represents non-parametric smoothing function, which is cubic spline in this study and ε is the residual error. *Xi* is the environmental variables such as the volume transport of the Tsushima Warm Current and the Kuroshio, zonal and meridional current velocity in the Goto-Nada Sea, spawning area and spawning latitude. These six variables were tested to build the relationship with the log transformed transport success. To avoid overfitting, the models were ranked by lower Akaike's information criterion value, and model with lowest AIC was selected as the best model. In this study, environmental variables, which were included in the best model was considered as the influential factors determining the transport success.

4.2 Results

4.2.1 Modeled hydrodynamics

The modeled hydrodynamic field off the western coast of Kyushu was shown in Fig. 4.3. The modeled surface current well reproduced the Tsushima Warm Current in the northern region. The volume transport passing through eastern channel was 1.42 Sv (average of March to April), and this almost agreed with the observed value by ADCP (Fukudome et al., 2010). In the southern part of the domain, the Kuroshio generated a cyclonic eddy. In the Goto-Nada Sea,

relatively weak current (< 0.1 m s^{-1}) was generated, as reported by Odamaki (1982). Time series of the modeled and observed zonal current velocities were shown in Figure 4.4. The model skill score and RMSE were 0.54 and 0.025 m s^{-1} at M1, 0.63 and 0.024 m s^{-1} for M2, respectively. At the M1, modeled hydrodynamic well captured reciprocating current out of the Sasebo Bay. At the M2, modeled current reproduced relative short-term (3 days~) variability, although shorter (~2 days) variation could not be reproduced adequately, because this method interpolated the monthly OFES data to daily value linearly.

4.2.2 Observed and simulated distribution of anchovy egg and larvae

Observed egg and larval distributions were shown in Figure 4.5. The high densities of eggs and larvae were found in the Goto-Nada Sea, and they were also seen in the main stream of the Tsushima Warm Current in May, associated with increase of the SST. The SST range, where egg density had more than 1.0 ind. per tow, was 13.7–19.6˚C and 15.7–20.1˚C in April and May, respectively (Fig. 4.6). In both months, no egg was collected in the southern region where the SST exceeds 21˚C.

The trajectories of the released particle for 30 days were shown in Fig. 4.7. General transport patterns were identified as three types that moved the Tsushima Warm Current, the Kuroshio and the Goto-Nada Sea. Particles that moved westward were likely to be transported to northeast by the Tsushima Warm Current. In this case, most of the particles exited the domain from the northeast boundary within 12 days on average, and some of them could retain in the area along the northwest coast of the Goto Islands and off the Hirado Peninsula. Particles that were entrained in the eddy associated with intrusion of the Kuroshio, tended to remain in the southern Goto-Nada Sea even after 20 days, and most of these particles were not transported to the coastal fishing zone. The surface current in the Goto-Nada Sea tended to carry particles to the region along the coast of Seihi Peninsula and Tachibana Bay by eastward current. The model result was supported by the observed larval distribution that larvae were distributed along the western coast of Kyushu (Fig. 4.5).

Most of the observed larval distribution was consistent with that of eggs, however, eggs and larval density in May has relatively increased compared with April. In addition, larval density in the south of the Goto-Nada Sea was higher than egg abundance but lower in the further south region in May. The kernel density analysis identified the highest density area in the south of the Goto-Nada Sea (Fig. 4.8) where the eddy formed (Fig. 4.3). The kernel density

was relatively high in the north of the Goto-Nada Sea, and the simulated distribution of particles over the domain agreed with the observed larval distribution (Fig. 4.9).

The satellite chl-*a* images showed that primary production was high around the Goto islands and coastal area of the Kyushu, but low in the southern Kuroshio region (Fig. 4.10). A cyclonic eddy with relative high chl-*a* concentration was found in the center of the eddy in the south of the Goto-Nada Sea in April 28, 2005 (Fig. 4.10). The vertical profile of the eddy at the section of 32.8˚N was shown in Fig. 4.11. The cold-water upwelling was identified in the modeled vertical structure in the case of the cyclonic eddy. On the other hand, anti-cyclonic eddy was found in the south of the Goto-Nada Sea with relative warm-water and low chl-*a* concentration in May 14, 2007 (Fig. 4.10). In this case, the water column at the section of 31.5˚N was stratified (Fig. 4.11).

4.2.3 Temporal change in the transport success

Transport success in the offshore zone has increased since the 1990s whereas the transport success in the coastal zone has decreased (Fig. 4.12). As a result of regime-averaged comparison, the offshore transport success in the warm-regime II was significantly higher than that in the warm-regime I, whereas the transport success in the coastal zone was significantly low in the warm-regime II compared with that in the warm-regime I (t-test, $p < 0.05$, Fig. 4.13). The kernel density in the south of the Goto-Nada Sea was also lower in the cold-regime and warm-regime II compared with that in the warm-regime I, and the kernel density in the north of the Goto-Nada Sea was higher in the cold-regime and warm-regime II than that in the warm-regime I (Fig. 4.8).

4.2.4 Relationship between the transport success and environmental conditions

The best model for the transport success in the offshore zone is below,

ln(transport success) = *s*(volume transport of the Tsushima Warm Current)+*s*(volume transport of the Kuroshio)+s(spawning area)
+*s*(spawning latitude)+*s*(zonal current velocity in the Goto-Nada Sea)+*s*(meridional current velocity of the Goto-Nada Sea)

The best model selected all explanatory variables, but the volume transport of the Tsushima Warm Current, spawning area and spawning latitude were statistically significant.

The model for the offshore zone implied that a strong influence of the volume transport of the Tsushima Warm Current and the spawning area and spawning latitude on the transport success (Table 4.1). The volume transport of the Tsushima Warm Current showed a negative relationship with the transport success (Fig. 4.14). The spawning area and latitude showed negative and positive relationship with the transport success, respectively.

The best model for the coastal zone is below.

ln(transport success) = s(zonal current velocity in the Goto-Nada Sea)+s(spawning latitude)

On the other hand, the GAM for the coastal zone selected the zonal current velocity in the Goto-Nada Sea and spawning latitude. The relationship between transport success and zonal current velocity in the Goto-Nada Sea showed that the effect of current velocity becomes strong when the eastward current dominates with two exceptions of 1998 and 2007 having low confidence level (Fig. 4.15). The spawning area showed the negative effect on the transport success.

Long-term variations of the environmental variables which had significant effect on the transport success, were shown in Figure 4.16. The volume transport of the Tsushima Warm Current and zonal current velocity in the Goto-Nada Sea showed small decreasing trend. The spawning area and latitude shifted to the northern region approximately 0.4 degree, and the spawning area has decreased.

The relationship of the juvenile and immature anchovies catch with egg and larval abundance in the ECS was examined. The low egg and larval abundance was found in the 1980s, but it began to increase in the 1990s (Fig. 4.17). The offshore catch showed significant correlation with the abundance of egg ($r = 0.647$, $p < 0.01$) and catch of larvae ($r = 0.724$, $p < 0.01$, Fig. 4.18), but neither egg ($r = 0.173$, $p > 0.05$) nor larvae ($r = 0.282$, $p > 0.05$) showed significant relationship with coastal catch.

4.3 Discussion

4.3.1 Distribution of anchovy eggs and larvae related to the environmental conditions

The spawning of anchovy off the western Kyushu spatially varied, however the possible spawning temperature was restricted within about 6 ˚C. Previous study showed wider and higher temperature range of spawning for the Japanese anchovy off the Pacific coast (Takasuka et al., 2008). However, off the western Kyushu, higher SST (> 21 ˚C) associated with the

Kuroshio seems to limit the spawning of anchovy. It was therefore suggested that interannual variations of the Kuroshio intrusion could be responsible for determining the southern limit of the spawning ground. However, the spawning and transport of eggs and larvae in the other months should be considered for further understanding of recruitment variability in western coast of Kyushu. As a result of the comparison of distribution of egg in April and May, it was suggested that the main stream of the Tsushima Warm Current could be a spawning ground with the warming of the surface water.

The patterns of particle trajectory indicated that most of the released particles are able to reach the fishery ground within 30 days after release. It was suggested that the horizontal current in the Goto-Nada Sea and Tsushima Warm Current would have important role in the transport of the eggs and larvae. The particles entrained in the eddy associated with the Kuroshio were unlikely to be transported to the offshore and coastal zones. On the other hand, surface current in the Goto-Nada Sea and the Tsushima Warm Current were likely to contribute the recruitment of anchovy both in the offshore and coastal fishery zones.

Observed distribution of eggs and larvae suggested that they are transported to the northern and eastern region where are the high chl-*a* concentration area, and some of the eggs and larvae are entrained in the frontal eddy caused by intrusion of the Kuroshio (Fig. 4.7). The satellite images and modeled hydrodynamics suggested that the upwelling of the nutrient rich water enhances primary production in the south of the Goto-nada Sea (Fig. 4.10). Regarding the role of the frontal eddy in larval anchovy, Kimura et al. (1997) showed an enhanced primary production in the eddy caused by the frontal disturbance of the Kuroshio along the central Pacific coast. In addition, the elevated primary production and copepods abundance were favorable for the entrained larval anchovy (Nakata et al., 2000). In the waters off the western coast of Kyushu, the occurrence of the cyclonic eddy was more frequent than anti-cyclonic eddy, and hence, the cyclonic eddy would be a favorable area for growth and survival of the larval anchovy, although entrained larvae were infrequently transported to the offshore and coastal zones. Simulated egg and larval distribution also agreed with those observed characteristics, and therefore the model approach can be useful for the prediction of egg and larval supply in the fishing ground.

4.3.2 Change in the transport success and its relation with climate change

In the offshore zone, the transport success has increased since the 1990s, corresponding

to the fluctuations in the offshore catch. The negative relationship between the transport success in the offshore zone and the Tsushima Warm Current indicated that the eggs and larvae are likely to be retained in the offshore zone under the condition of weak strength of the Tsushima Warm Current. In other words, strong Tsushima Warm Current tends to transport eggs and larvae away from the offshore zone. The positive relationship between the transport success and spawning latitude suggests that the northward expansion of spawning ground is favorable for the offshore retention of the eggs and larvae. From the above results, it was concluded that the weakened volume transport of the Tsushima Warm Current and the northern expansion of spawning ground allowed eggs and larvae more likely to be transported to the offshore zone. This model-based conclusion was supported by the results of relationship of the catch with the eggs and larval abundance. Positive correlations of the offshore catch with eggs and larval abundance indicates that the recruitment variability in the offshore zone is more vulnerable to the initial distribution and amount of egg in the spawning season. These results have clarified the factors for the recently flourished offshore catch that was not explained by the variation in the wind-stress (Chapter 3).

On the other hand, the transport success in the coastal zone has decreased unlike those in the offshore zone. The GAM analysis revealed that the zonal current velocity in the Goto-Nada Sea and spawning latitude are primary factors regulating the transport success in the coastal zone. Positive relationship between transport success and zonal current velocity in the Goto-Nada Sea indicates that the stronger eastward current makes it possible for larvae to reach the coastal fishing zone. On the other hand, negative relationship between the transport success and the spawning latitude indicate that the northern shift of spawning ground was not favorable for the successful transport of larval anchovy to the coastal zone. As the result of the relationship of the catch with the egg abundance and catch of larval anchovy suggested that the coastal catch is more susceptible to the surface current condition between the spawning ground and fishing area. Since the current velocity has weakened and the spawning latitude has shifted to north, both factors have negatively influenced the long-term transport success in the coastal zone. It is therefore concluded that the recently reduced catch in the coastal zone is attributed by the low transport success of the anchovy eggs and larvae.

As demonstrated in the Chapter 3, the averaged catch differed among three regimes. The regime-averaged transport success also showed a significant difference between warm-regime I and warm-regime II, corresponding to those of the regime-averaged catch.

These results can be a reason for difference in the regime-averaged catch between the same warm-regimes. On a basin scale, multi-decadal fluctuations in the stock abundance of pelagic fishes generally exhibits a good agreement with the variation in ambient temperature induced by global climate change because of their optimal temperature for growth and survival. However, this study explained the fluctuations by the multi-decadal changes in the formation of the spawning ground and transport success. Similar approach has investigated the recruitment variability of anchovy (Huggett et al., 2003; Itoh et al., 2009). In the southern Benguela, Hutchings et al. (1998) found restricted spawning ground of South African anchovy (*Engraulis capensis*) for successful recruitment. Furthermore, Roy et al. (2007) revealed that environmental shift alters the distribution of the spawner leading recruitment failure of South African anchovy. A small change in the spawning ground due to the warming of SST has potential to lead major changes in the recruitment of anchovy, and thus continuous global warming trend may constitute a great threat to the sustainable fishery in the study region.

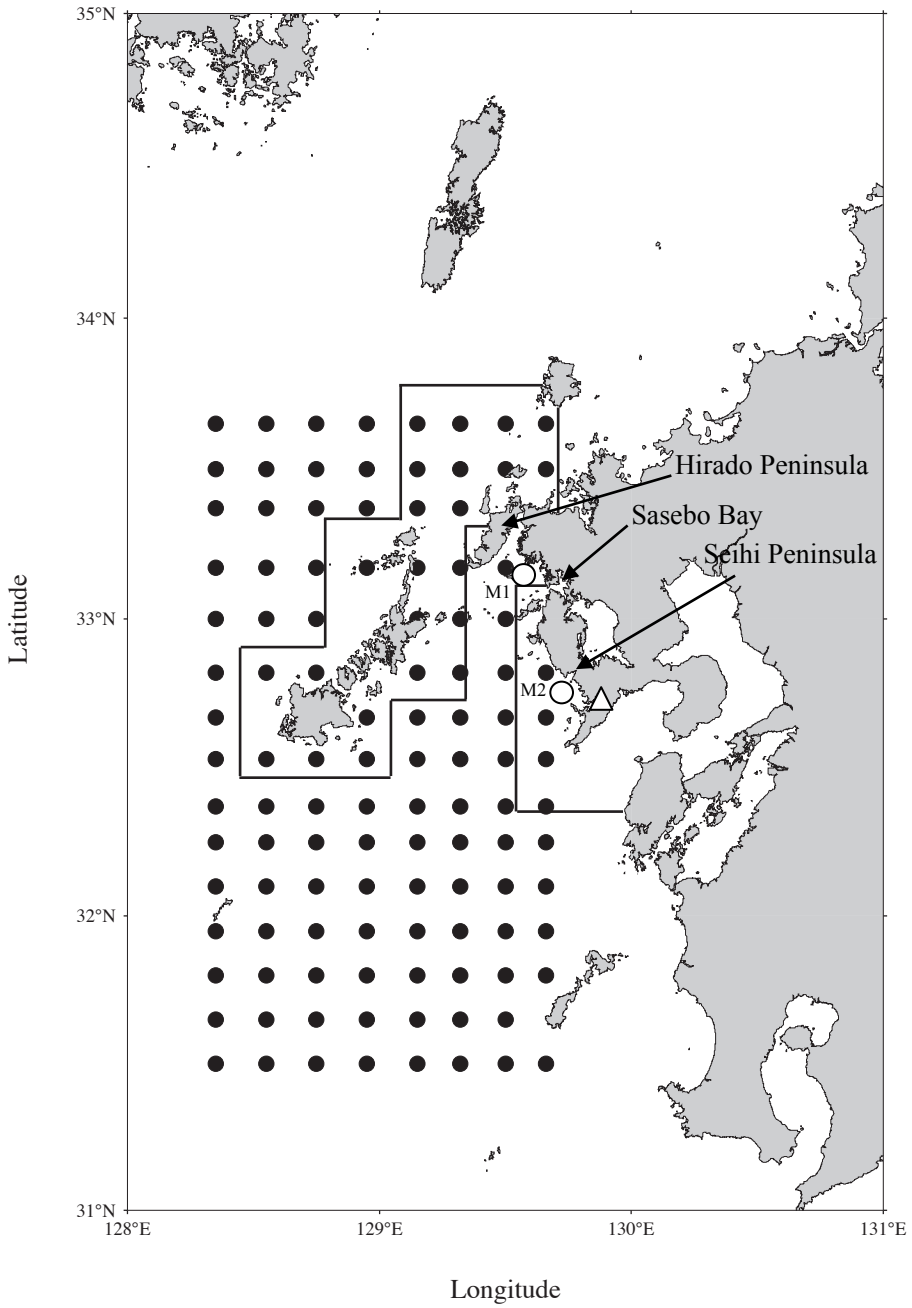

Fig. 4.1 Map of the modeled area. Black circles indicate particle release points. Solid lines indicate boundaries of offshore and coastal zones. Japan Meteorological Agency, Nagasaki Marine Observatory, is represented by triangle. White circles indicate coastal mooring stations.

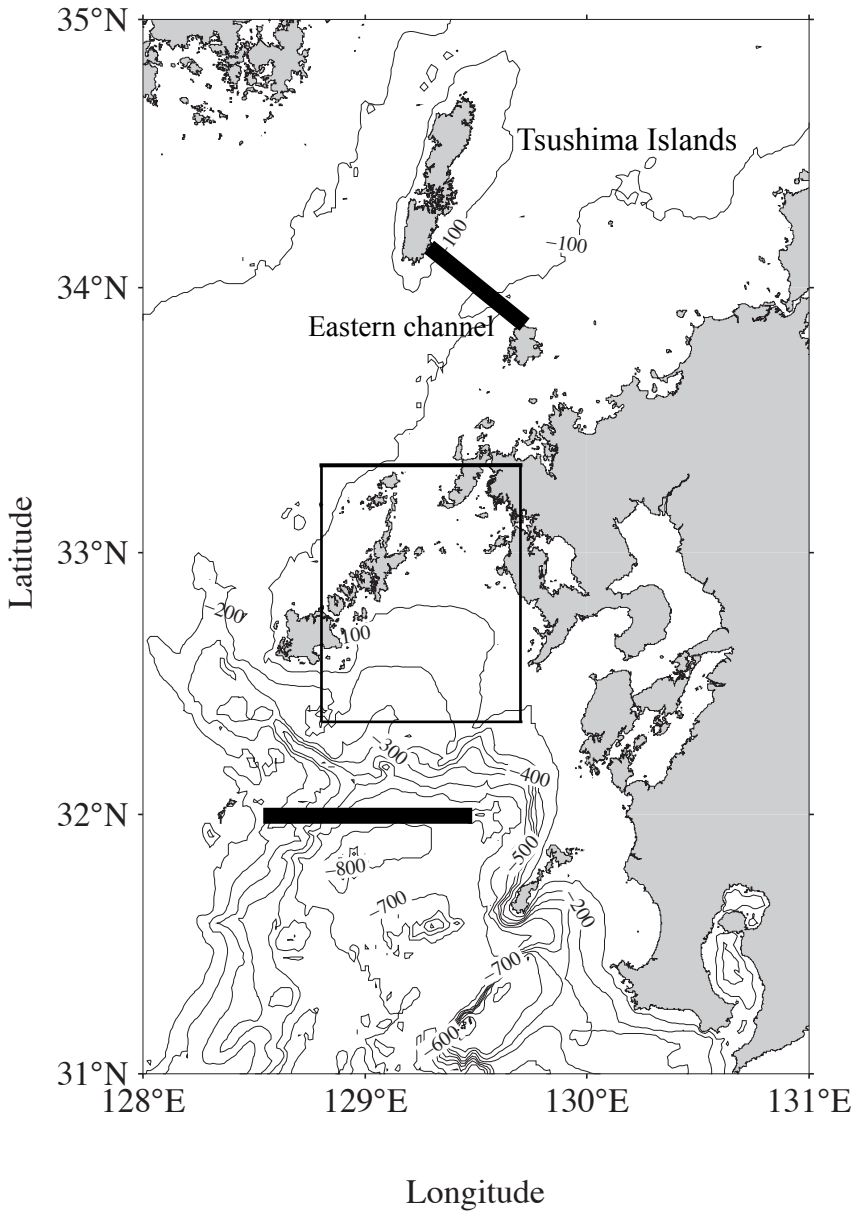

Fig. 4.2 Definitions of environmental conditions. Bold lines indicate each sections for calculating the volume transport of the Tsushima Warm Current and Kuroshio Current. The rectangle indicates the area definition of the Goto-Nada Sea defined for this study.

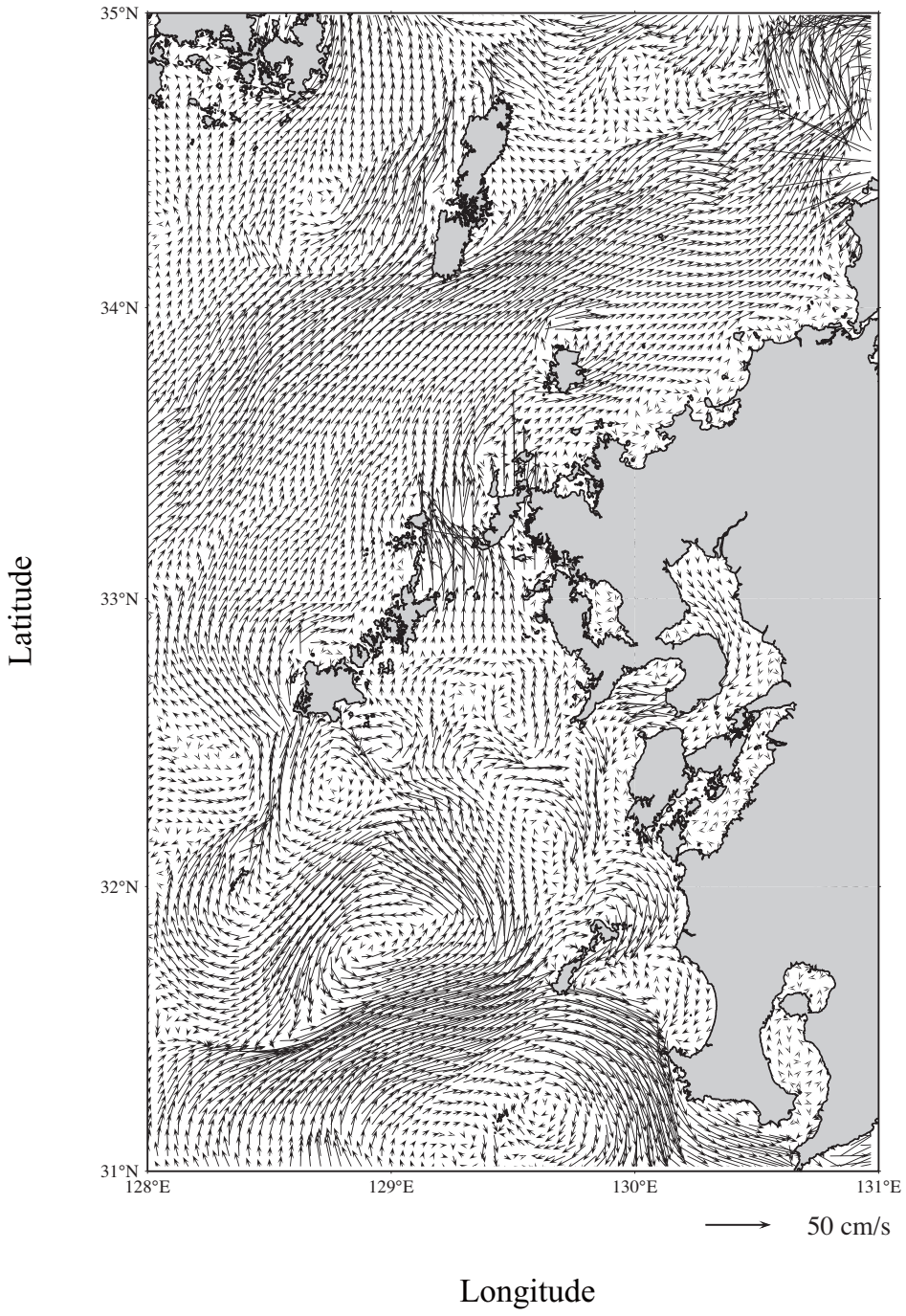

Fig. 4.3 Modeled hydrodynamic field off western Kyushu in April 1 1960. Arrows indicate current direction and speed.

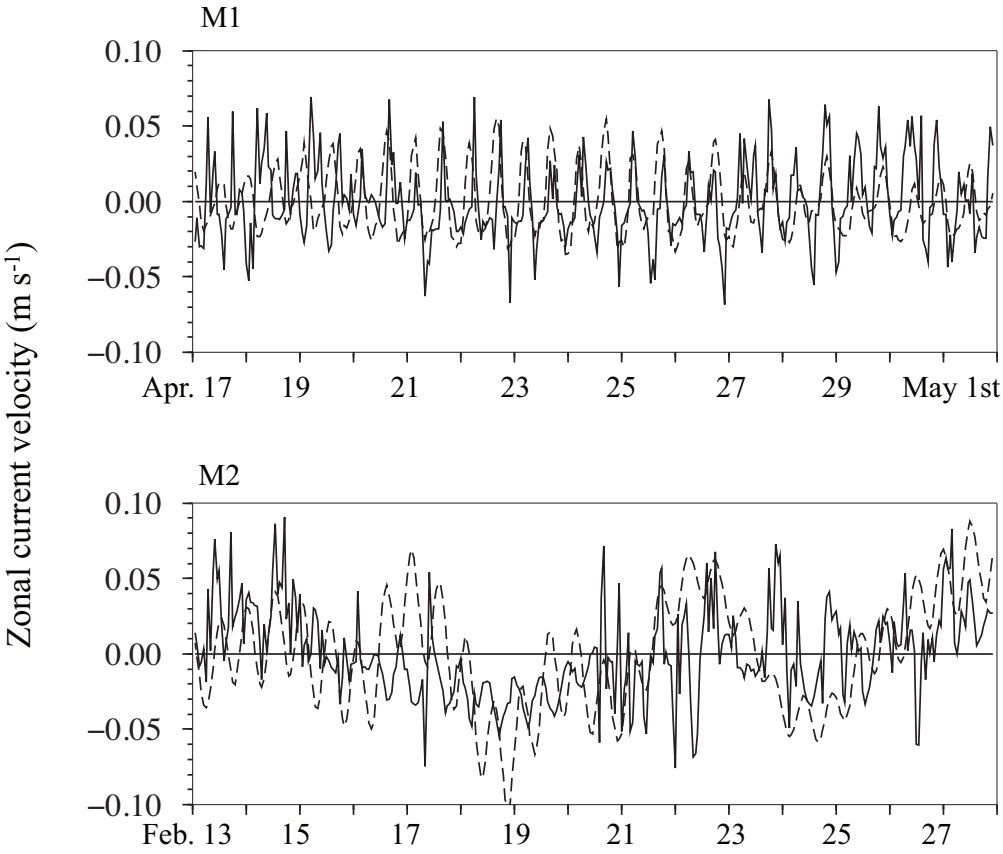

Fig. 4.4 Times series of modeled (dashed line) and observed (solid line) zonal current velocity at M1 in 1977 and M2 in 1999.

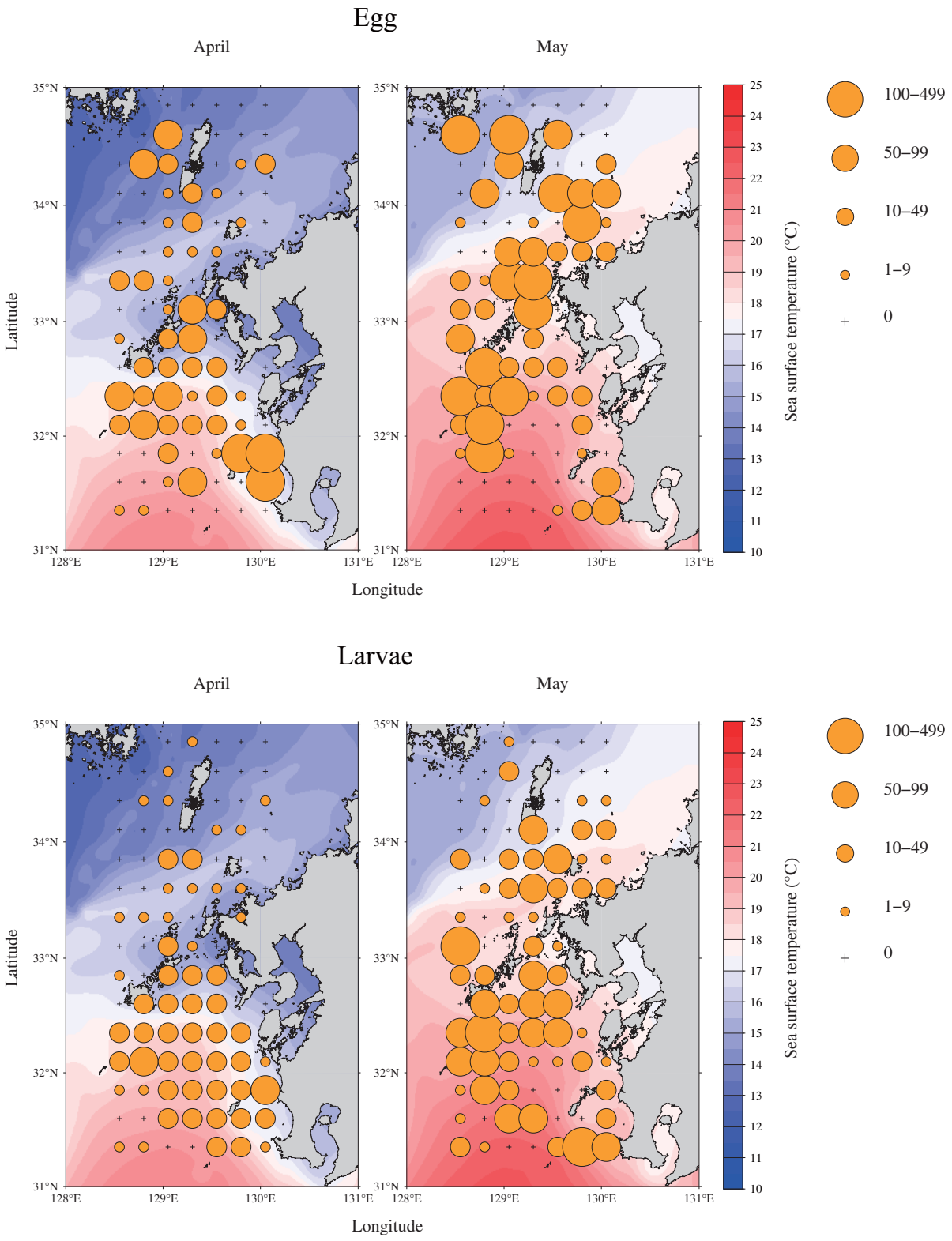

Fig. 4.5 Observed eggs and larval distributions off western Kyushu in April and May averaged from 1960 to 1973. Size of the circle indicates the number of eggs or larvae (ind. per tow). Background color indicates SST averaged from 1960 to 1973.

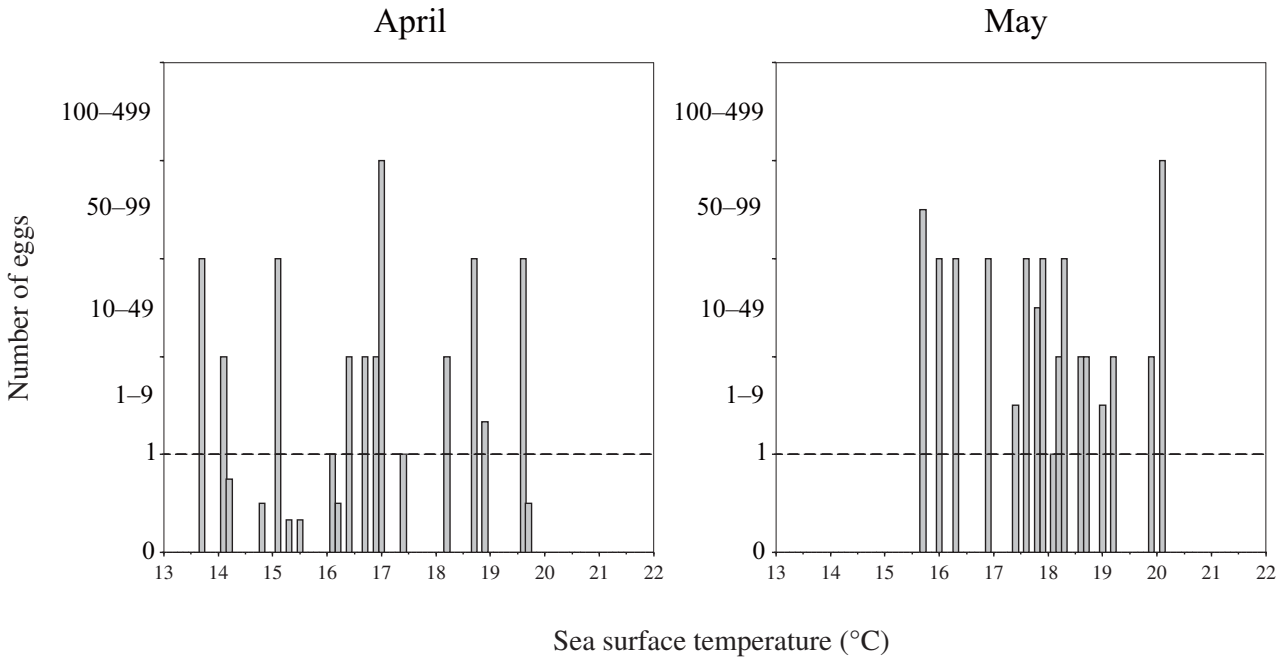

Fig. 4.6 Number of eggs at 0.1˚C interval between 13–22˚C. Dashed lines indicate 1.0 individual per tow.

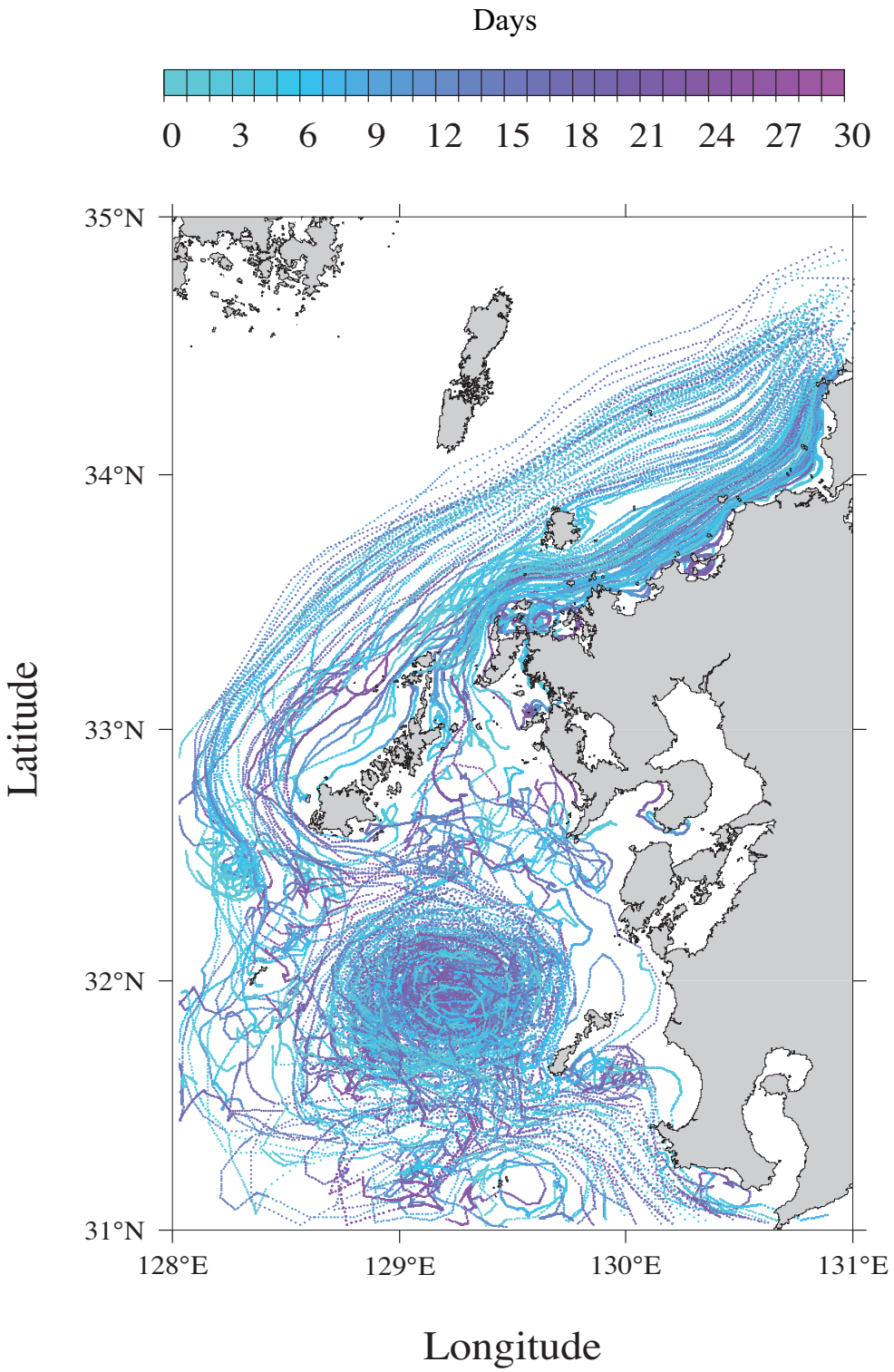

Fig. 4.7 Trajectories of particle for 30 days. Color indicates elapsed time since the release.

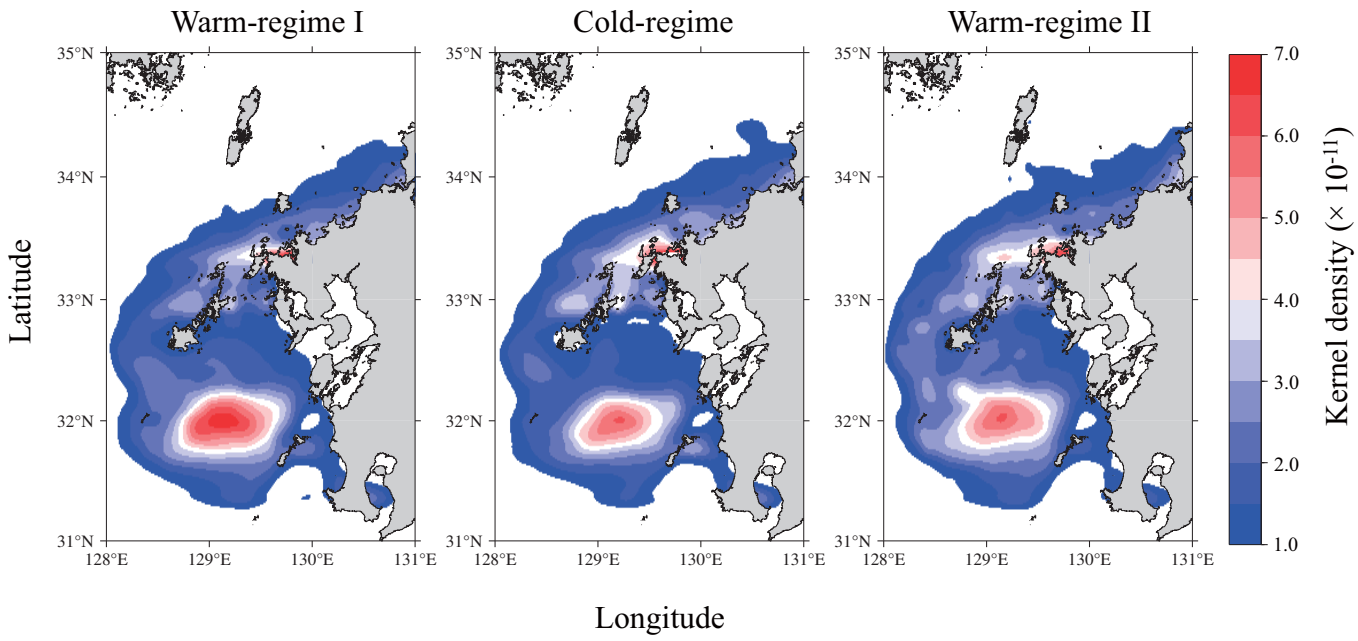

Fig. 4.8 Simulated particle distribution represented by kernel density in three regimes.

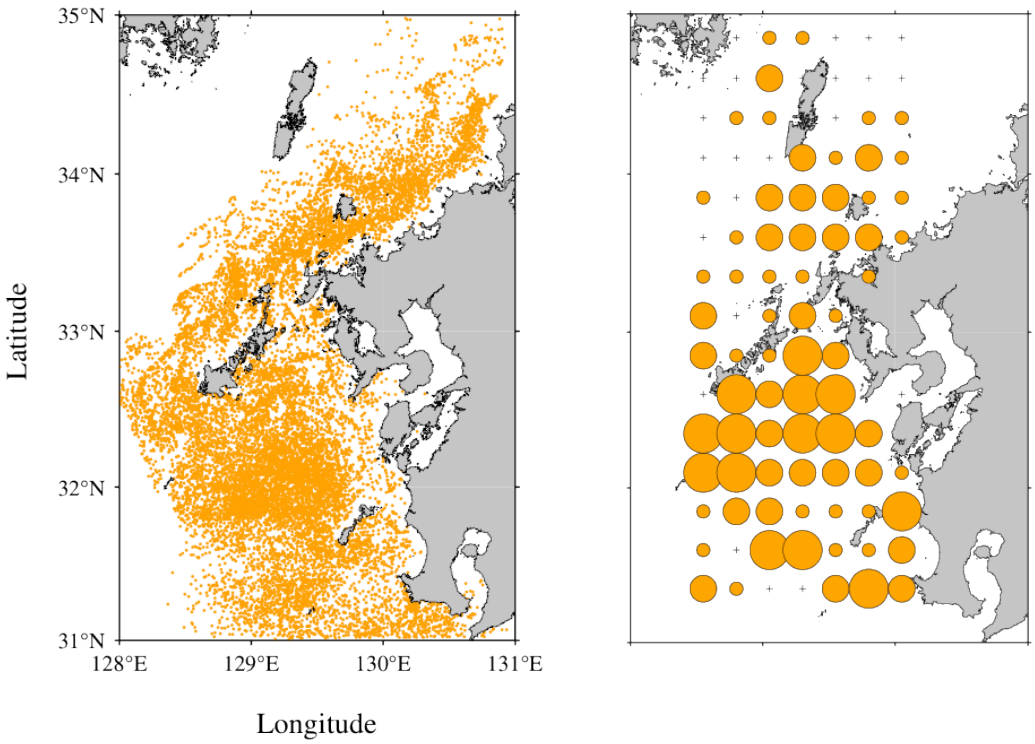

Fig. 4.9 Simulated (left) and observed (right) larval distribution.

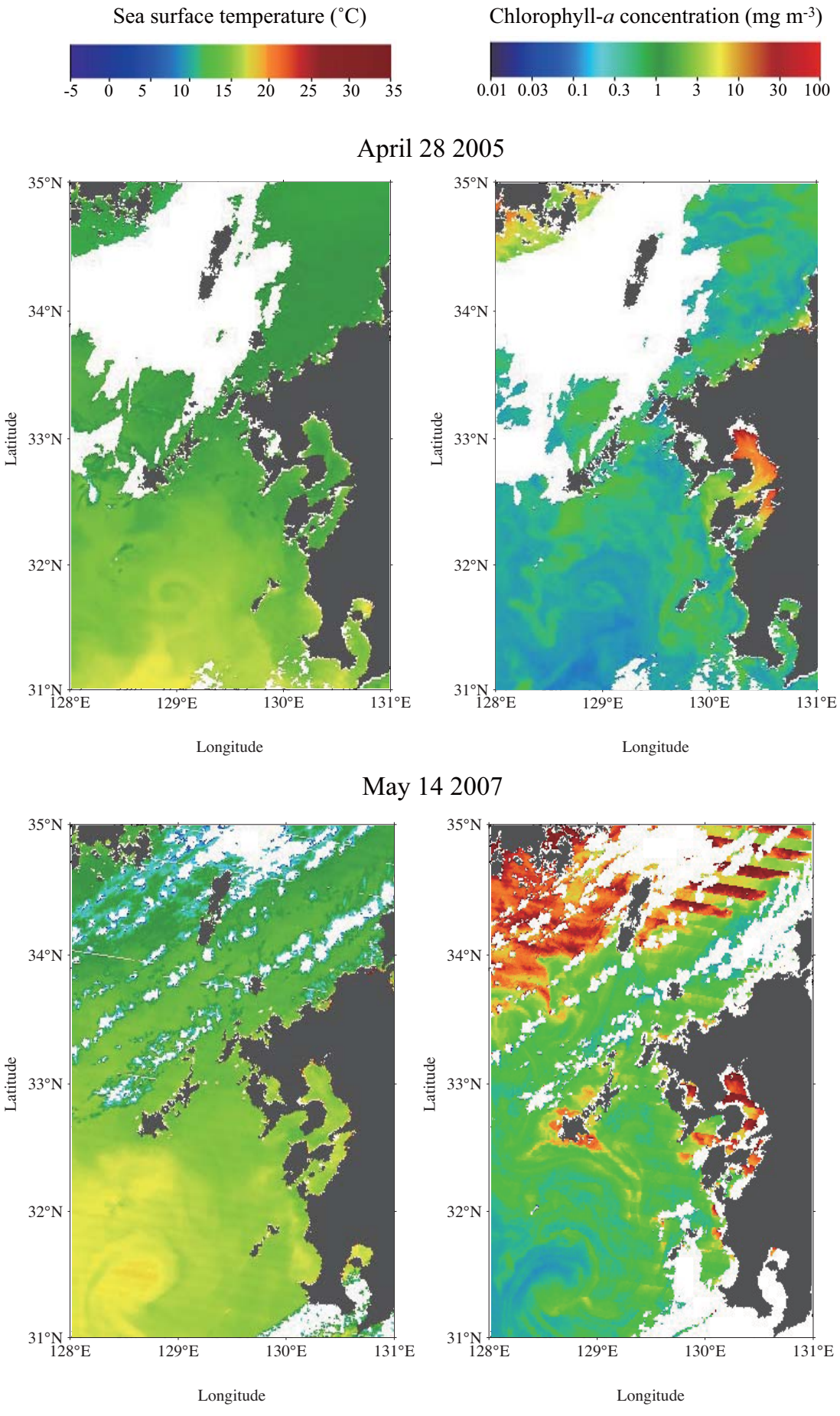

Fig. 4.10 Satellite images of the SST (left) and chlorophyll-*a* concentration (right) showing the cyclonic eddy (upper) and anti-cyclonic eddy (lower).

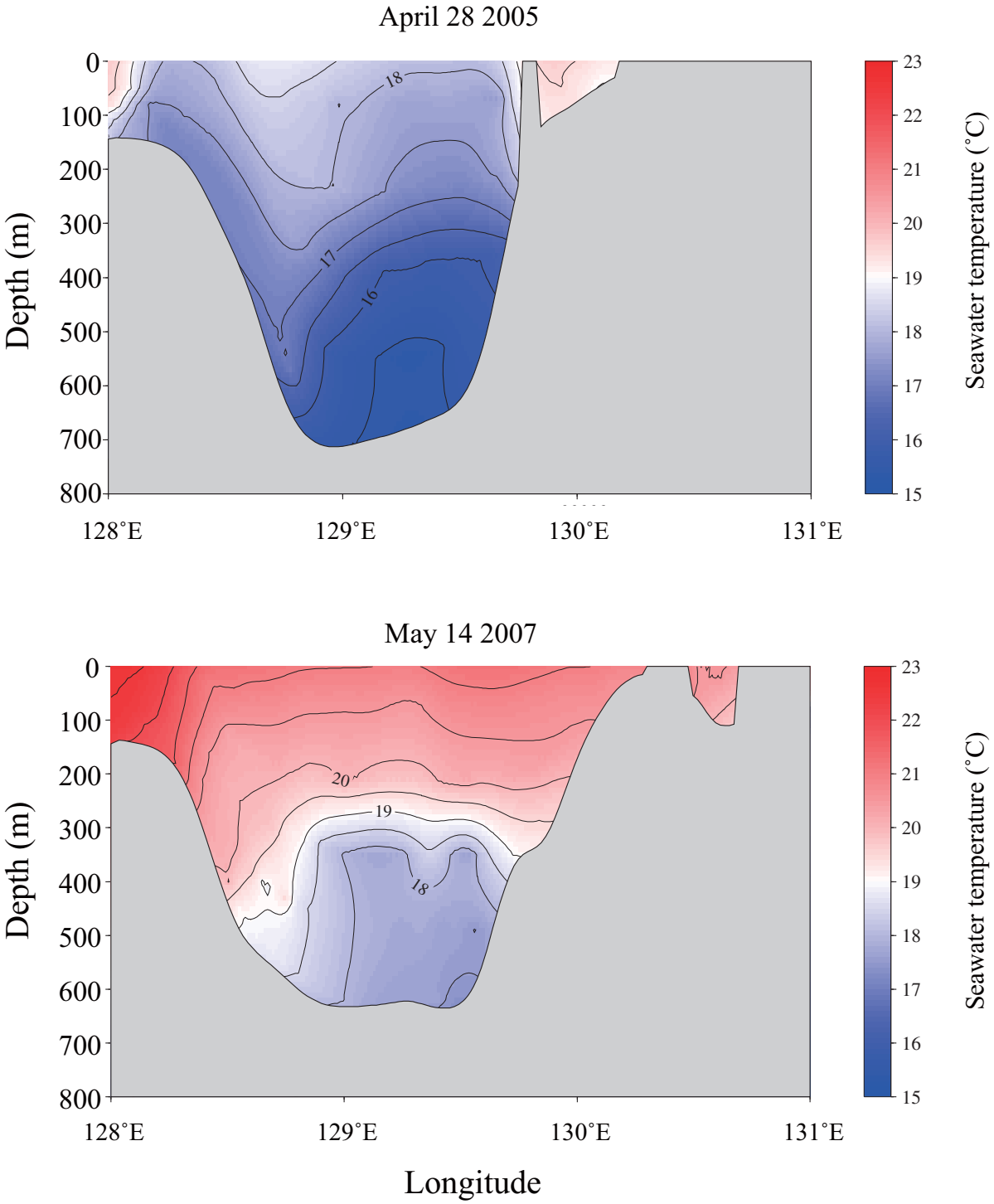

Fig. 4.11 The vertical profile of the seawater temperature at the section of 32.8˚N (upper) and 32.5˚N (lower).

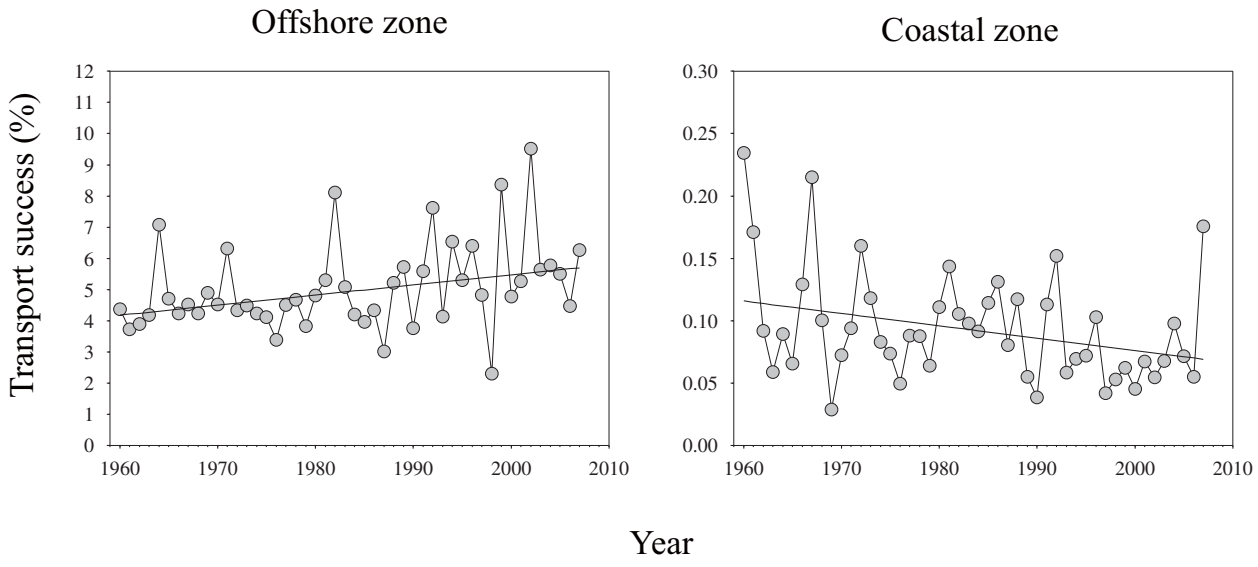

Fig. 4.12 Time series of the transport success in the offshore (left) and coastal (right) zones. Linear trend was indicated by solid lines.

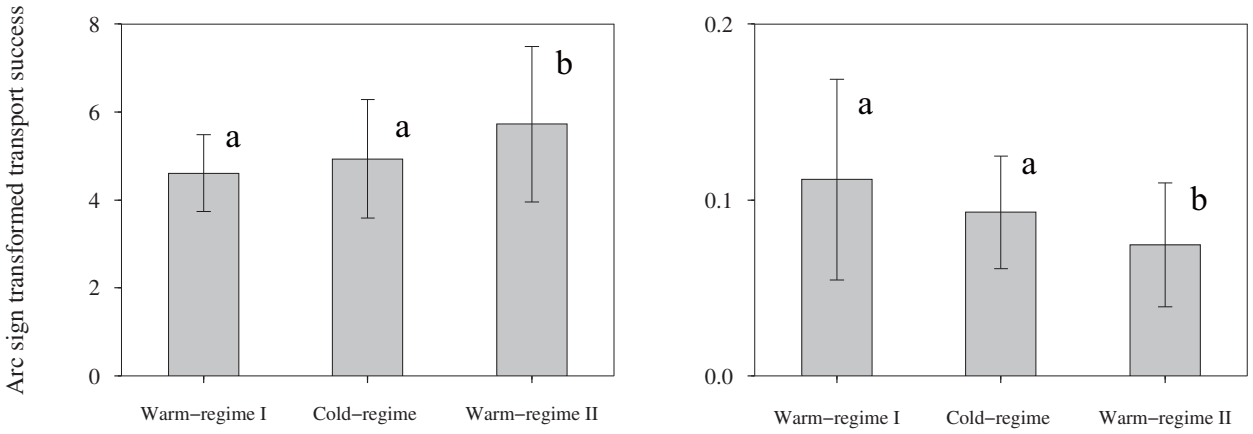

Fig. 4.13 Regime averaged transport success in the offshore (left) and coastal (right) zones. Error bar indicates SD. The different letters in each panel indicate significant differences.

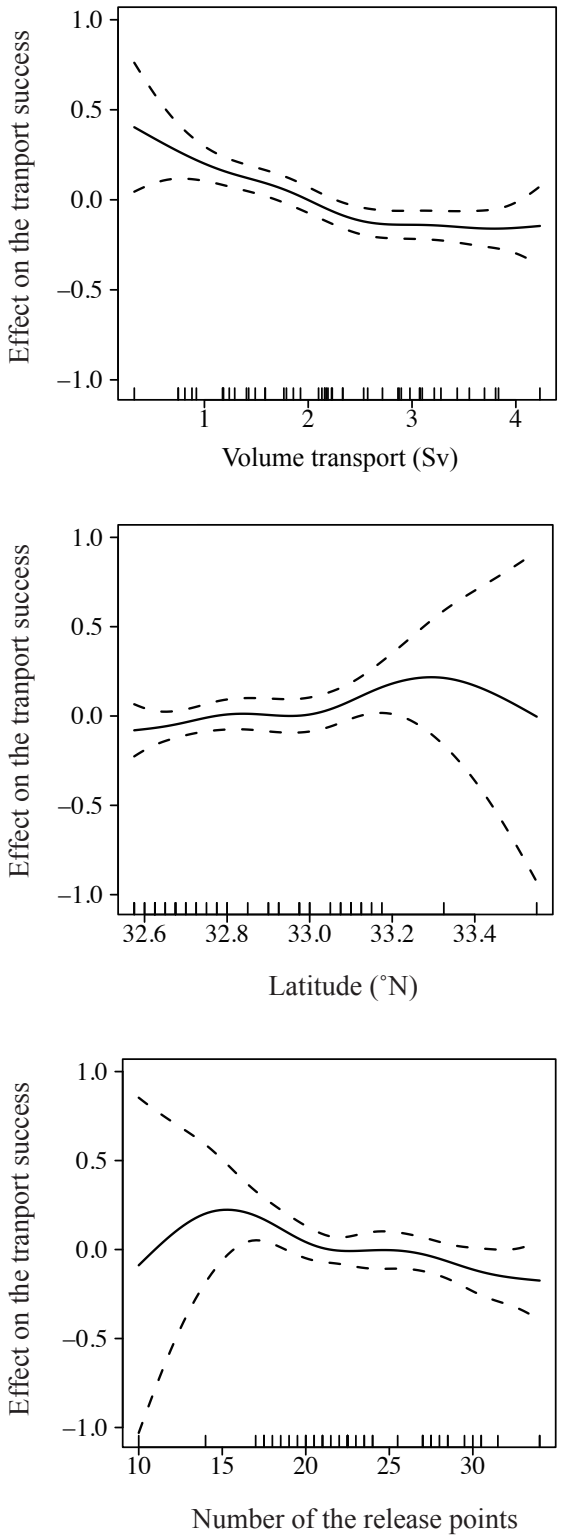

Fig. 4.14 Relationships between the transport success in the offshore zone and environmental variables. Dashed line indicates 95% confidence interval. Ticks at the bottom represents data points.

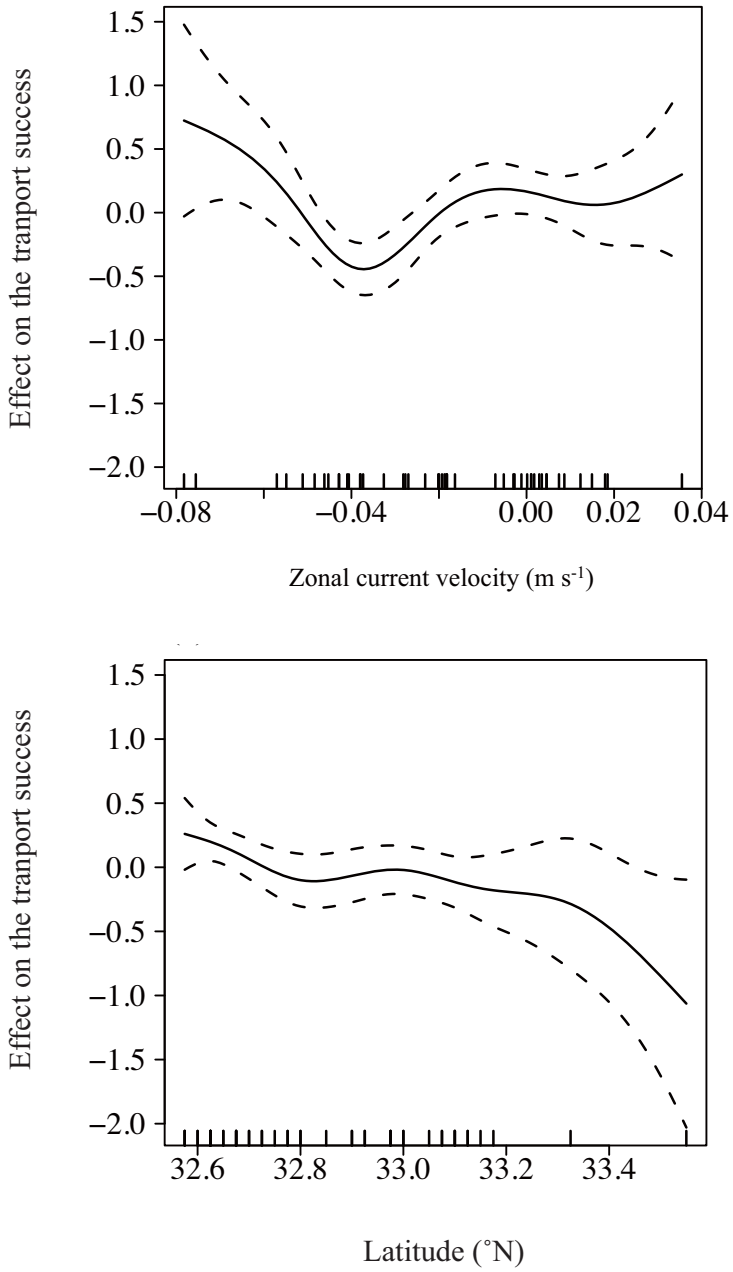

Fig. 4.15 Relationships between the transport success in the coastal zone and environmental variables. Dashed line indicates 95% confidence interval. Ticks at the bottom represents data points.

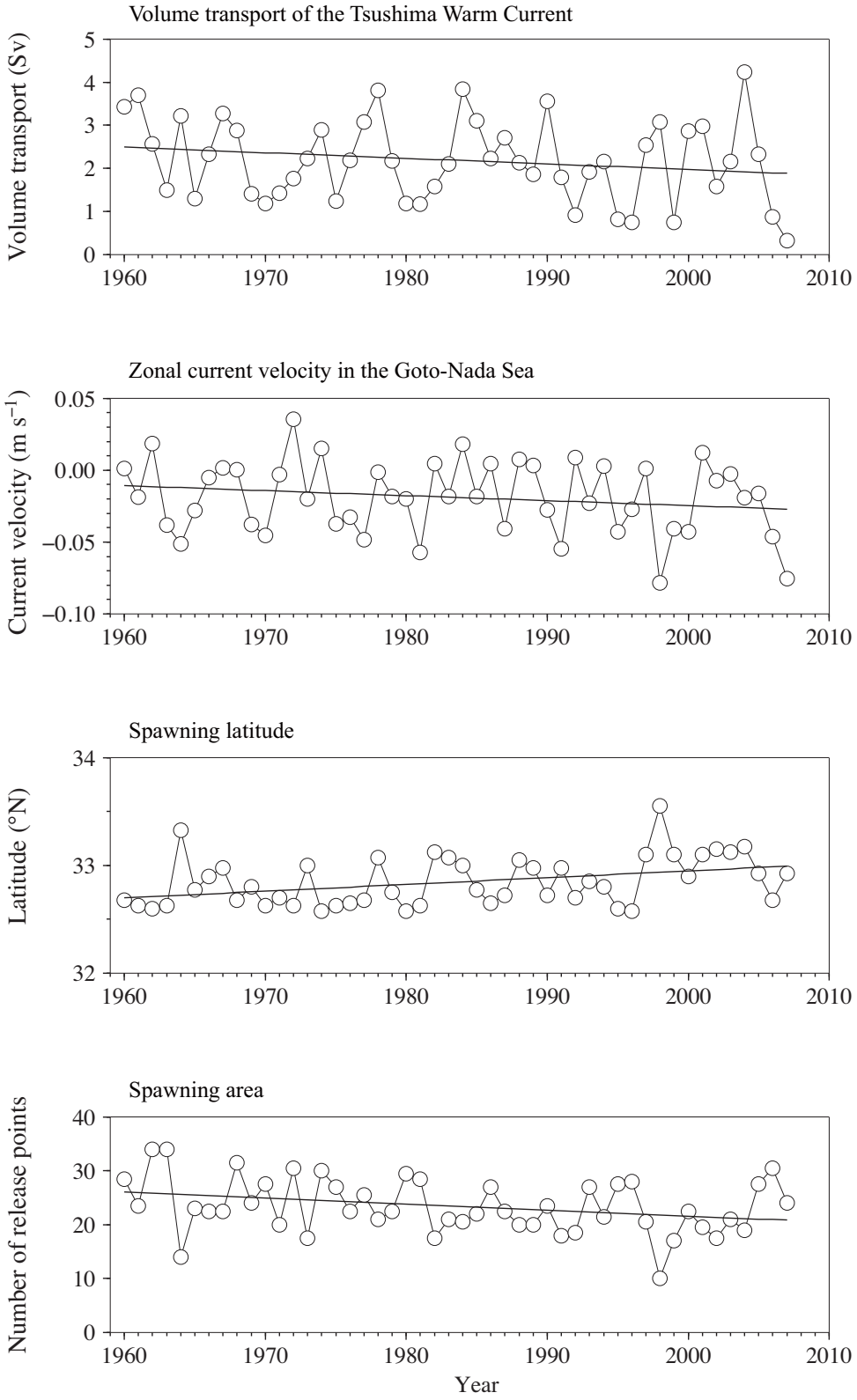

Fig. 4.16 Time series of environmental conditions which were estimated to have influence on the transport success. Solid lines represent linear trends.

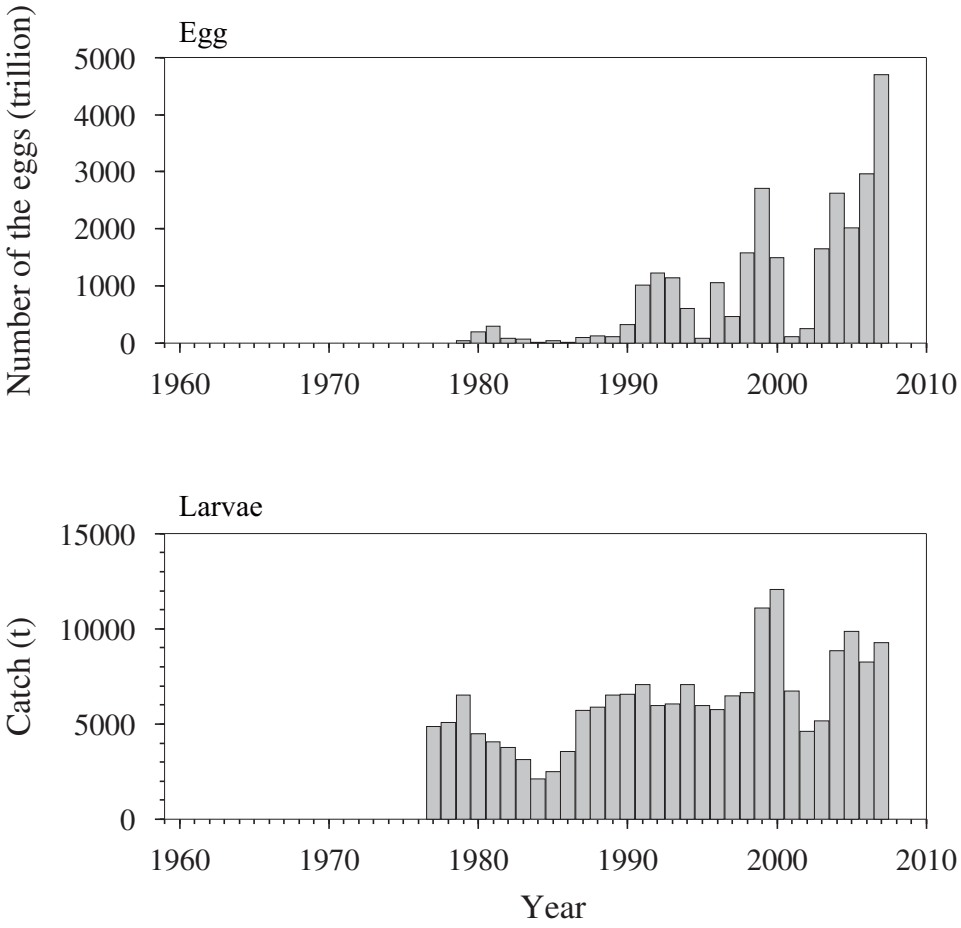

Fig. 4.17 Time series of abundance of egg and catch of larval anchovy in the East China Sea.

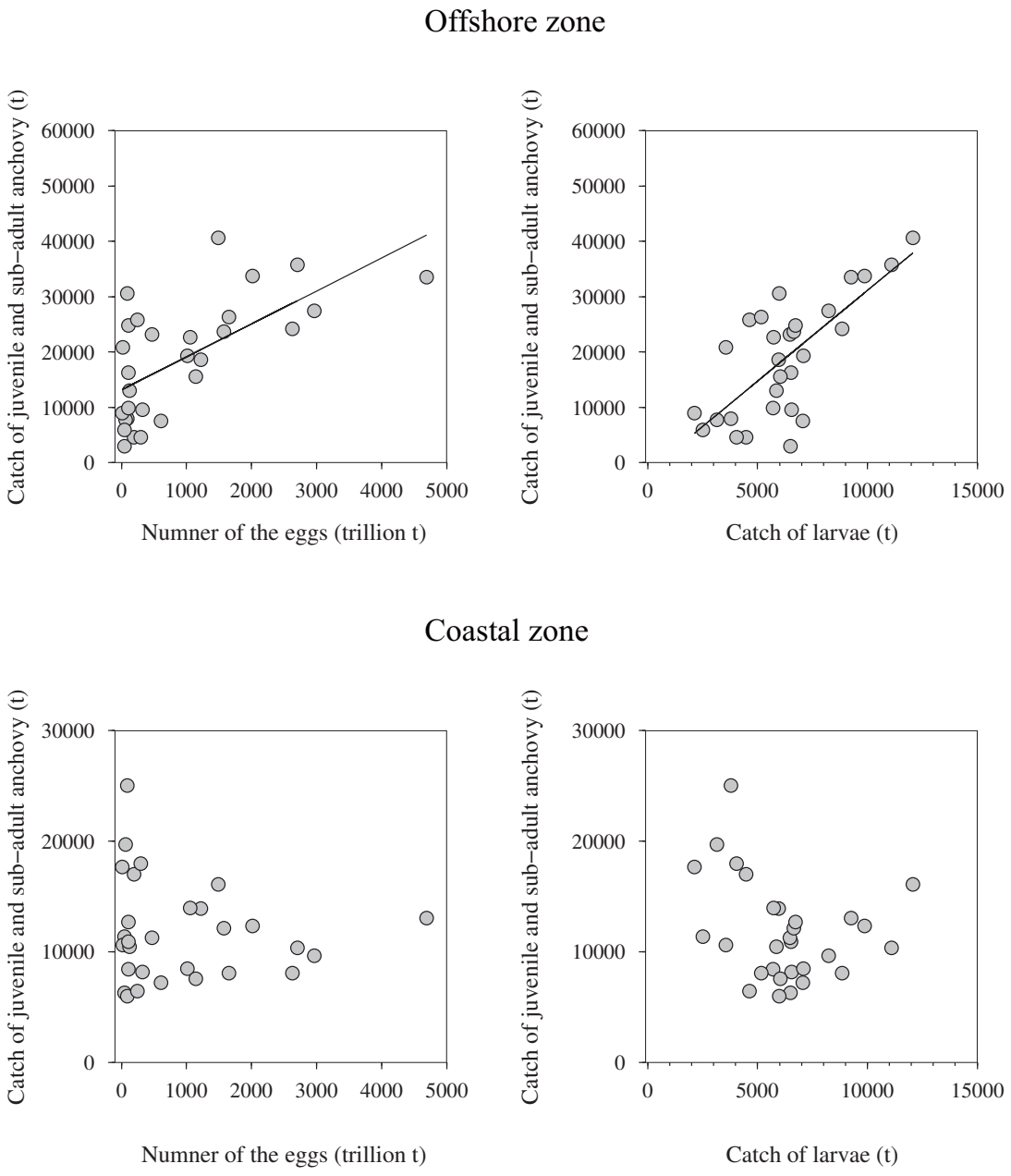

Fig. 4.18 Comparison of the catch of juvenile and sub-adult anchovy in the offshore and coastal zones with eggs and larval abundance in the East China Sea.

Table. 4.1 Effective degrees of freedom, *p*-value of the selected variables, and deviance explained and generalized cross validation (GCV) of the best model for Offshore and coastal zones transport success.

Offshore zone				
Predictors	Effective degrees of freedom	*p*-value	Deviance explained (%)	GCV
Volume transport of the Tsushima Warm Current	3.846	0.001	90.5	0.026
Volume transport of the Kuroshio	3.876	0.103		
Zonal current velocity in the Goto-Nada Sea	4.347	0.092		
Meridional current velocity in the Goto-Nada Sea	4.006	0.193		
Spawning area	4.169	0.018		
Spawning latitude	3.572	0.001		

Coastal zone				
Predictors	Effective degrees of freedom	*p*-value	Deviance explained (%)	GCV
Volume transport of the Tsushima Warm Current	-	-	46.6	0.169
Volume transport of the Kuroshio	-	-		
Zonal current velocity in the Goto-Nada Sea	5.153	0.001		
Meridional current velocity in the Goto-Nada Sea	-	-		
Spawning area	-	-		
Spawning latitude	4.040	0.027		

- indicates not selected

Chapter 5

Estimation of the future change of anchovy recruitment in response to global warming

The recent interest of fisheries oceanography is heading for the future projection of fisheries resources after global warming (Kimura et al., 2010; Blanchard et al., 2012; Tian et al., 2012; Okunishi et al, 2012). Since the south of the ECS is functioning as the spawning ground for many other fishes, and anchovy in this sea has an important role as prey organism for those predatory fishes, changes in the anchovy stock may have a great impact on the marine ecosystems. In this chapter, future changes in coastal ocean environment and anchovy recruitment were investigated on the basis of anthropogenic global warming scenario.

5.1 Data and methods

5.1.1 Evaluation of the future environmental change

Future environmental changes were analyzed using the result of the Model for Interdisciplinary Research on Climate (MIROC) high-resolution forecasting experiment (Kawamiya et al., 2005). MIROC forecasting experiments were conducted under the IPCC A2 carbon dioxides emission scenario of Special Report on Emission Scenarios (SRES, IPCC, 2000). The SRES A2 emission scenario assumes an undergoing very heterogeneous society characterized by a strong regional identity and high economic development. Under the A2 scenario, atmospheric CO_2 is estimated to reach 30 Gt yerar^{-1} in 2100 (Fig. 5.1). MIROC consists of 0.1˚ horizontal grid and 26 vertical layers with data of water temperature, salinity and horizontal and vertical current velocities.

In order to investigate the biological influence of global warming on larval anchovy, change in growth rate assumed to be temperature dependent was considered. Three days-mean growth rate (mm day^{-1}) before capture was calculated by a function of the SST (Yasue and Takasuka 2009, Fig. 5.2), as follows.

$$Growth\ rate = 0.108 + 0.023SST \tag{6.1}$$

Temporal change in growth rate was calculated using spatially averaged SST over the model domain. As for the prey environment for larval anchovy, winter (December to February)

mixing layer depth was estimated. Since copepods are dominant prey organism for anchovy (Islam and Tanaka, 2009) and the zooplankton biomass is correlated with the phytoplankton biomass in the ECS (Hwang et al., 2013), this study assumed that winter mixing layer can be used as an indicator of the food availability through the primary production in spring bloom. The mixing layer depth was defined as the depth that the temperature vertically changes more than 0.5 ˚C.

5.1.2 Hydrodynamic model

To simulate future ocean circulation in the study area, hydrodynamic model was developed using Delft3D-FLOW (Delft Hydraulics, 2008). Model area ranged from 31 to 35˚N and 128 to 131˚E, and consisted of a 2×2 km orthogonal grid cell. The vertical resolution has 5 σ-grid layers with a 20% thickness of the depth. The model bathymetry was constructed from 500 m mesh data obtained from JODC. The model boundary conditions were forced by daily horizontal current velocity at west and south boundaries, and hourly tidal height at north and east boundaries. The MIROC-high was used for forcing west and south boundaries. Since MIROC-high has 0.1˚ horizontal resolutions, model results were linearly interpolated to 0.02˚ for the calculation of the coastal circulation model. The tidal height at the north and east boundaries were calculated using NAO.99Jb model (Matsumoto et al., 2000). The model sea surface was forced by wind-stress obtained from MIROC-high. Air temperature, relative humidity and cloudiness from MIROC-high were used for the calculation of the heat exchanges at the model surface simulated with the Ocean heat flux model (Delft Hydraulics, 2008). All lateral boundaries were forced by water temperature and salinity. The horizontal eddy viscosity and diffusivity were 1.0 m^2 s^{-1} and 10 m^2 s^{-1}. Larger scale horizontal eddy turbulence was computed with Horizontal Larger Eddy Simulation (Delft Hydraulics, 2008). The background vertical eddy viscosity and diffusivity were set to 1.0×10^{-3} m^2 s^{-1}. The viscosity and diffusivity were calculated by *k-ε* turbulence model. The model calculations were started from January 1 to May 31 with a time step of 60s for every 10 years during 1950–2100.

5.1.3 Particle tracking experiment

To quantify the future change in the transport process of anchovy eggs and larvae, particle tracking model was run with Delft3D-PART (Delft Hydraulics, 2007). Particle tracking simulations were conducted using the output of the three-dimensional hydrodynamic

model. A thousand particles were released from the spawning ground in April 1 and May 1. Release points were determined considering spawning temperature determined by the same method used in the Chapter 4. Assuming the passive larval duration time, released particles were tracked for 30 days. Definition of the transport success followed the previous chapter. Particle tracking simulation was conducted every 10 years from 1950 to 2100, and averaged transport success for 1950–1990 was defined as the base line (BL) state, which represents before global warming, and 2020–2100 as after global warming. Environmental factors affecting the transport success were also investigated.

5.2 Results

5.2.1 Change in the transport success

The changes in the transport success from 2020 to 2100 are shown in Figure 5.3 with the BL transport success. The BL transport successes were 6.2% in the offshore zone and 0.2% in the coastal zone. Under the A2 scenario, transport successes were lower (4.2%) than the BL in the offshore zone, whereas those to the coastal zone (0.2%) did not show clear differences with the BL (Fig. 5.3).

The changes in the environmental factors such as the volume transport of the Tsushima Warm Current, zonal current velocity of the Goto-Nada Sea, spawning area and spawning latitude are shown in Figure 5.4. The volume transport of the Tsushima Warm Current in theBL was estimated to be 1.8 Sv, whereas that of average of after global warming was projected to be 2.4 Sv. The spawning latitude predicted to shift to north, and reached up to 0.5 degree from the BL. The spawning area in the study region has reduced after global warming with 0.5 degree northern shift of the spawning latitude, and those two factors showed significant negative correlation (r = -0.94, $p < 0.05$). With those changes in environmental conditions, the high kernel density of the particles shifted to the northern region, and the main stream of the Tsushima Warm Current seem to be a center area of particle distribution after global warming (Fig. 5.5).

5.2.2 Changes in growth rate and vertical mixing layer depth

The SST in the study region was 15˚C in the BL, and increased to 19˚C in 2100. As a result of growth rate estimation, it was expected to be higher than the BL (0.53 mm day^{-1}), and reached to 0.60 mm day^{-1} after global warming. The vertical mixing layer depth after global

warming showed shallower depth (average 90 m) than that in the BL (110 m on average)(Fig. 5.6).

5.3 Discussion

Under the global warming scenario, the SST would increase by 4˚C in the study region. In general, large temperature change can be a major factor influencing species-dependent distribution (Huse and Ellingsen, 2008), growth and mortality (Drinkwater, 2005; Donelson et al., 2010; Neuheimer et al., 2011). However, this increased SST may not seriously impact on anchovy vital functions, because of their high temperature optima for growth (peak at 22 ˚C, Takasuka et al., 2007). Seawater temperature change resulted from global warming would induce indirect effect on anchovy recruitment through the shift of the spawning ground.

The eggs and larval transport simulation showed a decreasing projection in the transport success in the offshore zone. According to the result of the Chapter 4, it is clear that intensified Tsushima Warm Current and reduced spawning area due to the northern shift of optimal spawning ground are responsible for the future decline in the transport success. An intensified Tsushima Warm Current would transport the particles to the far northeast, and therefore a less amount of particles remained in the offshore fishery zone within 30 days. The suggested increasing trend of the volume transport of the Tsushima Warm Current under the global warming possibly originated with an acceleration of the Kuroshio owing to the changes in the wind-stress over the North Pacific (Sakamoto et al., 2005).

The future growth rate of larval anchovy was estimated to be faster than the BL. Similar studies have reported the significant change in the fish growth rate resulted from global warming. Ito et al. (2013) reported that the growth rate of juvenile Pacific saury (*Cololabis saira*) would decrease as a result from the increased SST. Hashioka and Yamanaka (2007) studied future ecosystem change in the western North Pacific using ecosystem model, and pointed out that spring bloom predicted to be decreased due to the reduced nutrient concentration after global warming. Field and laboratory experiments have revealed that the change in day length resulted from the future shift of the spawning season and area would cause change in the growth rate of marine fishes (Shoji et al., 2011). An acceleration of growth rate was projected in this study, however, field and laboratory experiments found that the growth rate in the higher temperature would be limited by the food availability (Takahashi and Watanabe, 2004). In this study, it is projected that the strengthened vertical stratification due to

the temperature rise, causes mixing layer depth to be shallower than the BL. It implies that a lower primary production during spring bloom would occur through the less nutrient supply from the deep water. Since zooplankton is main prey for larval anchovy, growth and survival of anchovy needs to be evaluated practically by the abundance of zooplankton. Here, zooplankton density of 650 ind. m^{-3} in the western coast of Kyushu is assumed with reference to Tanaka et al. (2006). Future change in the zooplankton biomass has not been estimated in the ECS. As a reference, Ito (2007) investigated future change in the zooplankton biomass using ecosystem model, and reported that the zooplankton biomass estimated to be decreased by 50% in the Kuroshio-Oyashio mixed water region. According to the above knowledge, the zooplankton biomass is assumed to drop to approximately 300 ind. m^{-3} in the western coast of Kyushu in 2100. Furthermore, rearing experiments done by Takahashi and Watanabe (2004) reported that the lower survival rate of larval anchovy in the high temperature condition (21˚C) than that in the low temperature (17˚C) under the same food supply level of 300 nauplii $fish^{-1}$ d^{-1}. Since the SST in the western coast of Kyushu is estimated to increase to 19˚C in 2100, larval anchovy would experience low survival condition due to the low zooplankton availability.

The low food availability resulted from the decreased primary production would limit larval growth, which consequently results in low survival. Thus, even if the growth rate were accelerated by increased temperature, reduced food availability would limit the growth and survival of larval anchovy in the future. In this study, the food availability was evaluated from the winter mixing depth, however recent studies reported the primary production in the ECS have decreased possibly due to the Three-Gorges Dam project (Chen, 2000). Therefore, the effects of future change in the nutrient supply from the Yangtze River should be considered in the future study. Although some of the recent studies reports the hiatus and uncertainty in global warming phenomenon (Fyfe et al., 2013; Kosaka and Xie, 2013), preliminary estimation of this study can provide a useful information on a possible effect of global warming on the marine ecosystem in the ECS.

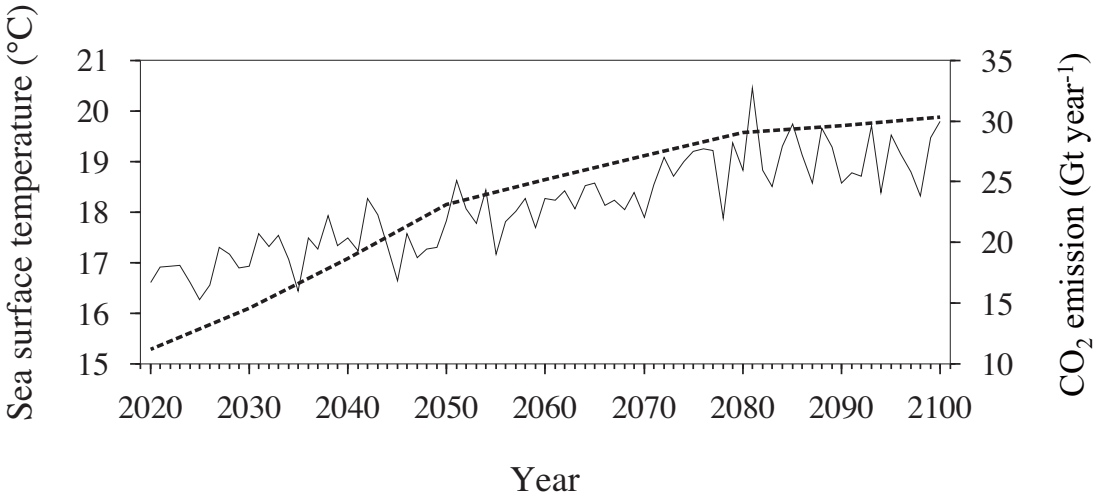

Fig. 5.1 Predicted changes in SST (solid line) in the study area and CO_2 emission (dashed line).

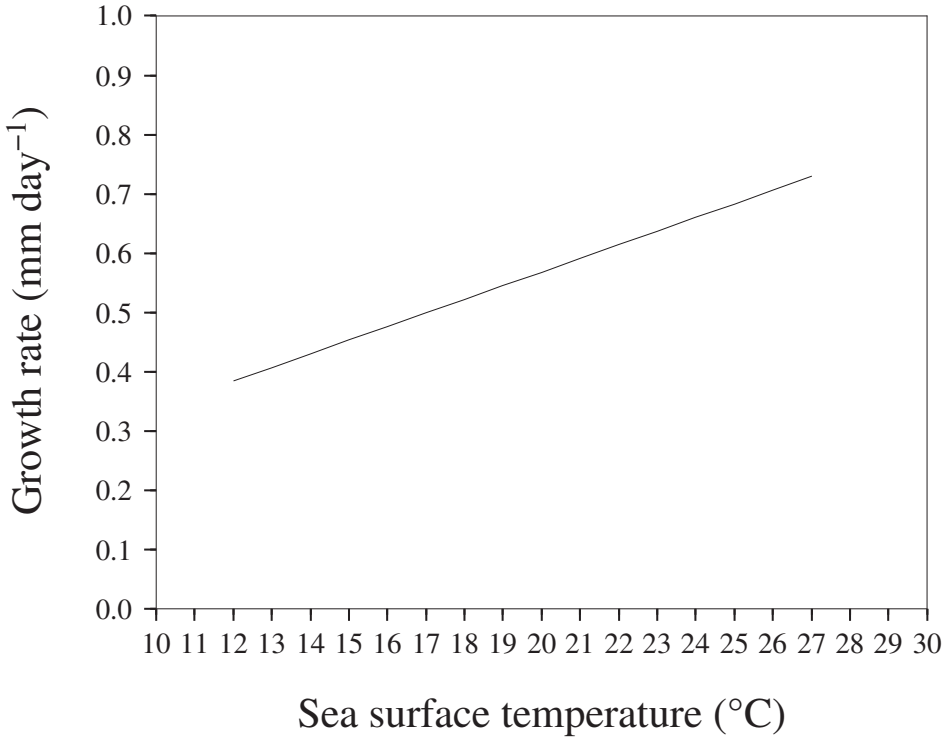

Fig. 5.2 Relationship between SST and larval growth rate proposed by Yasue and Takasuka (2009).

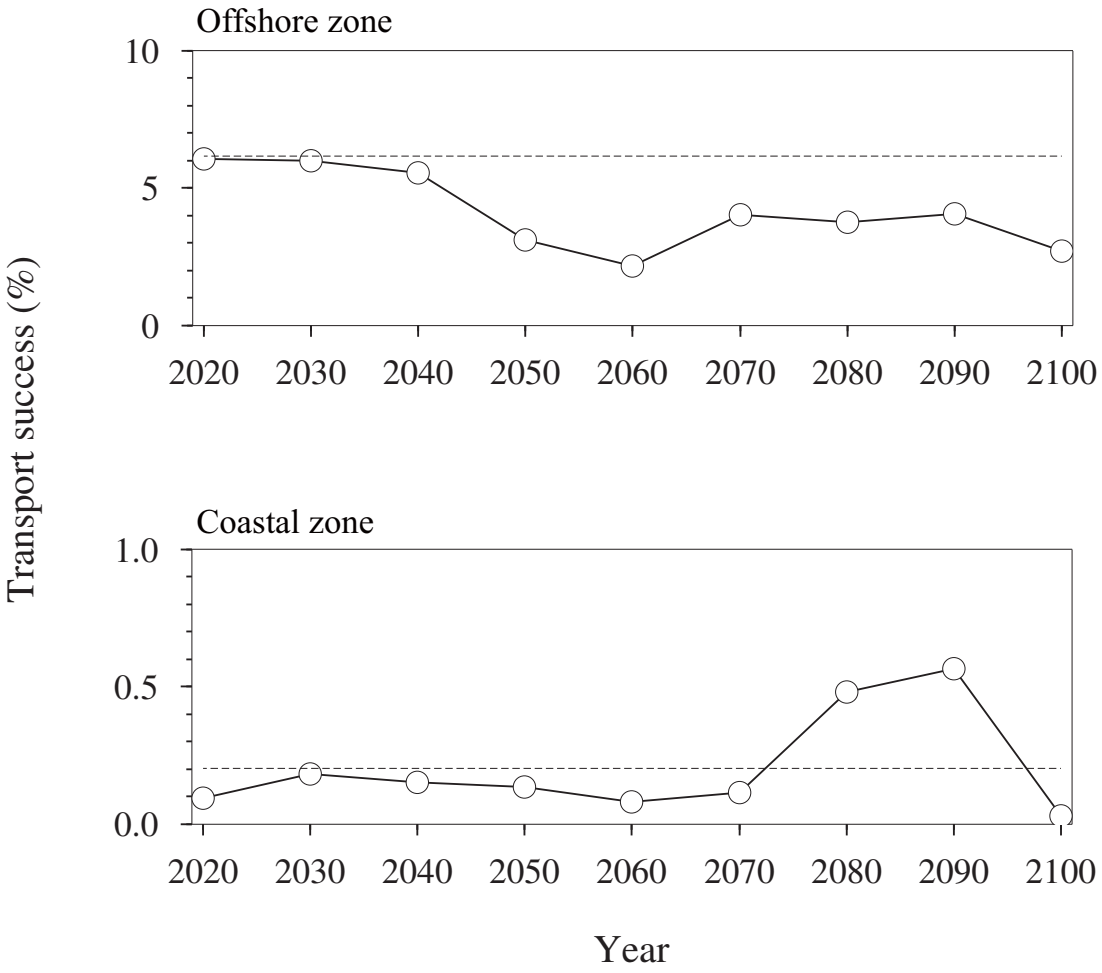

Fig. 5.3 Time series of the transport success in the offshore and coastal zones after global warming. Dashed lines represent the BL.

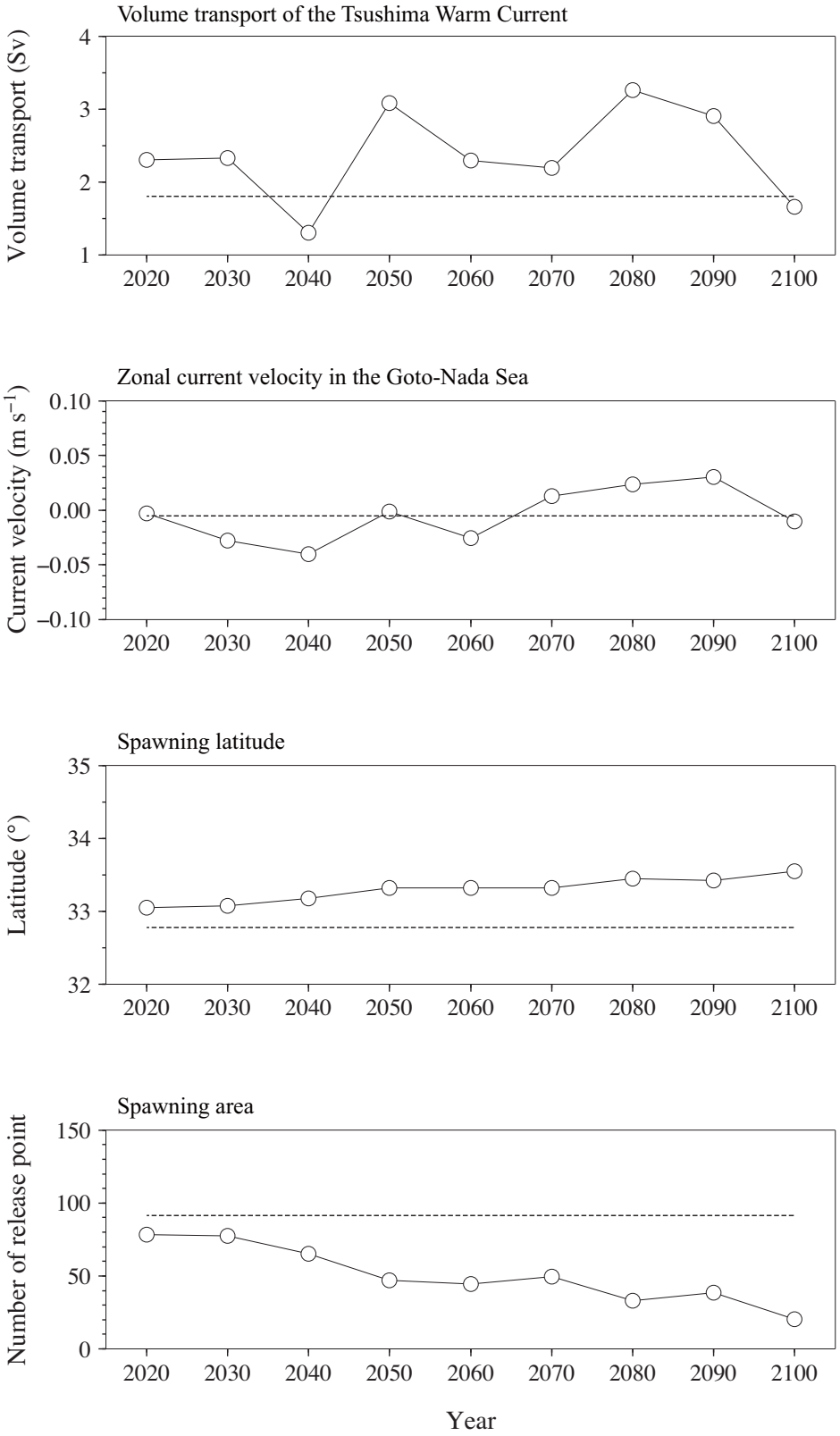

Fig. 5.4 Time series of environmental conditions which are estimated to have influence on the transport success. Dashed line represents the BL.

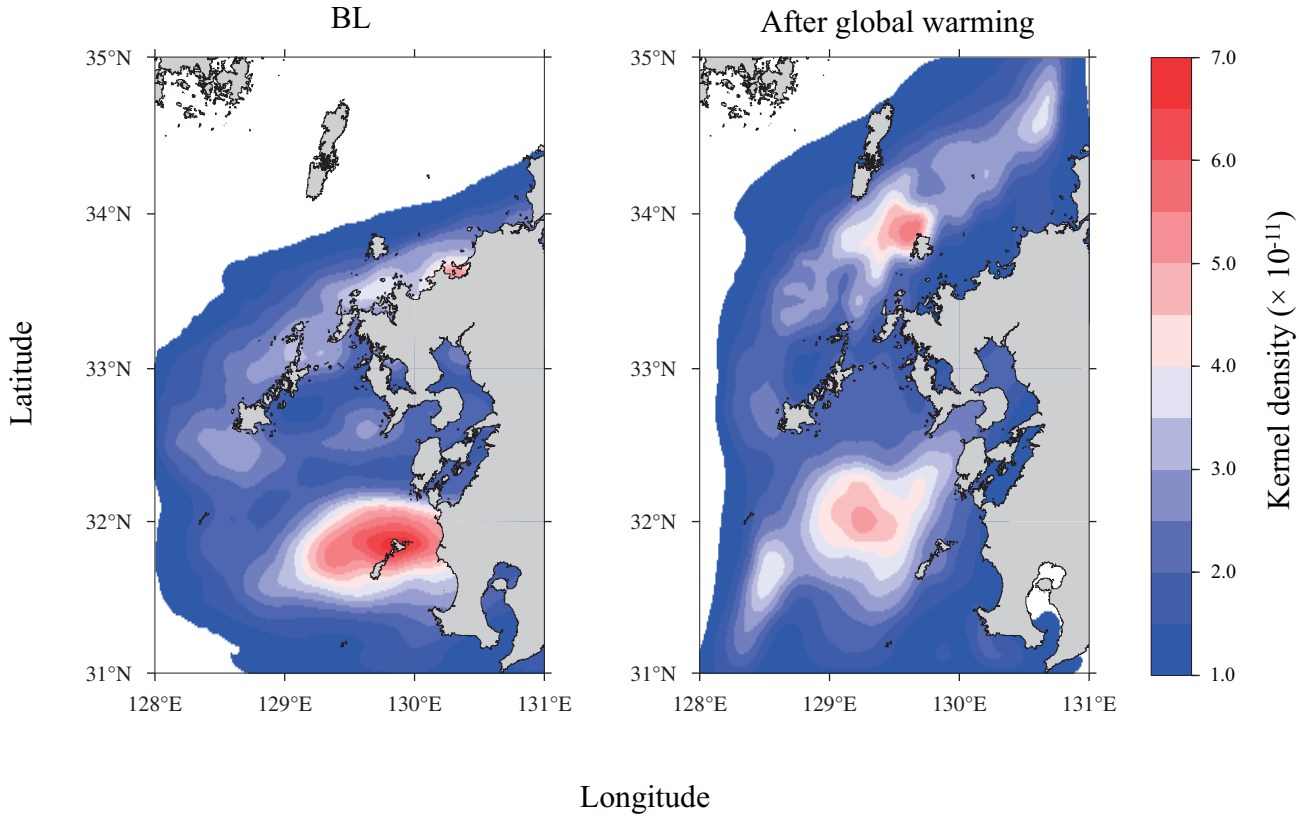

Fig. 5.5 Distribution of kernel density of the particles after 30 days in BL and after global warming.

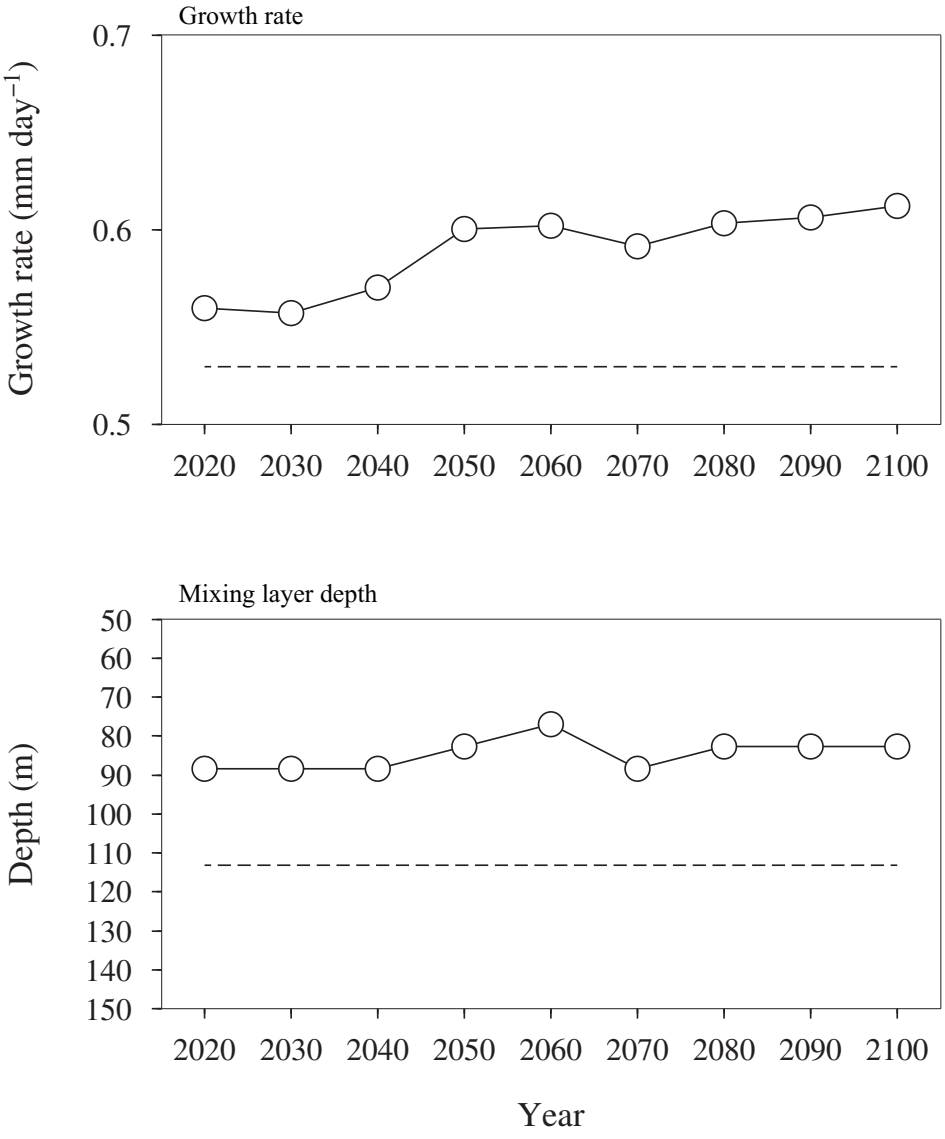

Fig. 5.6 Time series of the growth rate and mixing layer depth. Dashed lines represents the BL.

Chapter 6
General discussion

6.1 Impact of climate change on coastal ocean environment and fisheries resources

In this study, influence of global climate change on the regional scale environmental change was found to be significant. Although a number of studies have reported the SST trends in the regional ocean, present study is different in that this study achieved explaining the causes of the SST variation mechanistically and quantitatively, and also this study can be a persuasive case study that provides an applicable mechanism. In the Chapter 2, it was revealed that the changes in sunlight duration, air temperature, and wind speed caused long-term SST variations. In addition, those meteorological parameters showed a close linkage with the wider scale atmospheric change such as the East Asian monsoon and global dimming. Considering the fact that the sunshine reduction and wind decreasing trend have reported in widespread area, it is expected that changes in water temperature may commonly occur in most coastal areas in the mid-latitudes of the Northern Hemisphere in the same manner. In addition, the results confirm that monsoon-driven climate system possibly controls SST variation through the change in local meteorological conditions not only in Omura Bay, but also in the other coastal seas where the East Asian monsoon circulation covers. Quantitative analysis further proposes that coastal ocean can be a useful study area in terms of its role as a "sensor" reacting susceptibly to global climate change. These findings can be more important in this resourceful ocean, ECS, where the natural and human impacts seem dominant (Paerl, 2006). It is also notable that this study showed the reason why the effect of global warming is more evident in winter than in summer, by the fact that the reduced sunlight in summer decreases SST. As discussed in the Chapter 2, CO_2 emission would increase the amount of cloud, and consequently would result in decline of sunlight. Therefore, human activities in the coastal area may also contribute to the regional environmental change. From the results of this study, it is concluded that large-scale climate change effects should be included in the analysis of SST variation, even in local-scale coastal waters.

Multi-decadal variation in the SST could not explain the regional fluctuations in the anchovy catch in the western coast of Kyushu (Chapter 3). The wind condition, which has an important role in regional SST variation (Chapter 2), also could be a key environmental factor

that influences on the regional anchovy catch. The numerical simulations suggested a significant variation in the transport success of anchovy eggs and larvae, and its effect on the coastal fishery (Chapter 4). This finding should be taken into account for the overall understanding of the stock fluctuations, especially in the coastal fishing ground, because the transport process probably becomes dominant in the smaller scale.

As discussed in the Chapter 2–4, the climate variability has remarkably influenced the regional ocean-atmospheric conditions and fisheries resources since the 1960s to the present. Although species that have wider temperature range for spawning and growth, generally insensitive to climate change (Peck et al., 2013), this study proposed the risk of temperature rise that brings on the formation of spawning ground in unfavorable location which consequently leads transport failure. The relationships between the location of spawning ground and recruitment success have been well studied on many fisheries resources (Kimura et al., 2001; Sundby and Nakken, 2008; Rosa et al., 2011). In the present state, the restricted spawning area for the anchovy off the western coast of Kyushu benefit for them to reach the coastal highly productive zone. It is generally accepted that low temperature is threat to larval anchovy, therefore adult anchovy migrates offshore warm waters for spawning where is relative low food availability area. In terms of the strategy of anchovy recruitment, the temperature-dependent restricted spawning area may have been resulted from maximizing the transport success to the favorable nursery ground and minimizing the risk facing low food availability in the offshore water. Previous studies focusing basin scale ocean have discussed the mechanism of multi-decadal fluctuations in pelagic fishes in terms of the direct temperature effect on the growth and survival. On the other hand, this study demonstrated that a small temperature change in the spawning ground have potential to induce large change in the stock fluctuations through the transport process. In the small scale, transport process thought to be equally as influential as the growth and survival conditions.

Future anthropogenic global warming also has potential to result in the serious state for the reproduction of anchovy (Chapter 5). The continuously increasing trend of SST would lead to further shift of the spawning ground toward north, resulting in recruitment failure through the unsuccessful transport of eggs and larvae. In addition to the degraded transport conditions, this study also suggested changes in the growth rate and food availability after global warming. The future food availability would be lowered due to the reduced primary production resulted from the shoaling of the mixing layer depth. As results of unsuccessful transport and low food

availability, the recruitment success of anchovy would decrease after global warming.

The importance of the understanding of fluctuation mechanism of the anchovy stock in terms of their role of key organism linking the lower and higher trophic levels thought to be large particularly in the ECS. Pacific bluefin tuna, which is known as one of the predatory fishes for anchovy (Yamanaka, 1963) has their spawning ground in the south of the ECS. It is reported that the restricted spawning ground of Pacific bluefin tuna is advantageous for successful transport to the nursery ground around Japan (Kitagawa et al., 2010). The results of this study implied that the future oceanic changes in the marginal seas in the ECS could be a threat to Pacific bluefin tuna because Kuroshio transports larvae to the western coast of Kyushu, which is known as one of their habitats for feeding and overwinter (Kitagawa et al., 2006). The simulated distribution of the present larval anchovy (Fig. 4.8) overlapped with that of juvenile Pacific bluefin tuna estimated by archival tags (see Kitagawa et al., 2006, Fig. 2). It implies that the distribution of juvenile Pacific bluefin tuna is partly related to the presence of anchovy. If so, global warming could determine the distribution of the Pacific bluefin tuna through not only the change in the ambient temperature but also availability of the Japanese anchovy. Throughout above results, it is concerned that global warming would affect anchovy and their predatory fishes in the study area. Thus, global warming may affect broad range of trophic levels of fisheries resources in the study area.

6.2 Problems of the present modeling approach

The present modeling study has successfully demonstrated a considerable contribution of the transport success to the catch of anchovy. In many cases, studies on larval transport processes are based on field sampling, and needs spatially and temporally varied collection with simultaneous measurement of physical oceanographic conditions. The modeling approach can be a useful tool when a phenomenon needs to be tested, because it enables to estimate eggs and larval transport process quantitatively. This study has demonstrated an effectiveness of the modeling approach and supported a hypothesis from observational data analysis.

However, on the other hand, the modeling in this study has some limitations. Since the experiments focused only on the transport process (Chapter 4), the results of particle tracking experiments could not fully reproduce the observed fluctuations in anchovy catch. For example, as shown in the Chapter 4, the observed distribution of egg abundance spatially varied, however, because of the limitation of available egg data, a constant number of eggs were

released from each possible spawning ground. This would lead mismatch between observed and modeled fluctuations in catch. This problem can be resolved in the next steps by releasing the spatially weighted number of particles based on the field sampling.

The second problem lies in the period from release to endpoint of particle. As many studies have already reported, fishes in early life stages experience a high mortality (Hjørt, 1914). For small pelagic fishes, such as sardine and anchovy faces risks of mortality in all life stages. During egg and larval stages, seawater temperature and food availability limit the growth and survival (Takahashi and Watanabe, 2005; Takasuka et al., 2007), and predation pressure by other species (e.g. Japanese jack mackerel and moon jellyfish, Takasuka et al., 2007; Masuda, 2009) would affect the recruitment. Takahashi and Watanabe (2004) reported that the recruitment success of the Japanese anchovy in the Kuroshio-Oyashio transition region depends on the growth rate during the metamorphosing stage. Those previous studies suggest that the present model needs to be improved by incorporating those biotic factors.

The third problem is in the estimation of the future larval growth rate (Chapter 5). The response of growth rate to the ambient temperature estimated by Yasue and Takasuka (2009) would be different among the areas due to different food availabilities. Therefore, further study requires applying the growth-temperature relationship, which is estimated by the sampling in the study area.

6.3 Contributions of this study and future prospects

In this study, the complex coastal environmental variability has been revealed. Since similar seawater temperature trends have been identified in the other coastal waters, large-scale climatic factors may commonly affect ocean environmental variations. Thus, this study proposes to consider the effect of large-scale climatic change in the analysis of the regional ocean environmental conditions. It is therefore desirable that the other case studies examine the generality of the findings of this study. The regional modeling approach has contributed to the understanding of the fluctuation mechanism of the coastal anchovy catch, and this finding can be a useful knowledge for the fishery management. For the efficient fishery, the forecasting of the anchovy recruitment from days to weeks needs to be accomplished by using more reproducible boundary condition derived from an ocean data assimilation model.

6.4 Conclusion

From the results of the present study, significant changes in ocean and atmospheric changes were detected. Quantitative analyses revealed that those regional environmental changes have been attributed by large-scale climate change. Combined observed and modeled analyses identified the environmental factors affecting the spatial and temporal fluctuations in the catch of the Japanese anchovy. The influence of anthropogenic global warming on the future ocean environment and anchovy stock was predicted, and showed serious changes in the distribution of anchovy. These changes could impact on whole marine ecosystems in the ECS. In addition, the knowledge obtained by this study would profit the fisheries management in coastal ocean.

Summary

Long-term trends in ocean-climate environment condition in Omura Bay

Long-term trends in SST in Omura Bay were investigated using heat balance estimates based on a daily data set obtained for 40 years (1955–1995). SST during the heating period (from March to August) tended to decrease, whereas that during most of the cooling period (from September to February) increased during these 40 years. The maximum rates of SST decrease and increase were found to be 0.020˚C $year^{-1}$ in August and 0.028˚C $year^{-1}$ in January. The sea surface heat flux analysis revealed that shortwave radiation flux decreased in the heating period due to decrease in solar radiation, resulting in a decrease in SST. In the cooling period, the increase in SST was attributed to the decrease in latent and sensible heat fluxes due to increased air temperature and decreased wind speed. These climatic changes affecting SST in Omura Bay showed a close linkage with global dimming and the East Asian monsoon circulation.

Effect of wind-stress on the catch of Japanese anchovy

Effect of wind-stress on the annual catch of the Japanese anchovy off northwestern Kyushu for the period between 1963 and 2009 was investigated. Regime shift analysis detected several step changes in catch and environmental variables. Since the mid-1980s, the anchovy catch in the coastal fishery zones has declined, while the catch in the offshore zone has increased. The decline of catch in the coastal zones showed a significant correlation with the long-term variations in prevailing north-northeastward wind-stress over the Goto-Nada Sea during spring spawning season. The results indicated that weakened north-northeastward winds caused the recent low recruitment of anchovy through low levels of wind-induced eggs and larval transport from the offshore spawning ground to the coastal nursery areas, resulting in the potential shift of nursery area to the northwestern offshore region. Thus, as well as the growth-favorable ambient temperature, transport process would play an important role on long-term fluctuations in anchovy abundance in these coastal seas.

Modeling eggs and larval transport process and its relation to catch fluctuations

To investigate the potential influence of change in the eggs and larval transport on the recruitment of the Japanese anchovy off western coast of Kyushu, the numerical simulation using a coupled hydrodynamic and particle tracking model were conducted from 1960 to 2007.

In the study region, annual catch of anchovy in the offshore zone has increased since the mid–1980s, while those in the coastal zone has declined since the mid–1970s. Particle tracking experiments revealed that increased and decreased transport success in the offshore and coastal zones, respectively. It was also suggested that the warming trend in the SST contributed to the increased transport success due to the northern shift of spawning ground. Weakening trend in the coastward current in the Goto-Nada Sea and shift of the spawning ground reduced the amount of transported eggs and larvae. The results implied that transport process have contributed to the recently flourished catch in the offshore zone and decreased catch in the coastal zone. This study showed that the changes in transport success induced by environmental condition change has potential to impact on the recruitment of anchovy off western coast of Kyushu.

Estimation of the future change of anchovy in response to the global warming

Climate change possibly alters ocean state even in coastal waters, and could induce significant change in fish recruitment. Effect of global warming on the eggs and larval transport of the Japanese anchovy in the western Kyushu was investigated using a coupled hydrodynamic and particle tracking model. An atmosphere-ocean coupled model has predicted future environmental change under the IPCC A2 scenario. Using the predicted model result, this study revealed that the eggs and larval transport process would change and affect recruitment of anchovy more than the impact of an increased SST of 4˚C. Particle tracking experiment showed transport successes in the offshore zone would be lowered compared with those in the 1950–1990s. It was also revealed that the intensified Tsushima Warm Current and shift of spawning ground would decrease retention rate in the offshore zone. Estimated increase in the SST also would change the biological condition such as the growth and survival of larval anchovy. The larval growth rate was estimated to be faster than the present state. Strengthened stratification seems to limit the nutrient supply leading to a low primary production during spring bloom, and it may restrict the food availability.

On the whole, this study revealed the effect of climate change on the regional ocean environment and fisheries resources with a focus on the western coast of Kyushu located in continental margin of the ECS. Regional environmental changes due to global warming are not well studied and thus, the findings of this study would be useful for fisheries management and understanding of marine ecosystem.

Bibliography

Abakumova GM, Feigelson EM, Russak V, Stadnik VV (1996) Evaluation of long-term changes in radiation, cloudiness, and surface temperature on the territory of the former Soviet Union. J Clim 9:1319–1327

Aiken CM, Navarrete SA, Pelegrí JL (2011) Potential changes in larval dispersal and alongshore connectivity on the central Chilean coast due to an altered wind climate. J Geophys Res 116:1–14

Aksoy B (1997) Theoretical and Applied Climatology Variations and Trends in Global Solar Radiation for Turkey. Theor Appl Climatol 58:71–77

Ando H, Kashiwagi N, Ninomiya K, Ogura H (2003) Long term trends of seawater temperature in Tokyo Bay. Oceanogr Japan 12:407–413

Belkin IM (2009) Rapid warming of large marine ecosystems. Prog Oceanogr 81:207–213

Blanchard JL, Jennings S, Holmes R, Harle J, Merino G, Allen JI, Holt J, Dulvy NK, Barange M (2012) Potential consequences of climate change for primary production and fish production in large marine ecosystems. Philos Trans R Soc Lond B Biol Sci 367:2979–89

Borja A, Uriarte A, Egana J, Motos L, Valencia V (1998) Relationships between anchovy (*Engraulis encrasicolus*) recruitment and environment in the Bay of Biscay (1967–1996). Fish Oceanogr 7:375–380

Boyce DG, Lewis MR, Worm B (2010) Global phytoplankton decline over the past century. Nature 466:591–6

Brander K (2010) Impacts of climate change on fisheries. J Mar Syst 79:389–402

Brochier T, Echevin V, Tam J (2013) Climate change scenarios experiments predict a future reduction in small pelagic fish recruitment in the Humboldt Current system. Glob Chang Biol:1–13

Budyko MI (1956) The heat balance of the earth's surface, translated into Japanase by Uchijima Z. Kasen Suion Chosakai, Gidrometeoizdat, Leningr (in Russian) pp. 254

Chavez FP, Ryan J, Lluch-cota SE, Niquen C M, Miguel N (2003) From anchovies to sardines and back : Multidecadal change in the Pacific Ocean. Science 299:217–221

Chen CTA (2000) The Three Gorges Dam: reducing the upwelling and thus productivity in the East China Sea. Geophys Res Lett 27:381–383

Chen TR, Yu KF, Shi Q, Li S, Gilbert J. Price, Wang R, Zhao M (2009) Twenty-five years of change in scleractinian coral communities of Daya Bay (northern South China Sea) and its response to the 2008 AD extreme cold climate event. Chinese Sci Bull 54:2107–2117

Churchill JH, Runge J, Chen C (2011) Processes controlling retention of spring-spawned Atlantic cod (*Gadus morhua*) in the western Gulf of Maine and their relationship to an index of recruitment success. Fish Oceanogr 20:32–46

Clark NE, Eber L, Laurs RM, Renner JA, Saur JFT (1974) Heat exchange between ocean and atmosphere in the eastern North Pacific for 1961-71. NOAA Tech Rep NMFS SSRF:632–682

Cook T, Folli M, Klinck J, Ford S, Miller J (1998) The relationship between increasing sea-surface temperature and the northward spread of *Perkinsus marinus* (Dermo) disease epizootics in oysters. Estuar Coast Shelf Sci 46:587–597

Cowen RK, Sponaugle S (2009) Larval dispersal and marine population connectivity. Ann Rev Mar Sci 1:443–466

Cutforth HW, Judiesch D (2007) Long-term changes to incoming solar energy on the Canadian Prairie. Agric For Meteorol 145:167–175

Delft Hydraulics (2007) Delft3D-PART user manual. Delft

Delft Hydraulics (2008) Delft3D-FLOW user manual. Delft

Ding Y (1994) Monsoons over China. Kluwer Academic Publisher

Donelson J, Munday P, McCormick M, Pankhurst N, Pankhurst P (2010) Effects of elevated water temperature and food availability on the reproductive performance of a coral reef fish. Mar Ecol Prog Ser 401:233–243

Drinkwater K (2005) The response of Atlantic cod (*Gadus morhua*) to future climate change. ICES J Mar Sci 62:1327–1337

Fukudome K, Yoon J, Ostrovskii A (2010) Seasonal volume transport variation in the Tsushima Warm Current through the Tsushima Straits from 10 years of ADCP observations. J Oceanogr 66:539–551

Fyfe JC, Gillett NP, Zwiers FW (2013) Overestimated global warming over the past 20 years. Nat Clim Change 3:767–769

Gaines S, Bertness M (1992) Dispersal of juveniles and variable recruitment in sessile marine species. Nature 360:579–580

Goffart A, Hecq J, Legendre L (2002) Changes in the development of the winter-spring phytoplankton bloom in the Bay of Calvi (NW Mediterranean) over the last two decades: a response to changing climate? Mar Ecol Prog Ser 236:45–60

Gong G-C, Chang J, Chiang K-P, Hsiung T-M, Hung C-C, Duan S-W, Codispoti LA (2006) Reduction of primary production and changing of nutrient ratio in the East China Sea: Effect of the Three Gorges Dam? Geophys Res Lett 33:L07610

Gordon AL, Giulivi CF (2004) Pacific decadal oscillation and sea level in the Japan/East Sea. Deep Sea Res Part I Oceanogr Res Pap 51:653–663

Halpern BS, Walbridge S, Selkoe K a, Kappel C V, Micheli F, D'Agrosa C, Bruno JF, Casey KS, Ebert C, Fox HE, Fujita R, Heinemann D, Lenihan HS, Madin EMP, Perry MT, Selig ER, Spalding M, Steneck R, Watson R (2008) A global map of human impact on marine ecosystems. Science 319:948–52

Hamada T, Kyozuka Y (2001) Numerical simulation of water exchange in Omura Bay. Soc Nav Archit Japan

Han J, Wang H (2007) Interdecadal variability of the East Asian summer monsoon in an AGCM. Adv Atmos Sci 24:808–818

Harley C, Hughes AR (2006) The impacts of climate change in coastal marine systems. Ecol Lett 9:228–241

Hashioka T, Yamanaka Y (2007) Ecosystem change in the western North Pacific associated with global warming using 3D-NEMURO. Ecol Modell 202:95–104

Hatanaka H, Kawahara S, Uozumi Y (1967) Comparison of life cycles of five ommastrephid squids fished by Japan: *Todarodes pacificu*, *Illex illecebrosus*, *Illex argentinus*, *Nototodarus sloani sloani* and *Nototodarus sloani gouldi*. NAFO Sci Coun Stud 9:59–68

Hayward TL (1997) Pacific Ocean climate change: atmospheric forcing, ocean circulation and ecosystem response. Trends Ecol Evol 12:150–154

Hinrichsen H (2001) Testing the larval drift hypothesis in the Baltic Sea: retention versus dispersion caused by wind-driven circulation. ICES J Mar Sci 58:973–984

Hiyama Y, Yoda M, Ohshimo S (2002) Stock size fluctuations in chub mackerel (*Scomber japonicus*) in the East China Sea and the Japan/East Sea. Fish Oceanogr 11:347–353

Hjort J (1914) Fluctuations in the great fisheries in northern Europe viewed in the light of biological research. Rapp Proces-verbaux des Reun Cons Perm Int pour I'Exploration la Mer 20:1–229

Hollowed AB, Bond NA, Wilderbuer TK, Stockhausen WT, Teresa ZA, Beamish RJ, Overland JE, Schirripa MJ (2009) A framework for modelling fish and shellfish responses to future climate change. ICES J Mar Sci 66:1584–1594

Hori ME, Ueda H (2006) Impact of global warming on the East Asian winter monsoon as revealed by nine coupled atmosphere-ocean GCMs. Geophys Res Lett 33:2–5

Huggett J, Fréon P, Mullon C, Penven P (2003) Modelling the transport success of anchovy *Engraulis encrasicolus* eggs and larvae in the southern Benguela: the effect of spatio-temporal spawning patterns. Mar Ecol Prog Ser 250:247–262

Huse G, Ellingsen I (2008) Capelin migrations and climate change – a modelling analysis. Clim Change 87:177–197

Hutchings L, Barange M, Bloomer SF, Boyd AJ, Crawford RJM, Huggett JA, Kerstan M, Korrûbel JL, Oliveira JAA de, Painting SJ, Richardson AJ, Shannon LJ, Schülein FH, Lingen CD van der, Verheye HM (1998) Multiple factors affecting South African anchovy recruitment in the spawning, transport and nursery areas. S Afr J Mar Sci 19:211–225

Hwang S, Kang H, Son Y, Jang M, Choi K (2013) Collapse of the Crustacean Mesozooplankton in the Northern East China Sea: Effects of the Three Gorges Dam? J Coast Res 292:1464–1469

Hyodo R, Gotoh K (2000) Tidal flow simulation for the effect of seabed configuration on exchange rate of sea water in Omura Bay. Proc Hydraul Eng 44:487–491

Iida T, Mizobata K, Saitoh S-I (2012) Interannual variability of coccolithophore *Emiliania huxleyi* blooms in response to changes in water column stability in the eastern Bering Sea. Cont Shelf Res 34:7–17

Iizuka S, Ming SH (1989) Formation of anoxic bottom waters in Omura Bay. Bull Coast Oceanogr 26:75–86

IPCC (2000) Special Report on Emission Scenarios. pp. 599

IPCC (2013) Working group I contribution to the IPCC fifth assessment report climate change 2013 : The physical science basis final draft underlying Scientific-Technical Assessment.

Iseki K, Kiyomoto Y (1997) Distribution and settling of Japanese anchovy (*Engraulis japonicus*) eggs at the spawning ground off Changjiang River in the East China Sea. Fish Oceanogr 6:205–210

Ishii M, Hasegawa K, Kakino K (2008) Long-term fluctuations of the water quality in Tokyo Bay [Japan] judged from a data set of Chiba prefecture. Bull Jpn Soc Fish Oceanogr 72:189–199

Ishii T, Kondo J (1987) Seasonal variation of the heat balance of the East China Sea. Tenki 34:517–526

Islam MS, Tanaka M (2008) Diet and prey selection in larval and juvenile Japanese anchovy *Engraulis japonicus* in Ariake Bay, Japan. Aquat Ecol 43:549–558

Ito S (2007) Responses of Pacific saury and herring projected under a global warming scenario. Kaiyo Mon 39:303–308

Ito S, Okunishi T, Kishi M J., Muyin W (2013) Modelling ecological responses of Pacific saury (*Cololabis saira*) to future climate change and its uncertainty. ICES J Mar Sci 70:980–990

Itoh S, Yasuda I, Nishikawa H, Sasaki H, Sasai Y (2009) Transport and environmental temperature variability of eggs and larvae of the Japanese anchovy (*Engraulis japonicus*) and Japanese sardine (*Sardinops melanostictus*) in the western North Pacific estimated via numerical particle-tracking experiments. Fish Oceanogr 18:118–133

Iversen S, Zhu D, Johannessen A, Toresen R (1993) Stock size, distribution and biology of anchovy in the Yellow Sea and East China Sea. Fish Res 16:147–163

Katoh O, Teshima K, Kubota K, Tsukiyama K (1996) Downstream transition of the Tsushima Current west of Kyushu in summer. J Oceanogr 52:93–108

Kawamiya M, Yoshikawa C, Kato T, Sato H, Sudo K, Watanabe S, Matsuno T (2005) Development of an integrated earth system model on the Earth Simulator. Earth Simulator 4:18–30

Kawasaki T (1983) Why do some pelagic fishes have wide fluctuations in their numbers? Biological basis of fluctuation from the viewpoint of evolutionary ecology. FAO Fish Rep 291:1065–1080

Kimura S, Inoue T, Sugimoto T (2001) Fluctuation in the distribution of low-salinity water in the North Equatorial Current and its effect on the larval transport of the Japanese eel. Fish Oceanogr 10:51–60

Kimura S, Kasai A, Nakata H, Sugimoto T, John Simpson, Cheok J (1997) Biological productivity of meso-scale eddies caused by frontal disturbances in the Kuroshio. ICES J Mar Sci 54:179–192

Kimura S, Kato Y, Kitagawa T, Yamaoka N (2010) Impacts of environmental variability and global warming scenario on Pacific bluefin tuna (*Thunnus orientalis*) spawning grounds and recruitment habitat. Prog Oceanogr 86:39–44

Kitagawa T, Kato Y, Miller MJ, Sasai Y, Sasaki H, Kimura S (2010) The restricted spawning area and season of Pacific bluefin tuna facilitate use of nursery areas: A modeling approach to larval and juvenile dispersal processes. J Exp Mar Bio Ecol 393:23–31

Kitagawa T, Sartimbul A, Nakata H, Kimura S, Yamada H, Nitta A (2006) The effect of water temperature on habitat use of young Pacific bluefin tuna *Thunnus orientalis* in the East China Sea. Fish Sci 72:1166–1176

Kondo J (1975) Air-sea bulk transfer coefficients in diabetic conditions. Boundary-Layer Meteorol 9:91–112

Kondo A, Isobe A, Shinohara M (2005) Long-term variations of water temperature in Fukuoka bay and their possible cause. Oceanogr Japan 14:399–409

Kosaka Y, Xie S-P (2013) Recent global-warming hiatus tied to equatorial Pacific surface cooling. Nature 501:403–7

Kozasa E (1975) Distribution of plankton in the western seas of Kyushu [Japan]. Bull Seikai Reg Fish Res Lab 13:1–13

Kuroda H, Oshimo S, Yasuda T (2012) Stock assessment and evaluation for Tsushima Warm Current stock of Japanese anchovy (fiscal year 2011). In Marine Fisheries Stock Assessment and Evaluation for Japanese Waters (Fiscal Year 2011/2012). Fish Agency Fish Res Agency Japan: pp. 1735

Kuwaoka M (1976) Resent fluctuation of the fisheries aspect of anchovy in the coast of the southern Nagasaki Prefecture. Bull Nagasaki Prefectual Inst Fish:25–32

Lehodey P, Senina I, Sibert J, Bopp L, Calmettes B, Hampton J, Murtugudde R (2010) Preliminary forecasts of Pacific bigeye tuna population trends under the A2 IPCC scenario. Prog Oceanogr 86:302–315

Li H, Dai A, Zhou T, Lu J (2010) Responses of East Asian summer monsoon to historical SST and atmospheric forcing during 1950–2000. Clim Dyn 34:501–514

Lie H, Cho C, Lee J (1998) Separation of the Kuroshio water and its penetration onto the continental shelf west of Kyushu. J Geophys Res 103:2963–2976

Liepert BG (1997) Recent changes in solar radiation under cloudy conditions in Germany. Int J Climatol 17:1581–1593

Liepert BG (2002) Observed reductions of surface solar radiation at sites in the United States and worldwide from 1961 to 1990. Geophys Res Lett 29:1–4

Liley JB (2009) New Zealand dimming and brightening. J Geophys Res 114:1–9

Linnane A, James C, Middleton J, Hawthorne P, Hoare M (2010) Impact of wind stress anomalies on the seasonal pattern of southern rock lobster (*Jasus edwardsii*) settlement in South Australia. Fish Oceanogr 19:290–300

Lluch-Belda D (1989) World-wide fluctuations of sardine and anchovy stocks: the regime problem. S Afr J Mar Sci 8:195–205

Masuda R (2009) Ontogenetic changes in the ecological function of the association behavior between jack mackerel *Trachurus japonicus* and jellyfish. Hydrobiologia 206:269–277

Masumoto Y, Sasaki H, Kagimoto T, Komori N, Ishida A, Sasai Y, Miyama T, Motoi T, Mitsudera H, Takahashi K, Sakuma H, Yamagata T (2004) A fifty-year eddy-resolving simulation of the world ocean –preliminary outcomes of OFES (OGCM for the Earth Simulator)–. Earth Simulator 1:35–56

Matsumoto K, Takanezawa T, Ooe M (2000) Ocean tide models developed by assimilating TOPEX/POSEIDON altimeter data into hydrodynamical model: a global model and a regional model around Japan. J Oceanogr 56:567–581

Matsuoka M, Miyaji K, Katoh O (2002) Some observations on the spawning depth of the Japanese sardine, Sardinops melanostictus, and the Japanese anchovy, *Engraulis japonicus*, off southern Kyushu, Japan. Bull Fish Res Agency 2:15–23

Matsuyama Y (1999) Harmful efect of dinoflagellate *Heterocapsa circularisquama* on shellfish aquaculture in Japan. JARQ 33:283–293

Miyazawa Y, Zhang R, Guo X, Tamura H (2009) Water mass variability in the western North Pacific detected in a 15-year eddy resolving ocean reanalysis. J Oceanogr 65:737–756

Nagasaki Prefecture (2006) White paper on fisheries of Nagasaki Prefecture fiscal year of 2006. (in Japanese)

Nagasaki Prefecture (2008) Marine lab Nagasaki.

Nagata H, Ogawa Y, Hirai M, Hirakawa K (1996) Geographical and seasonal changes of water transparency in the seas adjacent to Japan. Bull Japan Sea Natl Fish Res Inst 46:1–24

Nakamura H, Furushima Y (2000) The variation of the environment factor related to the occurrence of oxygen-deficient water mass in Oomura Bay. Rep Japan Mar Sci :1–14

Nakamura H, Lin G, Yamagata T (1997) Decadal climate variability in the North Pacific during the recent decades. Bull Am Meteorol Soc 78:2215–2225

Nakamura Y, Ichinomiya S, Hayakawa N, Nishimura H (1989) Sea surface heat transfer and its effects on the formation of coastal bay anoxia. Bull Nagaoka Univ Technol 11:69–81

Nakata H, Hirano T (1988) Wind effects on the transport of red sea bream larvae from a coastal spawning ground adjacent to Shijiki Bay. Nippon Suisan Gakkaishi 54:1545–1552

Nakata H, Kimura S, Okazaki Y, Kasai A (2000) Implications of meso-scale eddies caused by frontal disturbances of the Kuroshio Current for anchovy recruitment. ICES J Mar Sci 57:143–152

Neuheimer AB, Thresher RE, Lyle JM, Semmens JM (2011) Tolerance limit for fish growth exceeded by warming waters. Nat Clim Chang 1:110–113

Neumann T (2010) Climate-change effects on the Baltic Sea ecosystem: A model study. J Mar Syst 81:213–224

Nielsen E, Bagge O, MacKenzie BR (1998) Wind-induced transport of plaice (*Pleuronectes platessa*) early life-history stages in the Skagerrak-Kattegat. J Sea Res 39:11–28

Noguchi Y (2001) Secular variations of SST and air temperature on the Pacific side of the Tohoku region, northern Japan. J Meteorol Soc Japan 48:747–757

Odamaki M (1982) Tidal and permanent current patterns in Goto-Nada. Bull Coast Oceanogr 19:112–120

Ogawa N (1976) Mechanism of migration of anchovy, *Engraulis japonica*, towards the shore in Goto-nada and Tachibana Bay, western Kyushu [Japan]. Bull Seikai Reg Fish Res Lab 48:1–22

Ohshimo S (1996) Acoustic estimation of biomass and school character of anchovy *Engraulis japonicus* in the East China Sea and Yellow Sea. Fish Sci 62:344–349

Ohshimo S (2004) Spatial distribution and biomass of pelagic fish in the East China Sea in summer, based on acoustic surveys from 1997 to 2001. Fish Sci 70:389–400

Ohshimo S, Tanaka H, Hiyama Y (2009) Long-term stock assessment and growth changes of the Japanese sardine (*Sardinops melanostictus*) in the Sea of Japan and East China Sea from 1953 to 2006. Fish Oceanogr 18:346–358

Okazaki Y, Nakata H (2007) Effect of the mesoscale hydrographic features on larval fish distribution across the shelf break of East China Sea. Cont Shelf Res 27:1616–1628

Okunishi T, Ito S, Hashioka T, Sakamoto TT, Yoshie N, Sumata H, Yara Y, Okada N, Yamanaka Y (2012) Impacts of climate change on growth, migration and recruitment success of Japanese sardine (*Sardinops melanostictus*) in the western North Pacific. Clim Change 115:485–503

Paerl HW (2006) Assessing and managing nutrient-enhanced eutrophication in estuarine and coastal waters: Interactive effects of human and climatic perturbations. Ecol Eng 26:40–54

Paraso M, Valle-Levinson A (1996) Meteorological influences on sea level and water temperature in the lower Chesapeake Bay: 1992. Estuaries 19:548

Peck M a., Reglero P, Takahashi M, Catalán IA (2013) Life cycle ecophysiology of small pelagic fish and climate-driven changes in populations. Prog Oceanogr 116:220–245

Perry RI, Cury P, Brander K, Jennings S, Möllmann C, Planque B (2010) Sensitivity of marine systems to climate and fishing: Concepts, issues and management responses. J Mar Syst 79:427–435

Perry AL, Low PJ, Ellis JR, Reynolds JD (2005) Climate change and distribution shifts in marine fishes. Science 308:1912–5

Rodionov S, Overland J (2005) Application of a sequential regime shift detection method to the Bering Sea ecosystem. ICES J Mar Sci 62:328–332

Rosa AL, Yamamoto J, Sakurai Y (2011) Effects of environmental variability on the spawning areas, catch, and recruitment of the Japanese common squid, *Todarodes pacificus*

(Cephalopoda: Ommastrephidae), from the 1970s to the 2000s. ICES J Mar Sci 68:1114–1121

Rouault M, Pohl B, Penven P (2010) Coastal oceanic climate change and variability from 1982 to 2009 around South Africa. African J Mar Sci 32:237–246

Roy C, Lingen C van der, Coetzee J, Lutjeharms J (2007) Abrupt environmental shift associated with changes in the distribution of Cape anchovy *Engraulis encrasicolus* spawners in the southern Benguela. African J Mar Sci 29:309–319

Sakamoto TT (2005) Responses of the Kuroshio and the Kuroshio Extension to global warming in a high-resolution climate model. Geophys Res Lett 32:L14617

Sassa C, Konishi Y, Mori K (2006) Distribution of jack mackerel (*Trachurus japonicus*) larvae and juveniles in the East China Sea, with special reference to the larval transport by the Kuroshio Current. Fish Oceanogr 15:508–518

Sato N, Takahashi M (2001) Long-term variations of the Baiu frontal zone and midsummer weather in Japan. J Meteorol Soc Japan 79:759–770

Schwartzlose R, Alheit J, Bakun A (1999) Worldwide large-scale fluctuations of sardine and anchovy populations. S Afr J Mar Sci 21:37–41

Sherman K, Belkin IM, Friedland KD, O'Reilly J, Hyde K (2009) Accelerated warming and emergent trends in fisheries biomass yields of the world's large marine ecosystems. AMBIO A J Hum Environ 38:215–224

Shoji J, Toshito S, Mizuno K, Kamimura Y, Hori M, Hirakawa K (2011) Possible effects of global warming on fish recruitment: shifts in spawning season and latitudinal distribution can alter growth of fish early life stages through changes in daylength. ICES J Mar Sci 68:1165–1169

Stanhill G, Kalma JD (1995) Solar dimming and urban heating in Hong Kong. Int J Climatol 15:933–941

Stenevik EK, Sundby S (2007) Impacts of climate change on commercial fish stocks in Norwegian waters. Mar Policy 31:19–31

Sundby S, Nakken O (2008) Spatial shifts in spawning habitats of Arcto-Norwegian cod related to multidecadal climate oscillations and climate change. ICES J Mar Sci 65:6 953–962

Takagi N, Kenji M, Hideaki N (2009) Structure and variation of the north to northeastward current observed on the continental margin of the Amakusa-nada and southern part of Goto-nada through winter to spring. Bull Jpn Soc Fish Oceanogr 73:172–180

Takahashi M, Watanabe Y (2004) Growth rate-dependent recruitment of Japanese anchovy *Engraulis japonicus* in the Kuroshio–Oyashio transitional waters. Mar Ecol Prog Ser 266:227–238

Takahashi M, Watanabe Y (2005) Effects of temperature and food availability on growth rate during late larval stage of Japanese anchovy (*Engraulis japonicus*) in the Kuroshio–Oyashio transition. Fish Oceanogr 14:223–235

Takasuka A, Oozeki Y, Aoki I (2007) Optimal growth temperature hypothesis: Why do anchovy flourish and sardine collapse or vice versa under the same ocean regime? Can J Fish Aquat Sci 64:768–776

Takasuka A, Oozeki Y, Kubota H (2008) Multi-species regime shifts reflected in spawning temperature optima of small pelagic fish in the western North Pacific. Mar Ecol Prog Ser 360:211–217

Tanaka H (2006) Feeding habits and gill raker morphology of three planktivorous pelagic fish species off the coast of northern and western Kyushu in summer. J Fish Biol 68:1041–1061

Tanaka M, Nakajima C (1975) Heat balance at he sea surface over Hiuchinada Sea. Disaster Prev Res Inst Annu 18:589–595

Tanaka H, Ohshimo S, Takagi N, Ichimaru T (2010) Investigation of the geographical origin and migration of anchovy *Engraulis japonicus* in Tachibana Bay, Japan: A stable isotope approach. Fish Res 102:217–220

Tian Y, Kidokoro H, Watanabe T (2006) Long-term changes in the fish community structure from the Tsushima warm current region of the Japan/East Sea with an emphasis on the impacts of fishing and climate regime shift over the last four decades. Prog Oceanogr 68:217–237

Tian Y, Kidokoro H, Watanabe T, Igeta Y, Sakaji H, Ino S (2012) Response of yellowtail, *Seriola quinqueradiata*, a key large predatory fish in the Japan Sea, to sea water temperature over the last century and potential effects of global warming. J Mar Syst 91:1–10

Tomosada A (1994) Long-term variations of water temperature around Japan. Bull Tohoku Natl Fish Res Inst 56:1–45

Ward J (1963) Hierarchical grouping to optimize an objective function. J Am Stat Assoc 58:236–244

Warner JC (2005) Numerical modeling of an estuary: A comprehensive skill assessment. J Geophys Res 110:C05001

Watanabe T (1990) Study on formation processes of SST anomalies in the western North Pacific: Role of the East Asian winter monsoon. Doctral Thesis. Tohoku University

Wild M (2009) Global dimming and brightening: A review. J Geophys Res 114:1–31

Xu M, Chang C-P, Fu C, Qi Y, Robock A, Robinson D, Zhang H (2006) Steady decline of East Asian monsoon winds, 1969–2000: Evidence from direct ground measurements of wind speed. J Geophys Res 111:1–8

Yabe H, Shoji U, Watanabe H (1966) Studies on the early life history of bluefin tuna *Thunnus thynnus* and on the larvae of the southern bluefin tuna T. maccoyii. Rep Nankai Reg Fish Res Lab 23:95–129

Yamamoto M (2003) The Long-term variations in water temperature and salinity in Bisan-Seto, the central Seto Inland Sea. Bull Japanese Soc Fish Oceanogr 67:163–167

Yamanaka H (1963) Synopsis of biological data on kuromaguro *Thunnus orientalis* (Temminck & Schlegel) 1942 (Pacific Ocean). FAO Fish Rep 49

Yamashita K (1984) Relation between the distribution of Sardine eggs and larvae and fishing condition of "Shirasu" in the Goto nada. Bull Nagasaki Prefectual Inst Fish 10

Yang YH, Zhao N, Hao XH, Li CQ (2009) Decreasing trend of sunshine hours and related driving forces in North China. Theor Appl Climatol 97:91–98

Yasuda T, Hanawa K (1999) Composite analysis of North Pacific subtropical mode water properties with respect to the strength of the wintertime East Asian monsoon. J Oceanogr 55:531–541

Yasue N, Takasuka A (2009) Seasonal variability in growth of larval Japanese anchovy *Engraulis japonicus* driven by fluctuations in sea temperature in the Kii Channel, Japan. J Fish Biol 74:2250–68

Yeh S-W, Kim C-H (2010) Recent warming in the Yellow/East China Sea during winter and the associated atmospheric circulation. Cont Shelf Res 30:1428–1434

Yoda M, Ohshimo S, Hiyama Y (2004) Estimation of the spawning ground of jack mackerel in the East China Sea based on the catch statistics and biometric data. Bull Jpn Soc Fish Oceanogr 68:20–26

Zenitani H, Kimura R (2007) Elemental analysis of otoliths of Japanese anchovy: trial to discriminate between Seto Inland Sea and Pacific stock. Fish Sci 73:1–8

Acknowledgements

I would like to express my sincere gratitude to supervising professor Dr. S. Kimura, Atmosphere and Ocean Research Institute & Graduate School of Frontier Sciences, the University of Tokyo. I have been fortunate to have an opportunity to work as a part of his team, and to gain scientific skills and knowledge in the field of fisheries oceanography. His support and encouragement helped me throughout my years in Doctoral course. My dissertation would never have been completed without his invaluable instructions and suggestions.

I am deeply grateful to professor Dr. H. Nakata, Graduate School of Fisheries Science and Environmental Studies, Nagasaki University for encouragement, continuous help and advices, fruitful suggestions throughout my years from undergraduate days to doctoral course.

I am indebted to professor Dr. K. Shirakihara, Atmosphere and Ocean Research Institute & Graduate School of Frontier Sciences, the University of Tokyo, professor Dr. Y. Watanabe, Atmosphere and Ocean Research Institute, the University of Tokyo, associate professor Dr. K. Komatsu, Atmosphere and Ocean Research Institute & Graduate School of Frontier Sciences, the University of Tokyo, associate professor Dr. T. Kitagawa, Atmosphere and Ocean Research Institute, the University of Tokyo and associate professor Dr. S. Itoh, Atmosphere and Ocean Research Institute, the University of Tokyo, for reviewing my manuscript. Thanks are extended to professor Dr. H. Hasumi, Atmosphere and Ocean Research Institute, the University of Tokyo, for providing MIROC data.

Gratitude is expressed to project associate professor Dr. M. Yamamoto, Atmosphere and Ocean Research Institute & Graduate School of Frontier Sciences, the University of Tokyo, for his encouragement and fruitful suggestions. I would like to express my acknowledgement to research associate Dr. Y. Miyake, Atmosphere and Ocean Research Institute & Graduate School of Frontier Sciences, the University of Tokyo, for his technical advices that helped me learn a modeling study, and fruitful suggestions. Thanks are extended to scientific secretary Mrs. Y. Aoyama for support of my research life. I would like to acknowledge my colleagues for their kind advice, constant help and warm encouragement.

Finally, I would like to express my gratitude to my family for their understanding, support and encouragement.